NORTHWESTERN UNIVERSITY

Role of Hexokinase 2 in T Cell Metabolism

A DISSERTATION

SUBMITTED TO THE GRADUATE SCHOOL

IN PARTIAL FULLFILMENT OF THE REQUIREMENTS

for the degree

DOCTOR OF PHILOSOPHY

Field of Life Sciences

By

Manan M. Mehta

EVANSTON, ILLINOIS

December 2018

Abstract

T cells and cancer cells have many common features, including their need to proliferate and their metabolic requirements. In particular, glucose metabolism is highly upregulated in both cancer cells and T cells to support proliferation and other cellular functions. The first step of glycolysis is catalyzed by Hexokinase, which exists in 4 main isoforms. Hexokinase 2 (HK2) has been shown to be specifically upregulated in various types of cancers. Moreover, HK2 is required for tumor initiation, growth, and metastasis in different contexts. While this makes HK2 a potential target for cancer therapy, it is important to note that HK2 is also highly upregulated in T cells. It is unclear if inhibition of HK2 would adversely affect T cells by disrupting glucose metabolism. In the context of cancer therapy, T cell inhibition is not desirable, as it leaves patients susceptible to infections and could theoretically interfere with tumor immunity and potential immunotherapies. This thesis explores the necessity of HK2 in T cells in a variety of contexts. HK2 is largely dispensable for T cell activation, proliferation, and differentiation in vitro. In mouse models of inflammation and viral immunity, T cell function is mostly intact in the absence of HK2, with small differences in pathological inflammation. Suppressive T cell function is also spared in vivo when mice are deficient in HK2 in Regulatory T cells. Finally, we identify other potential metabolic difference between leukemic cancer cells and T cells. Together, the data show that HK2 functions mostly as a redundant enzyme in T cells and therefore it may serve as an attractive target for cancer therapy.

Acknowledgements

Many individuals have contributed in countless ways to help me during my graduate career, without whom this thesis would likely never have been completed. First I would like to thank my co-authors and the other individuals that directly contributed to the data I generated for this thesis. Sam Weinberg lent me his considerably valuable time in helping me to design and think through virtually every experiment and piece of data in this thesis. Lizzie Steinert's expertise in T cells allowed me to add some of the most convincing data in this thesis, the colitis and LCMV experiments. I thank Krishan Chhiba and the Paul Bryce lab for their help in designing and performing asthma experiments. RNA-seq and metabolomic experiments were made possible by the help of Carlos Martinez and Peng Gao, respectively. The help of the Harris Perlman lab was invaluable in evaluating the development of autoimmune disease. Of course, none of this would have been possible without our collaborator Nissim Hay who shared the HK2 mice used in all of my experiments. Additionally, I would like to thank the Jeff Rathmell lab for sharing their T cell differentiation protocols, and the Panos Ntziachristos lab for sharing their T-ALL leukemia protocols and reagents. The Northwestern cores facilities are incredibly useful resources, and I would be remiss to not mention their contribution to this thesis: the Mouse Histology and Phenotypic Core, High Throughput RNA-Seq Center, and Flow Cytometry Core all shared their equipment and skills in helping me to perform my experiments. The feedback of my thesis committee members – Chyung Ru Wang, Harris Perlman, and Scott Budinger – was also critical in improving my experiments and helping develop the story that eventually became this thesis. Finally, I must thank my advisor, Navdeep Chandel. Through all of the challenges we faced in this project, his vision and patience guided me in every decision I made.

Next I would like to thank everyone who contributed in other ways to this thesis. While their contributions did not lead to the generation of any individual graph or plot, their contributions nonetheless played a critical role in helping me complete my work. My parents worked hard to instill in me the confidence to achieve whatever I set my mind to. Their support, along with that of my sister, are the reason I was even in a position to seek a PhD. I must also thank all my friends, including my lab mates and fellow MSTP classmates; their presence in my life brought me the happiness and strength I needed to continue when experiments failed and failed again. The support of the MSTP office, in particular Jayms Peterson, helped keep me on track when I felt I wasn't. Last, I would like to thank my wife and daughter, Lopa and Leena. When I moved to Chicago in 2012 to begin my path in the MSTP, I had neither a wife nor a daughter. I never imagined how much their love could change my life. Their support and understanding kept me sane and motivated when I was at my lowest. Truly, I would not be where I am today without them.

Table of Contents

List of Figures

Chapter 1. Introduction – Role of Metabolism in T cell function

Chapter 3. Hexokinase 2 is dispensable for T cell dependent immunity

Chapter 1. Introduction – Role of Metabolism in T cell function

Portions of this chapter are from a previously published review by Manan Mehta, Sam Weinberg, and Navdeep Chandel.

Functions of metabolism

Metabolism is the process through which the cell changes the composition of different molecules inside itself. In some cases large molecules are broken down into smaller molecules, also known as catabolism. In other instances, small molecules are used to build larger molecules, also known as anabolism. The cell can alter its metabolic programs to serve its particular needs at any given time. For example, if energy is needed, catabolic process could be upregulated to generate ATP. The main metabolic pathways involve the production and consumption of amino acids, nucleic acids, fatty acids, and glucose. Mitochondria sit at the center of these pathways and act as a hub. The most relevant metabolites and metabolic pathways are highlighted in Figure 1.1 and Figure 1.2.

Though the cell is able to change its metabolism to suit its purposes, it is important to remember metabolism is not merely an output of the cell, it is also an input. The availability of certain metabolites can act as a signal to change the programming of the cell. One well studied example of this is the generation of reactive oxygen species (ROS) in periods of hypoxia, which in turn can cause an increase in the transcription factor needed to cope with hypoxia (Chandel, McClintock et al. 2000). Elegant systems such as this allow the cell to adapt to whatever environment it may find itself in and can be found in all cell types. This thesis mainly concerns

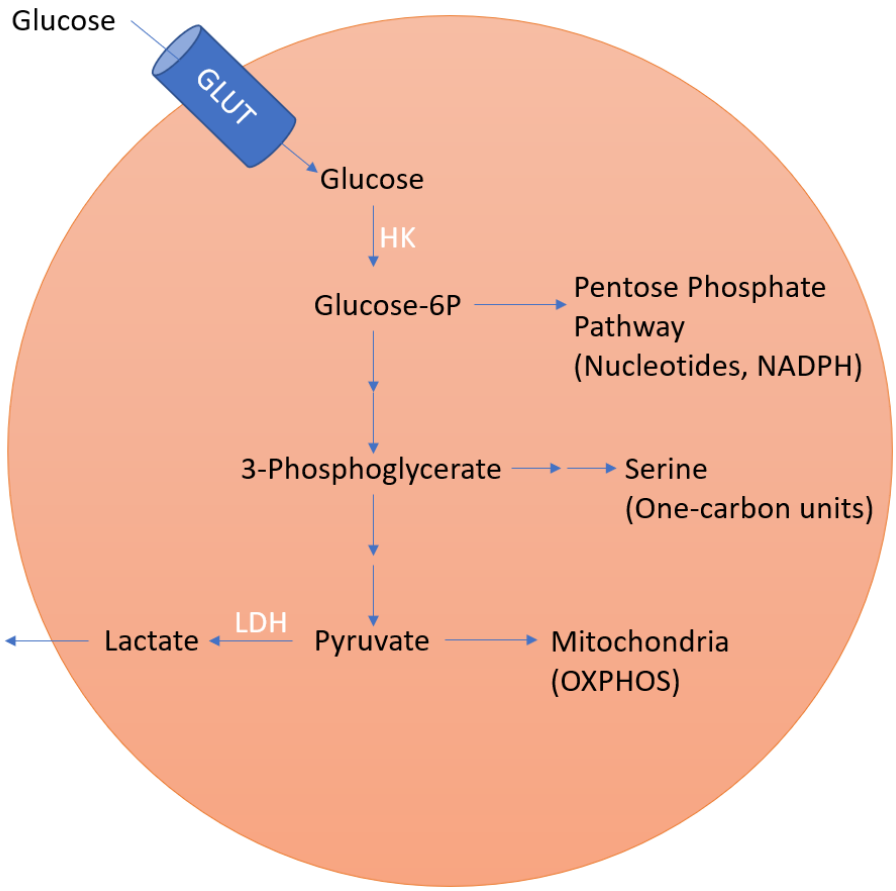

Figure 1.1 Important Glycolytic Intermediates and branch points. Glucose is taken up by the cell through glucose transporters such as those of the GLUT family. Hexokinase (HK) enzymes phosphorylate glucose as Glucose-6P to trap it in the cell. Glucose-6P can feed into the Pentose Phosphate Pathway, which produces building blocks for nucleotides as well as the reducing equivalent NADPH. Glucose-6P can be further metabolized to 3-phosphoglycerate, which can be used to generate Serine, an amino acid that plays an important role in one-carbon metabolism. Otherwise, 3-phosphoglycerate can be metabolized to pyruvate, where it can either be turned into lacate for secretion with lactate dehydrogenase or enter the mitochondria. Mitochondria can use pyruvate for oxidative phosphorylation (OXPHOS) to generate ATP.

Adapted from (Hamanaka and Chandel 2012)

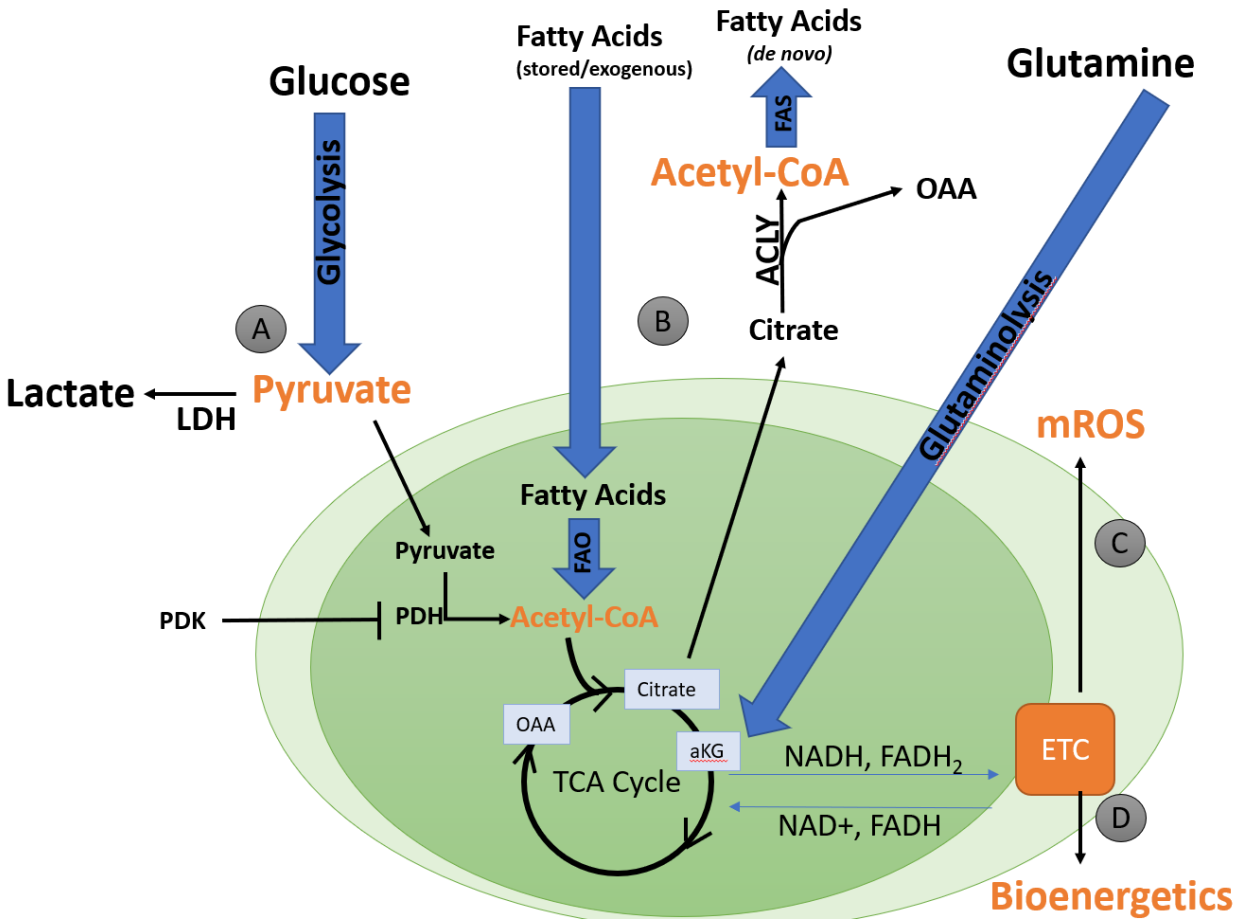

Figure 1.2. Important Metabolic Pathways. A. Pyruvate from glucose (or other sources) can either be reduced to lactate as the last step of glycolysis, or it can enter the mitochondria where it is metabolized to Acetyl-CoA by Pyruvate Dehydrogenase (PDH). The enzyme PDK inhibits PDH. **B.** Fatty Acids can be generated from Acetyl-CoA via Citrate through Fatty Acid Synthesis (FAS). Fatty Acids can also be broken down to Acetyl-CoA, which feeds the TCA cycle. Glutamine enters the TCA cycle through αKG. **C.** Reducing equivalents generated from TCA cycle and elsewhere drive the electron transport chain (ETC) which can generate reactive oxygen species (mROS) as well as **D** ATP.

Adapted from (Mehta, Weinberg et al. 2017)

the role of glucose metabolism in T cells, therefore the known roles of metabolism in T cell function will first be reviewed.

T cell activation

T cells play a critical role in the immune system, as they learn to recognize potential pathogens and either directly or indirectly attempt to attack the perceived threat. There are two main types of T cells, CD4+ T cells (helper T cells) and CD8+ T cells (cytotoxic T cells). Both cell types begin as naïve cells, but can become activated when presented with an antigen that it recognizes (Figure 1.3). Studies over the past couple decades have shown the various ways metabolism is changed during T cell activation and the functions of those metabolic changes.

Naïve T cells are metabolically quiescent, with low rates of oxygen consumption and glucose consumption (Sena, Li et al. 2013). However, stimulation of the T Cell Receptor (TCR) and costimulatory receptors leads to an increase in glycolytic and mitochondrial TCA cycle flux through activation of transcription factors and signaling pathways (Frauwirth, Riley et al. 2002, Wang, Dillon et al. 2011). In particular, in CD4+ T cells, signaling through the PI3K/Akt, AMPK, and ERK/MAPK pathways concomitant with activation of the MYC and nuclear receptor estrogen-related receptor-α (ERRα) transcriptional networks leads to increased rates of glucose and glutamine uptake, which can be metabolized through glycolysis and the TCA cycle respectively (Frauwirth, Riley et al. 2002, Carr, Kelman et al. 2010, Michalek, Gerriets et al. 2011, Wang, Dillon et al. 2011, Blagih, Coulombe et al. 2015). Simultaneously, CD4+ T cells greatly expand their ability to utilize these metabolites by increasing mitochondrial mass and capacity for OXPHOS (Sena, Li et al. 2013, Ron-Harel, Santos et al. 2016). Additionally,

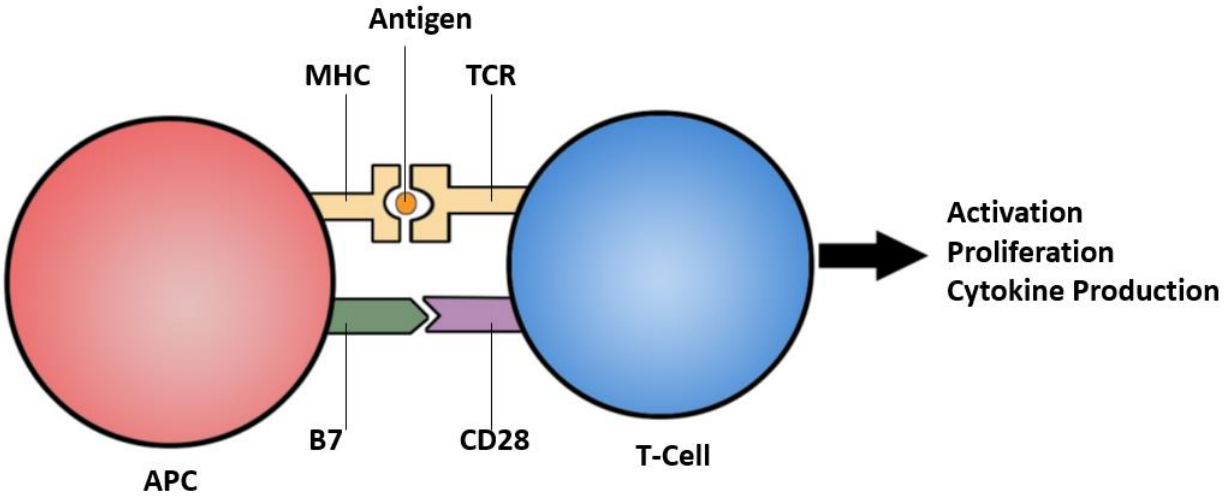

Figure 1.3 T cell activation. Antigen Presenting Cells (APCs) activate T cells through a primary signal and a secondary signal. The primary signal is initiated when an antigen is presented on a Major Histocompatability Complex and it is recognized by a T cell receptor (TCR). A secondary signal is also necessary, such as the B7-CD28 costimulatory interaction. After receiving these signals, the T cell is no longer naïve and becomes activated, proliferating and producing cytokines to address the perceived antigen threat. Activated T cell upregulate several metabolic pathways, including glycolysis and oxidative phosphorylation.

Adapted from (Sharma, Wagner et al. 2011)

activated CD4+ and CD8+ T cells increase serine-dependent mitochondrial one-carbon metabolism to support proliferation (Ron-Harel, Santos et al. 2016, Ma, Bantug et al. 2017).

Together, these metabolic changes constitute the metabolic phenotype of activated T cells. However, the aforementioned upregulation in glucose metabolism and mitochondrial metabolism has also been shown to be necessary for T cell activation. In the case of glucose metabolism, inhibition of glycolysis by reducing glucose concentration in media causes decreased proliferation and an inability to secrete IFN-γ (Jacobs, Herman et al. 2008). Interestingly, the effect on glucose is dose dependent, while the effect on IFN-γ has a threshold between 0.1 and 0.5 mM glucose at which secretion is abolished.

Mitochondrial metabolism is also necessary for important steps in T cell activation, such as production of the cytokine IL-2. Indeed, TCR-dependent calcium induces mitochondrial reactive oxygen species (mROS) which have been shown to be essential for CD4 T cell activation (Kaminski, Sauer et al. 2012, Sena, Li et al. 2013). T cells impaired in complex III of the electron transport chain (ETC) fail to induce NFAT translocation to the nucleus, resulting in decreased IL-2 mRNA upon TCR activation (Sena, Li et al. 2013). These changes in complex III deficient T cells are likely due to decreased mROS. Treatment of complex III deficient cells with exogenous H202 is sufficient to recover IL-2 production while treatment with mitochondrial targeted anti-oxidants abolishes TCR-dependent IL-2 production in WT cells (Sena, Li et al. 2013). Other sources of mROS such as complex I derived mROS and glycerol-3-phosphate

dehydrogenase derived mROS likely also contribute to T cell activation (Kaminski, Sauer et al. 2012).

An interesting observation is that loss of mitochondrial complex III results in impaired antigen-driven T cell responses in vivo but does not affect T cell proliferation upon adoptive transfer into lymphopenic mice (i.e. homeostatic proliferation) (Sena, Li et al. 2013). This indicates that complex III is necessary not for proliferation but to generate mROS in T cell activation. Furthermore, a recent study showed that complex IV deficient T cells do not have a deficit in T cell activation measured by IL-2 production (Tan, Yang et al. 2017). Complex III and IV deficient T cells would be expected to have similar changes in ATP production but could have differences in signaling through mROS, thus providing more evidence that changes due to complex III deficiency are not caused by bioenergetic deficits but rather metabolic signaling.

Together, these studies demonstrate the important role of glucose metabolism and mitochondrial metabolism in T cell activation. It is important to keep in mind the ways in which these pathways intersect. These pathways are intricate and are composed of a variety of different enzymes, and the roles of all of these components has yet to be fully elucidated.

CD4+ T cell subset differentiation

CD4+ T cells can be further subdivided into different subsets. Most CD4+ T cell subsets serve a similar purpose, they act to help promote inflammation. These effector (Teff) subsets include Th1, Th2, and Th17 cells, with each lineage specializing in certain forms of inflammation

(Figure 1.4). On the other hand, CD4+ T cells can also differentiate into regulatory (Treg) cells, which function to help control and modulate inflammation.

Each lineage is dependent on specific transcription factors and displays a unique metabolic phenotype in terms of what metabolic substrates and pathways are utilized. To date, the data suggest that an increase in glycolysis or repression of mitochondrial metabolism can increase inflammatory T cells while promoting mitochondrial metabolism increases Tregs (Michalek, Gerriets et al. 2011, Gerriets, Kishton et al. 2015). Inflammatory T cell subsets but not Tregs display elevated levels of glycolytic enzymes and lactate (Michalek, Gerriets et al. 2011, Gerriets, Kishton et al. 2015). The importance of glycolysis for Teff cells is highlighted by how loss of the glucose transporter GLUT1 diminishes glucose transport and glycolysis in vitro resulting in decreased cytokine-producing Th1, Th2 and Th17 cells but not Tregs (Macintyre, Gerriets et al. 2014). The decrease in Teff expansion due to loss of GLUT1 also reduced the ability to induce inflammatory disease in vivo such as graft versus host disease and colitis. Furthermore, GLUT1 overexpression promotes Teff numbers and inflammatory disease (Michalek, Gerriets et al. 2011). Although GLUT1 overexpression was sufficient to increase the number of Treg cells, it reduced their suppressive capacity (Gerriets, Kishton et al. 2016). Together these data imply that reducing glucose transport suppresses inflammatory T cells while increasing glucose transport supports inflammatory T cells.

Treatment of T cells with 2-DG inhibits differentiation of Th17 cells and promotes differentiation of Tregs, providing further evidence that glucose primarily supports Teff cells (Dang, Barbi et al. 2011, Shi, Wang et al. 2011). Tregs preferentially use glucose for pyruvate

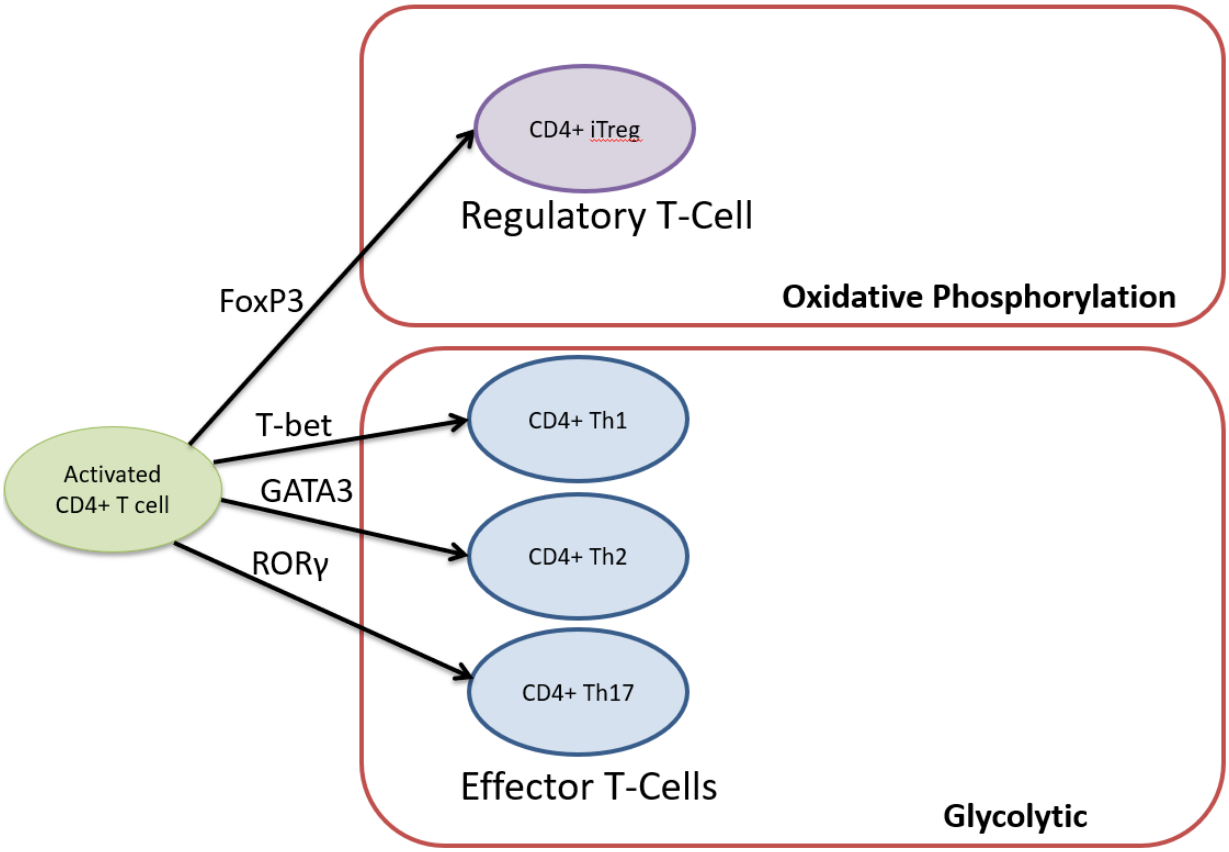

Figure 1.4. T cell subsets have different metabolic programs. CD4+ T cells can differentiate into different subsets with specialized functions. Each subset expresses certain lineage-specific transcription factors (FoxP3 for Treg, T-bet for Th1, GATA3 for Th2, and RORγ for Th17). Effector subsets tend to be more glycolytic in their metabolism while Treg cells rely more on oxidative phosphorylation.

Adapted from (Gerriets and Rathmell 2012)

oxidation rather than lactate production, and activation of pyruvate dehydrogenase (PDH) through genetic and pharmacologic means improves Treg differentiation and protects against experimental autoimmune encephalomyelitis (EAE) (Gerriets, Kishton et al. 2015). Thus, decreasing glucose flux through glycolysis appears to be a signal against Teff differentiation.

These data are further supported by the observation that genetic ablation of HIF-1α (hypoxia inducible factor 1α) phenocopies the effects of 2-DG (Shi, Wang et al. 2011). HIF-1α is a key regulator promoting glycolysis in Teff cells. Conversely, aberrant HIF-1α stabilization due to loss of VHL (a negative regulator of HIF) specifically in Tregs caused increased inflammation in mice and increased the propensity of these Tregs to secrete IFN-γ (Lee, Elly et al. 2015). These findings support the theory that increasing glucose flux through glycolysis increases inflammatory T cells while decreasing glucose flux through glycolysis increases suppressive Treg cells.

However, currently it is not clear whether it is increased glycolytic flux or diminished mitochondrial metabolism that promotes Teff cytokine producing cells. The challenge has been to decipher the mechanism by which these changes in metabolism cause an increase in Teff cells. The promotion of Tregs and suppression of Th17 cells by activating PDH in part can be rescued by administering the pan-antioxidant N-acetyl cysteine (NAC) suggesting increased mROS suppresses Th17 cell differentiation (Gerriets, Kishton et al. 2015). Diminishing respiration results in decreased mROS production and correlates with an increase in Teff cytokine producing cells; conversely increased mROS production is correlated with increased Treg formation

(Gerriets, Kishton et al. 2015). Others have speculated that ROS may modulate FoxP3 expression indirectly through its known effects on TCR signaling and NFAT (Newton, Priyadharshini et al. 2016).

The other mechanism aside from mROS could be the generation of TCA cycle metabolites controlling epigenetics. Th1 cells require expression of LDH to shunt pyruvate away from the mitochondria into lactate (Figure 1.5) (Peng, Yin et al. 2016). Genetic loss of LDH in T cells inhibits Th1 cytokine production due to shunting of pyruvate into the mitochondria, which lowers cytosolic acetyl-CoA levels necessary for histone modifications at loci critical for Th1 differentiation and function, such as the IFN-γ locus (Peng, Yin et al. 2016). Additionally, glucose metabolism may be required for optimal Th1 function through a post-transcriptional mechanism where increased glucose flux relieves GAPDH mediated suppression of IFN-γ translation (Chang, Curtis et al. 2013). Going forward, it will be important to understand the signaling mechanisms by which changes in metabolism control Teff cells and Tregs.

CD8+ T cell memory formation

An important function of T cells in general is the ability of the T cell to remember past threats and respond quickly to address them when seen again. T cell memory is often studied in CD8+ T cells, and CD8+ T cells can therefore be rudimentarily grouped as either memory or effector cells. For example, during a typical viral infection, T cells will rapidly divide as effector cells to clear the infection and then a small memory cell population will persistent long term in case of future infection with the same pathogen (Figure 1.6). Effector and memory T cells have differing

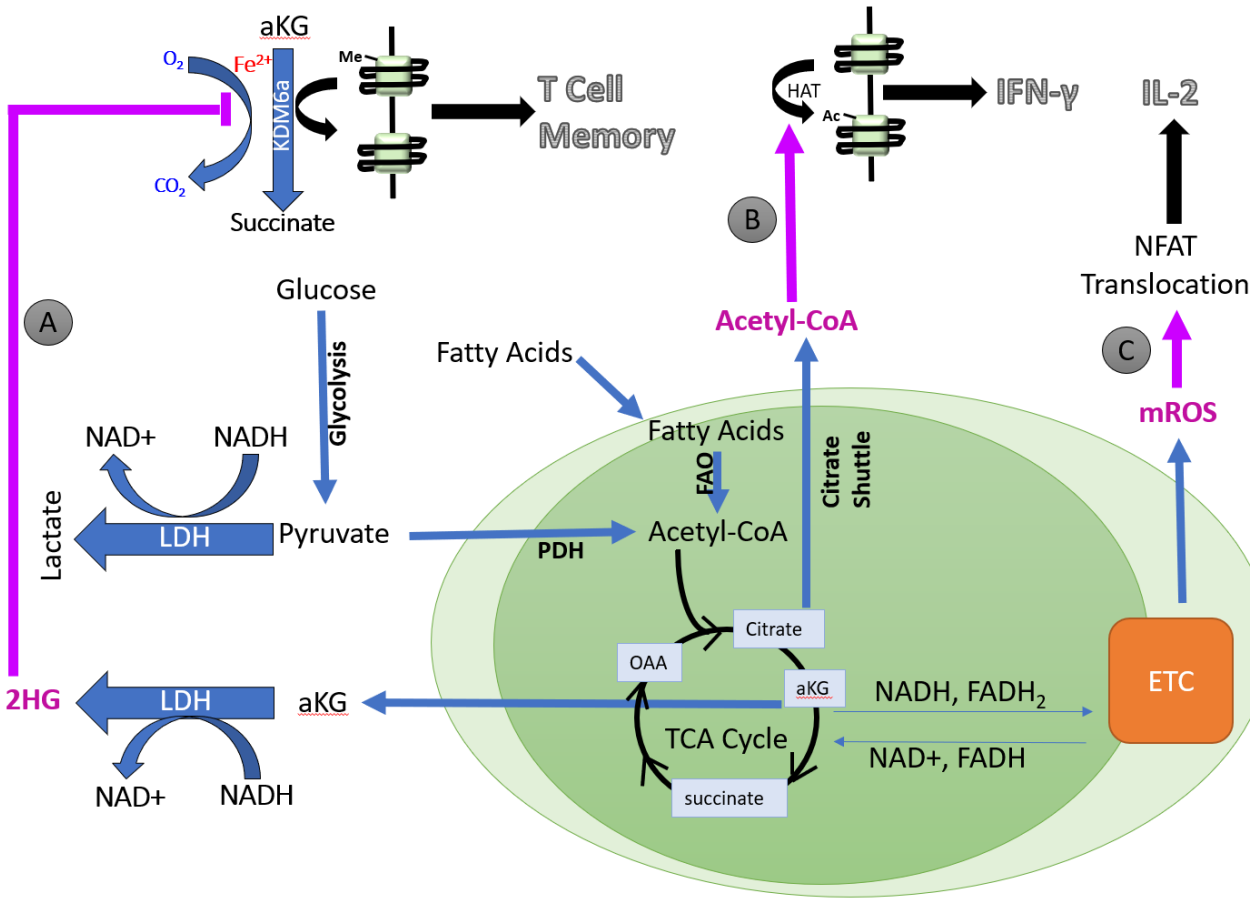

Figure 1.5. Mechanisms of metabolic control of T cell function. A. αKG can be reduced to 2HG under conditions which favor high NADH/NAD+ ratios through enzymes such as Lactate Dehydrogenase (LDH). 2HG inhibits αKG-dependent dioxygenase reactions such as histone lysine demethylases (KDM6a), potentially leading to a T cell memory phenotype through epigenetic changes. **B.** Typically, pyruvate from glycolysis is converted to lactate by LDH. Alternatively, pyruvate can enter the mitochondria and be oxidized by pyruvate dehydrogenase (PDH). The flow of pyruvate into the mitochondria instead of lactate may limit the availability of cytoplasmic acetyl-CoA used for histone acetylation reactions needed for IFNγ production. **C.** mROS generated at the ETC are necessary for NFAT mediated IL-2 production.

Adapated from (Mehta, Weinberg et al. 2017).

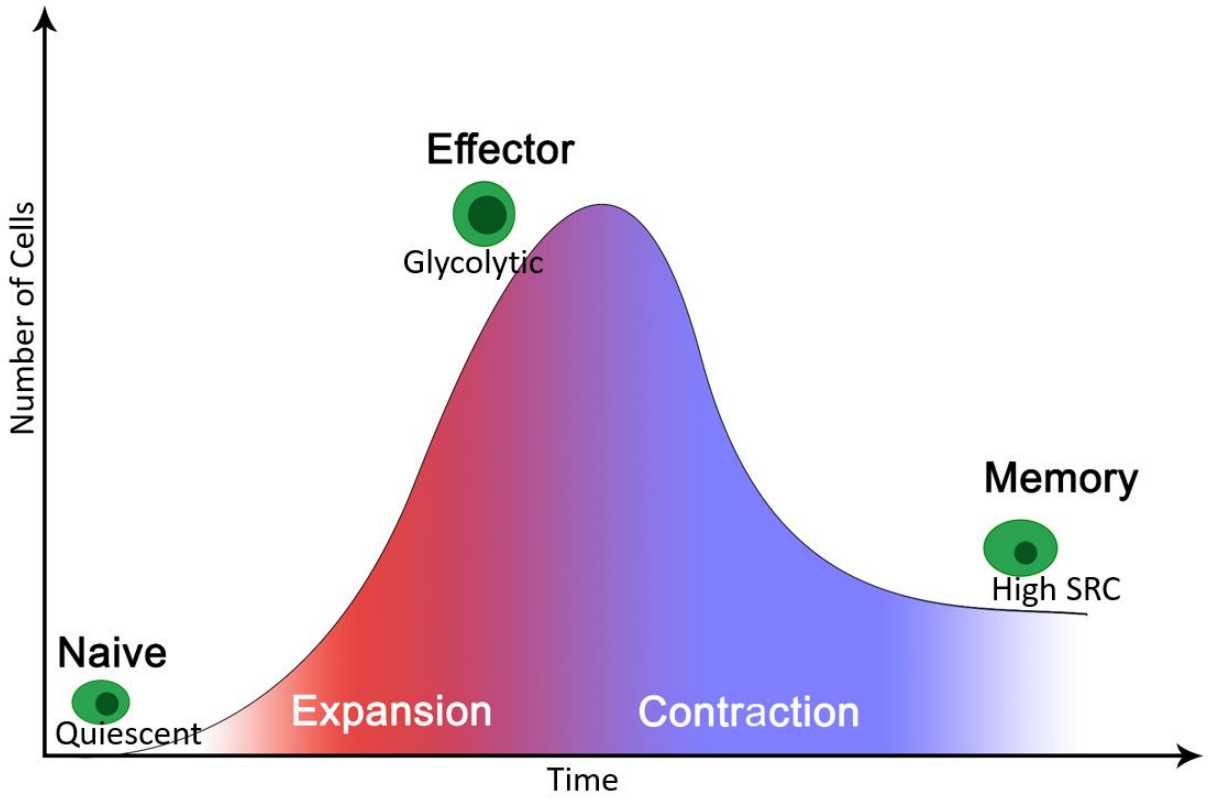

Figure 1.6. Memory and effector T cells have differing metabolic phenotypes. After T cells recognize a potential infectious pathogen, they become activate and expand as effector cells. While naïve cells are metabolically quiescent, effector cells are highly glycolytic. Once the infection is resolved, the population contracts into a memory population. Memory T cells are characterized by a high Spare Respiratory Capacity (SRC) and lower levels of glycolysis than effector cells.

Adapted from (Pearce, Poffenberger et al. 2013)

metabolic phenotypes and metabolism can also play a role in determining how effectively memory cells can form.

Effector T cells display mitochondria undergoing fission, whereas memory T cells have densely packed fused mitochondria (Buck, O'Sullivan et al. 2016). Early metabolic studies showed that memory cells tend to be more quiescent with a large capacity for mitochondrial oxidative phosphorylation (OXPHOS) while effector cells tend to be more glycolytic (Pearce, Walsh et al. 2009, van der Windt, Everts et al. 2012, Sukumar, Liu et al. 2013). However, one important idea that has emerged from studies is that increased glycolysis is a signal for effector function while increased OXPHOS is a signal for memory formation. In support of this, cells treated with 2-DG show enhanced memory formation while overexpression of the glycolytic enzyme phosphoglycerate mutase (PGAM) showed decreased memory formation (Sukumar, Liu et al. 2013).

In terms of mitochondrial metabolism, memory cells have a high spare respiratory capacity (SRC) (van der Windt, Everts et al. 2012). This means that they have the ability to support very high flux through the ETC, but do not use this respiratory capacity at baseline. The SRC is thought to be due to an increased capacity for fatty acid oxidation (FAO), implying that memory T cells use fatty acids for energy preferentially. However, memory T cells have decreased uptake of fatty acids when compared to effector T cells due to decreased CD36 expression (O'Sullivan, van der Windt et al. 2014). Instead, the source of fatty acids is stored intracellular triacylglyceride (TAGs) that are synthesized from glucose (O'Sullivan, van der Windt et al. 2014). In addition, FA/TAG synthesis has been shown to be necessary and sufficient for IL7-

dependent CD8 memory T cell longevity (Cui, Staron et al. 2015). The unexpected conclusion is that memory T cells apparently engage both FAO and FAS pathways, at least in vitro. Cells typically do not perform both FAO and FAS, as the resulting futile cycle would waste energy. If memory T cells do in fact engage in a futile cycle, glucose flux could play an even more important role in determining memory formation through its effects on FAS.

An important caveat to these findings is how the metabolism of tissue resident memory populations may differ from other memory populations. A recent study showed FAO was required for resident memory cell function by utilizing genetic knockouts of FABP4/5, a key pair of proteins responsible for intracellular FA transportation (Pan, Tian et al. 2017). Importantly, these proteins were not required for central memory T cell function.

Together, these studies showed a link between effector and memory T cells and glycolysis and OXPHOS, respectively. Going forward it will be important to verify the necessity of fatty acid driven oxidative phosphorylation in vivo by ablating genes essential for FAO, FAS, or ETC in memory T cells. While some inroads have been made in this area, the use of transgenic mouse models with inducible gene deletion would help dissect the role of metabolism in various phases of the immune response. For example, use of an inducible Cre could allow for the deletion of a metabolic gene after a stable memory population has formed to determine the necessity of a particular metabolic gene in maintaining functional memory cells.

Studies that have begun to use conditional knockouts of genes regulating metabolic pathways have demonstrated surprising results. For example, while initial studies suggested that glycolysis

is not essential for memory formation, recent in vivo studies have provided evidence that these conclusions may not hold true under all circumstances. Mice with T cells deficient in VHL have aberrant increases in glycolysis at the expense of some OXPHOS (Phan, Doedens et al. 2016). While these cells would be expected to preferentially become effector cells due to increased glycolysis, they do not have impairment in memory formation. On the contrary, loss of VHL accelerates memory T cell formation (Phan, Doedens et al. 2016). It is important to note that VHL deficient T cells preferentially form effector memory cells rather than central memory cells, and therefore some observed discrepancies with previous studies may simply be due to analysis of different types of memory T cells (Phan, Doedens et al. 2016).

An approach to decipher how metabolism controls T cell immune functions is to conduct metabolomics. Indeed, CD8 T cells deficient in VHL demonstrate through metabolomics that S-2-hydroxygluatrate (S-2HG) is the most abundant metabolite in these cells (Tyrakis, Palazon et al. 2016). S-2HG is generated by lactate or malate dehydrogenases using α-ketoglutarate (α-KG) as a promiscuous substrate. This reaction is coupled to oxidation of NADH to NAD+ (Figure 1.5) (Intlekofer, Dematteo et al. 2015). S-2HG is an antagonist to multiple α-KG dependent dioxygenases including histone demethylases and the TET family of enzymes that control DNA demethylation. Thus, increases in S-2HG can correlate with histone and DNA methylation. Specifically, in VHL deficient T cells, increased 2HG causes epigenetic changes that correlate with memory-like characteristics (Tyrakis, Palazon et al. 2016).

VHL deficiency or hypoxia increases S-2HG by elevating HIF-1α dependent expression of LDH-A (Intlekofer, Dematteo et al. 2015). How VHL deficiency or physiological hypoxia (1%

O2) increases the NADH/NAD+ ratio to drive this reaction is not clear. Hypoxia would increase the NADH/NAD+ ratio at oxygen levels below 0.5% O2 at which point respiration is inhibited. It is important to note that the key experiments regarding the necessity of S-2HG in controlling memory cells haves not been performed to date. S-2HG would have to be diminished in VHL deficient T cells to demonstrate the requirement of 2HG in controlling memory in this setting. Nevertheless, these findings suggest that controlling 2HG levels might be the key feature of how increasing glycolysis promotes memory function.

Interestingly, S-2HG levels also increase when the mitochondrial respiratory chain is inhibited resulting in elevated NADH/NAD+ ratio (Mullen, Hu et al. 2014). At first glance, this would predict that inhibition of respiration should increase memory CD8+ T cell formation. However, disrupting mitochondrial cristae in T cells due to Opa1 deficiency reduces electron flux through the respiratory chain and impairs memory T cell formation after infection (Buck, O'Sullivan et al. 2016). Importantly, Opa1 loss does not impair effector T cell response. Conversely, promoting mitochondrial respiratory chain flux due to loss of MCJ (methylation-controlled J protein) enhances the secretion, but not expression, of IFN-γ to provide increased protection against influenza virus infection (Champagne, Hatle et al. 2016). These results lead us to speculate that S-2HG would only promote memory function in conditions where the respiratory chain is not impaired, such as VHL deficiency. However, it is still not fully understood how the respiratory chain controls memory T cell function. It might be to sustain FAO-dependent metabolite production as well as generation of mROS for optimal memory function. How glucose metabolism and mitochondrial respiration work together to control CD8+ T cell memory

is an unanswered question that may be addressed in the future through further genetic and in vivo mouse models.

Glucose metabolism in tumor immunity

A growing field of immunology is the role of the immune system in cancer and how it may be harnessed for cancer therapy. Accordingly, recent work has shown how various aspects of tumor immunity can be controlled by metabolism. T cells are essential to the host immune response to cancer. Activated CD8 T+ cells exert cytotoxic effects on tumor cells. However, during cancer progression, the tumor microenvironment becomes immunosuppressive which reduces T cell mediated cytotoxicity (Rabinovich, Gabrilovich et al. 2007). Some of the mechanisms by which tumor cells exert their immunosuppressive effects may be through altering the metabolism of T cells.

For example, inhibiting mitochondrial function may inhibit the tumoricidal ability of T cells. Tumor-infiltrating T cells (TILs) display a loss of mitochondrial function due to a defect in PGC1α-programmed mitochondrial biogenesis. This effect is independent of PD-1 blockade or regulatory T cell suppression (Scharping, Menk et al. 2016). Ectopic PGC1α expression in T cells rescues mitochondrial function and induces more effective antitumor responses (Scharping, Menk et al. 2016). These data are supported by the observation that increasing mitochondrial fusion, which promotes mitochondrial metabolism in memory T cells, also enhances antitumor responses (Buck, O'Sullivan et al. 2016). In another study, adoptive transfer of melanoma-specific CD8+ T cells caused an improved antitumor response when specifically cells with low

mitochondrial membrane potential were transferred (Sukumar, Liu et al. 2016). This effect was attributed to an enrichment of cells engaging in OXPHOS/FAO and an enrichment of long-lived memory cells (Sukumar, Liu et al. 2016). Clearly, there is at least a correlation between metabolic phenotype, memory phenotype, and tumoricidal activity.

How the tumor microenvironment represses mitochondrial metabolism is not fully understood. The tumor microenvironment is limited in nutrients, which could repress T cell activation. Indeed, low glucose in the tumor microenvironment causes TIL dysfunction; recent studies suggest that cancer cells that consume high levels of glucose restrict glucose available to TILs thus preventing their ability to be cytotoxic to tumors (Chang, Qiu et al. 2015, Ho, Bihuniak et al. 2015). Restoring glucose flux and the glycolytic intermediate phosphoenolpyruvate is sufficient for optimal calcium dependent NFAT activation and boosts TIL anti-tumor responses (Chang, Qiu et al. 2015, Ho, Bihuniak et al. 2015). Furthermore, PHD null T cells, which have increased glycolysis through HIF-1α stabilization, are also more tumoricidal (Mamlouk, Kalucka et al. 2014). Oxygen can also be limiting in the tumor microenvironment due to high consumption by proliferative tumor cells. Providing supplemental oxygen to tumor bearing mice as a strategy to decrease tumor microenvironment hypoxia increases T cell infiltration and anti-tumor responses (Hatfield, Kjaergaard et al. 2015). Optimizing both glucose and mitochondrial metabolism are therefore both likely to be necessary for the optimal anti-tumor function of T cells.

The tumor microenvironment can alter T cell metabolism through checkpoint signaling such as upregulation of co-inhibitory molecules CTLA-4 and PD-1, and checkpoint blockade

immunotherapy may work in part by reversing those metabolic changes (Ho, Bihuniak et al. 2015). Interestingly, PD-1 binding has been shown to decrease glucose and glutamine uptake in T cells, causing an immunosuppressed phenotype (Ho, Bihuniak et al. 2015). Disrupting this co-inhibitory signaling increases glucose utilization in TILs, implying that metabolism in part mediates restored tumoricidal potential in TILs (Ho, Bihuniak et al. 2015). An exciting idea is to combine current metabolism therapies with checkpoint blockade. A recent study demonstrated that treating tumors with metformin (a complex I inhibitor) in combination with PD-1 blockade resulted in increased TIL function and tumor clearance (Scharping, Menk et al. 2017). However, it is unclear if this is due to the effects of metformin on the tumor, TILs, or a combination of both. In other experimental models, metformin has been shown to directly inhibit tumor cell mitochondrial complex I to inhibit tumorigenesis (Wheaton, Weinberg et al. 2014). Thus, metformin could have multiple mechanisms to serve as an anti-cancer agent.

Adoptive T cells can also be utilized for cancer therapy, such as CAR-T cell therapy. CAR-T cells are genetically engineered to recognize cancer cells and have been shown to create robust, durable responses to certain malignancies (Fesnak, June et al. 2016). One avenue of research has focused on how to improve responses by modulating the metabolism of the cells. For example, the choice of co-receptor in the CAR affects the metabolism of CAR-T cells and also their effectiveness; CARs that use 41BB instead of CD28 have increased mitochondrial mass and increased expression of ETC genes, leading to increased FAO (Kawalekar, O'Connor et al. 2016). These changes are correlated with enhanced survival and T cell memory, thus improving the antitumor response of the therapy (Kawalekar, O'Connor et al. 2016). Another strategy uses CD8+ T cells cultured in the presence of cell-permeable S-2HG. Subsequent transfer into tumor-

bearing hosts shows remarkably increased anti-tumor activity when compared to untreated T cells (Tyrakis, Palazon et al. 2016). This might be efficacious in controlling cell fate of T cells prior to adoptive transfer for immunotherapy. Looking forward, there is much excitement in the interconnection between the field of cancer and immunometabolism.

Hexokinase 2

One potential metabolic target to inhibit cancer cells is Hexokinase 2 (HK2). As mentioned previously, HK is the first step of glycolysis. There are four commonly expressed isoforms of HK (Wilson 2003). HK4, also known as glucokinase, is a low affinity isoform of HK that serves highly specialized functions in hepatocytes and pancreatic β-cells (Postic, Shiota et al. 2001). HK1, 2, and 3 have higher affinity for glucose and are therefore more suited for rapidly feeding glycolysis (Wilson 2003). In addition, HK1 and HK2 both have N-terminal sequences allowing them to associate with the mitochondrial membrane and gain access to mitochondrial ATP (Wilson 2003). HK1 is expressed through many different types of tissues while HK2 is expressed mostly in muscle and adipose tissue (Wilson 2003). However, HK2 is highly upregulated in many different types of cancer cells (Patra, Wang et al. 2013, Wang, Xiong et al. 2014, Botzer, Maman et al. 2016, Kishton, Barnes et al. 2016). Indeed, HK2 may specifically be required for cancer cells over other HK isoforms. For example, in a mouse model of Kras-driven lung cancer, HK2 was significantly upregulated compared to normal lung, but HK1 was not (Patra, Wang et al. 2013). More importantly, deletion of the Hk2 gene in the lung resulted in fewer tumors and increased survival. Furthermore, HK2 deficiency was shown to delay initiation of tumors in a mouse model of Neu-driven breast cancer and inhibit tumor growth of xenograft breast cancer (Patra, Wang et al. 2013). Similarly, HK2 deficiency decrease tumor growth and

reduced lung metastasis after neuroblastoma xenograft (Botzer, Maman et al. 2016). HK2 was also shown to be highly expressed in a mouse model of T cell acute lymphoblastic leukemia, and HK2 deficiency lead to delayed mortality (Kishton, Barnes et al. 2016). Finally, one study showed HK2 was upregulated in prostate cancer using in vivo Pten/p53 deficient mouse models, and that silencing of HK2 lead to diminished tumor burden in a prostate xenograft model (Wang, Xiong et al. 2014). Clearly, HK2 deficiency inhibits cancer in a wide variety of forms.

HK2 is also highly upregulated in T cells, however. In fact, it is one of the most upregulated glycolytic enzymes after T cell activation (Shi, Wang et al. 2011, Tan, Yang et al. 2017). It was previously unknown how HK2 inhibition would affect T cells, given its role in glucose metabolism. Based on the studies reviewed above, changes in glucose flux could potentially alter a wide variety of T cell functions, including T cell activation, proliferation, cytokine production, subset differentiation, and memory formation. The effects of HK2 inhibition on T cells are important, as T cell inhibition could limit the applicability of HK2 inhibition to cancer therapy. In this thesis, we report that HK2 is surprisingly not required for T cell function.

Chapter 2 – Materials and Methods

Mouse models

HK2fl/fl mice were previously generated (Patra, Wang et al. 2013). Genotyping was performed by PCR of genomic DNA using the following primers: HK2-F (CCCCTTCGCTTGCCATTAC), HK2-R (TGTCTTGGCTCAGATGTGAC), HK2-null (AACCACGACGCCCAATGATTTAG). HK2-F and HK2-R primers yields two bands on 2% agarose gel, a high molecular weight band for floxed gene and low molecular weight for wild-type. CD4-cre, Vav-iCre, FoxP3-YFP-Cre, CD45.1, IL-10-/- mice were obtained from Jackson Labs. Except where noted otherwise, approximately 2-4 month old adult mice of both sexes were used for experiments. Animals were not randomized to experimental groups, but were age-matched, sex-matched, and littermates where possible. No animals were excluded from analysis. Investigators were blinded to mouse genotypes for histological scoring but not blinded otherwise. All animals were housed and bred in the Northwestern animal vivarium and procedures were approved by Institutional Animal Care and Use Committee (IACUC) at Northwestern University.

T cell isolation and in vitro culture

Single cell suspensions of splenocytes were isolated by mechanically disrupting spleens from approximately 2-4 month old mice through a 70 uM strainer in 2% FBS/PBS. CD4+ T cells and CD8+ T cells were isolated from splenocytes using a negative selection magnetic bead kit according to manufacturer's protocol (StemCell). Resulting T cells were activated 1:1 with CD3/CD28 coated beads (Gibco) and 20 ng/mL IL-2 (peprotech) for 24-72 hours in RPMI 1640 media, 10% fetal bovine serum (FBS), 10 mM HEPES, 2mM glutamax, 50 uM beta-

mercaptoethanol with antibiotic/antimycotic. Typically, 100,000-200,000 cells were activated per well of 96 well plate. For proliferation experiments, cells were stained for 10 minutes with CFSE prior to activation according to manufacturer's protocol (ThermoFisher). For low glucose experiments, dialysed fetal bovine serum was used and glucose was added to glucose-free RPMI at indicated concentrations. For experiments requiring conditions biased for certain lineages, activation was altered as follows. Cells were activated with 5:1 irradiated splenocytes (3000 rad) and 2.5 ug/mL soluble anti-CD3 (ebiosciences). Cytokines and blocking antibodies were added to promote Th1 (10 ng/mL IL-12, 10 ug/mL anti-IL-4), Th2 (300 ng/mL IL-4, 10 ug/mL anti-IL-12, 10 ug/mL anti-IFNγ), Th17 (2 ng/mL TGFb, 20 ng/mL IL-6), and Treg (2 ng/mL TGFb) differentiation. Th0 consisted of base media without any additional cytokines or blocking antibodies. IL-12 obtained from peprotech; anti-IL-4, anti-IFNγ from biolegend; IL-6, anti-IL-12 from ebiosciences; IL-4/TGFb from R&D. Cells split 1:2 after 3 days and supplemented with additional media and IL-2 for 2 days before analysis.

Glucose assays

Oxygen consumption and extracellular acidification were measured on a 96 well Seahorse Analyzer (Agilent) as previously described (Sena, Li et al. 2013). Briefly, T cells (up to 250,000) were plated in wells pre-coated with cell-tak (Corning) according to manufacturer's protocol in 10 mM glucose containing media. After adhesion, glucose-free media was added to bring volume to 175 uL before starting assay, leaving approximately 2 mM glucose at start of assay. Assay was performed according to manufacturer's protocol using following final assay concentrations: 10 mM glucose, 2.5 uM oligomycin, 2 uM CCCP, 2 uM antimycin A, 2 uM rotenone, 25-50 mM 2-DG. HK activity and 2-DG uptake were measured on activated CD4+ and

CD8+ T cells by commercially available kits (BioVision and Promega, respectively) according to manufacture's protocols. 50,000 cells were plated for glucose uptake assay. HK lysates of 100,000-200,000 cells were flash frozen in liquid nitrogen prior to storage at -80C.

Flow Cytometry and Sorting

Single cell suspensions were resuspended in 2% FBS/PBS for surface staining, and the following antibodies were used as indicated (clone numbers in parenthesis): anti-CD4 (GK1.5, RM4-5), CD8 (53-6.7), CD45.2 (104), CD25 (PC61.5), CD69 (H1-2F3), CD44 (IM7), CD62L (MEL14), F4-80 (BM8), CD11c (N418), B220 (RA3-6B2), CD11b (M1/70), Gr-1 (RB6-8C5), NK1.1 (PK136), TER-119 (TER-119), CD19 (1D3). Viability was determined by staining with a nucleic dye, either propidium iodide (ThermoFisher), LIVE/DEAD Fixable Blue stain (ThermoFisher), or Ghost Dye Red 780 (Tonbo) and measuring unstained cells. For intracellular cytokine staining, cells were pretreated with 50 ng/mL PMA (Sigma), 1ug/mL ionomycin (Sigma), and protein transport inhibitor cocktail (ebiosciences) for approximately 4 hours (except in case of gp33 stimulation, which is performed as described below). For intracellular cytokines and transcriptions factors, cells were fixed with a Cell Fixation/Permeabilization Kit (BD) or FoxP3/Transcription Factor Staining Kit (ebiosciences) followed by staining with the following antibodies as indicated: anti-Tbet (O4-46), GATA3 (TWAJ), RORγt (B2D), FoxP3 (FJK-16s), IFNγ (XMG1.2), IL-4(11B11), IL-17a (17B7). Cell counts were measured by adding a known concentration of beads (Spherotech) to sample prior to analysis. Alternatively, cells were counted on a Cellometer (Nexcelom). gp33 monomer (D(b)/LCMV.GP33.KAVYNFATM) was obtained from the NIH Tetramer Core Facility and tetramerized according to their provided protocol. All samples were run on LSR Fortessa or FACSymphony flow cytometers (BD) and data was

analyzed using FlowJo software. Cells were sorted using the FASC Aria II (BD). Sorted cells were reanalyzed afterwards to ensure approximately 90% purity.

Protein extraction and Western Blot

Cells pellets were stored at -80C until resuspension and lysis. Protein content was quantified by BCA assay. 4-20% or Any kD polyacrylamide gels (Bio-Rad) were used to separate lysate proteins. Protein was then transferred to nitrocellulose membranes using Trans-Blot Turbo (BioRad). Membranes were blocked using 5% milk/TBS for 1 hour, washed with TBST, and then incubated in 5% BSA/TBST with anti-HK2 (Santa Cruz, product #6521, diluted approximately 1:500) and anti-β-actin (Sigma, catalog no. T9026/A2066; diluted 1:1000) or anti-GAPDH (Santa Cruz, clone C65, diluted 1:1000) overnight at 4C. HK1 and HK3 blotting performed similarly with antibodies from Cell Signaling (clone C35C4) and Abcam (catalog no. ab126217), respectively. Membranes were washed with TBST and incubated in appropriate secondary antibodies – donkey anti-goat or goat anti-rabbit IRDye 800CW (Li-cor, diluted 1:5000-1:10000 in 5% milk/TBST) and donkey anti-mouse or anti-rabbit IRDye 680RD (Li-cor, diluted 1:10,000 in 5% milk/TBST) for one hour at room temperature. Membranes were imaged with an Odyssey Fc Analyzer (Li-cor).

Real Time PCR

cDNA was generated using M-MLV Reverse Transcriptase (invitrogen) according to manufacture's protocol. cDNA, iQ SYBR Green Supermix (Bio-rad) and 200nM primers were mixed according to manufacturer's protocol and analyzed on the CFX384 Real Time System (Bio-rad). Alternatively, low quantity RNA samples were analyzed using a one step protocol

(Tonbo CybrFast 1-step RT-qPCR Lo Rox) and 0.1-1.0 pg of RNA according to manufacturers protocol. The following primer sequences were used: HK2-F (GTGTGCTCCGAGTAAGGGTG), HK2-R (CAGGCATTCGGCAATGTGG), HK1-F (AACGGCCTCCGTCAAGATG), HK1-R (GCCGAGATCCAGTGCAATG), HK3-F (TGCTGCCCACATACGTGAG), HK3-R (GCCTGTCAGTGTTACCCACAA), Hmgcs2-F (GAAGAGAGCGATGCAGGAAAC), Hmgcs2-R (GTCCACATATTGGGCTGGAAA), Chdh-F (TTCGGCTGGATGGACATGAC), Chdh-R (CTGCTTACAAGTGTCTGGACC), Ldhb-F (CATTGCGTCCGTTGCAGATG), Ldhb-R (GGAGGAACAAGCTCCCGTG), Prodh-F (GCACCACGAGCAGTTGTTC), Prodh-R (CTTTGTTGTGCCGGATCAGAG), Fbp1-F (CACCGCGATCAAAGCCATCT), Fbp1-R (AGGTAGCGTAGGACGACTTCA), b-Actin-F (CTAAGGCCAACCGTGAAAAG), b-Actin-R (ACCAGAGGCATACAGGGACA), RPL-19-F (GAAGGTCAAAGGGAATGTGTTCAA), and RPL-19-R (TTTCGTGCTTCCTTGGTCTTAGA). Some primer sequences obtained from PrimerBank database. Relative expression levels were calculated using ΔCT method by comparing genes of interest to the geometric mean of indicated housekeeping genes.

Colitis Model and Histology

IL10$^{-/-}$ mice were allowed to spontaneously develop colitis, typically between 8-14 weeks of age. Mice were euthanized if they lost greater than 20% of their body weight or if they developed rectal prolapse. IL-10$^{+/+}$ littermates were euthanized at approximately 13-15 weeks as controls. Colon, spleen, and mesenteric lymph nodes from euthanized mice were collected. Colons were fixed for 2 days in 10% neutral buffered formalin for H&E staining or immediately digested to isolate lamina propria cells as previously described and reproduced as follows (Steinert,

Schenkel et al. 2015). Colons were sliced into small pieces, followed by stripping epithelial cells with 0.154 mg/mL DTE in 10% HBSS/HEPES bicarbonate for 30 min at 37 C, shaking at 450 RPM. Tissues were then digested with 100U/mL type I collagenase (Worthington) in RPMI 1640, 5% FBS, 2 mM $MgCl_2$, $CaCl_2$ for 45 min shaking as before. Finally, tissues were mechanically disrupted using a gentleMACS spleen setting. Lymphocytes were enriched with a 44/67% Percoll gradient. Lymph nodes were mechanically disrupted in RPMI on scored plates to yield lymphocytes. Lymphocytes were analyzed by flow cytometry as described above. Fixed tissues were parrfin embedded, section, mounted, and stained with H&E by the Northwestern mouse histology core. Scoring was performed blinded according to established criteria (Erben, Loddenkemper et al. 2014).

OVA Immunization and Airway inflammation

OVA immunization and challenge was performed as previously described (Bryce, Mathias et al. 2006). 6-8 week old mice were sensitized to OVA by treating with intraperitoneal 10 mg OVA (Grade VI; Sigma-Aldrich) in alum (3 mg) or equal volume PBS/alum on days 0 and 14. On days 21-23, mice were challenged daily for 20 min with 1% OVA/PBS aerosolized by nebulizer. Mice were euthanized on day 24, trachea was cannulated, and lungs were flushed with PBS + 10% FCS + 1mM EDTA. Resulting BAL fluid was counted for total nucleated cell count, cells were cytospun onto slides, and supernatants were used for ELISA cytokine quantification. Differential counts were performed after staining slides with DiffQuik. Lung tissue was homogenized for RNA isolation (Qiagen) and analyzed by taqman probes according to manufacturer's protocol (ThermoScientific, probe numbers mm00445259_m1, mm00439646_m1, mm00434204_m1,

mm01168134_m1, mm00439618_m1). Remaining lung tissue was fixed and H&E stained as described above.

LCMV infection, CD8+ T cell restimulation, and Plaque assay

Adult mice were infected with 200,000 pfu LCMV-armstrong intraperitoneally. Peripheral blood was acquired by retroorbital bleeds on indicated days. Red blood cells were lysed in RBC lysis buffer (ebiosciences) and blood was analyzed by flow cytometry as described above. Mice were euthanized after 60 DPI and splenoyctes were isolated as described above. 1 million splenocytes per sample were stimulated with 30 ng/mL exogenous gp33-41 peptide (KAVYNFATM, genscript) for approximately 5 hours in the presence of GolgiPlug (BD), after which surface staining, tetramer staining, and intracellular cytokine staining were performed as described above. Alternatively, mice were euthanized at 3 and 8 DPI and liver and spleens were removed. 8 DPI spleens were sorted for CD8+ T cells which were used for RNA-seq and metabolomics as described below. Liver was homogenized and used to determine viral load by plaque assay as described in detail by others (Welsh and Seedhom 2008). Briefly, six serial dilutions of liver homogenate were added to a monolayer of Vero cells and overlayed with 0.5% agarose for 5 days, stained with neutral red for 1 day, and PFUs were counted.

Bone marrow isolation and leukemic transformation

Peripheral blood counts were obtained by retroorbital bleeds of mice and analysis on a Hemavet (Drew). Bone marrow from adult mice was harvested by dissecting pelvis, femur, and tibia. Bones were centrifuged for 5 minutes at 5000 rcf in an 18G-punctured 500 uL tube nested in a 1.5 mL tube. Platinum E cells were used to create Notch1-DE retrovirus by treating cells with

MIGR1-Notch1-DE plasmid and using the JetPrime manufacturer's protocol (plasmid and cell line gifted by Panagiotis Ntziachristos). Bone marrow was used with a CD117+ positive selection magnetic bead isolation kit (StemCell) to yield CD117+ cells. CD117+ cells were grown in Opti-Mem (ThermoFisher) supplemented with 10 ng/mL IL-3 (peprotech), 10 ng/mL IL-7 (peprotech), 50 ng/mL SCF (peprotech), 50 ng/mL Flt3L (peprotech), and 20 ng/mL IL-6 (ebiosciences). Cells were infected with Notch1-DE retrovirus by adding virus to cells, centrifugation at 2500 rpm at 25C for 90 minutes, incubation at 37C for 4 hours, and removal of virus replacing with previous media. Infection was repeated on the next day, after which cells were allowed to rest for 2 days. 75,000 lineage (CD4, CD8a, B220, CD11b, Gr-1, NK1.1, Ter-119) negative, GFP+ cells were sorted and mixed with 750,000 bone marrow cells from CD45.1 mice resuspended in PBS. Cells were adoptively transferred into lethally irradiated (1000 rad) CD45.1 mice by retroorbital injection. Mice were monitored over 6 weeks by analyzing peripheral blood with flow cytometry for CD45.2+GFP+CD4+CD8+ leukemic cells to ensure development of leukemia. Splenocytes were sorted for GFP+ leukemic cells and analyzed by RNA-seq (described below).

RNA-seq data acquisition and analysis

RNA processing was performed by the Northwestern High Throughput RNA-Seq Center, within the Division of Pulmonary and Critical Care. RNA quality and quantity were measured by using Agilent 4200 Tapestation and high Sensitivity RNA ScreenTape System (Agilent Technologies). SMART-Seq v4 Ultra Low Input RNA Kit (Takara Bio USA, Inc) was used to generate full-length cDNA and Nextera XT DNA sample preparation kit (Illumina Inc) was used to prepare

final library. An Illumina NextSeq 500 (Illumina Inc) was used to sequence library with single end sequencing (1x75 cycles) using NextSeq 500 High Output reagent kit (Illumina Inc). FASTQ reads were trimmed using Trimmomatic to remove end nucleotides with a PHRED score less than 30 and requiring a minimum length of 20 bp. Reads were then aligned to the mm10 genome using tophat version 2.1.0 using the following options --no-novel-juncs --read-mismatches 2 --read-edit-dist 2 --max-multihits 20 –library-type fr-unstranded. The generated bam files were then used to count the reads only at the exons of genes using htseq-count with the following parameters -q -m intersection-nonempty -s no -t exon. The R package edgeR was used to determine significance of differentially expressed genes, only genes with >2 fold change in expression and p-adj<0.01 were considered significant and included in heatmap. Genes were filtered for involvement in metabolism based on the KEGG mmu01100 genes. NCBI gene ids for mmu01100 pathway downloaded from http://rest.kegg.jp/link/mmu/mmu01100 and converted to gene names using the David Gene ID Conversion tool (https://david.ncifcrf.gov/conversion.jsp). Broad Institute GSEA software was used to perform a pre-ranked GSEA analysis using 3000 permutations and the Hallmark pathway database.

Metabolomics

Cell pellets were flash frozen in liquid nitrogen and stored at -80C until metabolite extraction. Samples pellets were thawed on ice, immediately resuspended and vortexed in 80% methanol, freeze thawed three times between liquid nitrogen and 37 C water bath, and centrifuged at 18,000 rcf for 10 minutes at 4C. Supernatants were transferred to new tubes and stored at -80 C until analysis. For analysis, samples were dried and resuspended in a volume adjusted so 500,000 cells' worth of metabolites were analyzed for targeted metabolomics. Samples were analyzed by

High-Performance Liquid Chromatography and High-Resolution Mass Spectrometry and Tandem Mass Spectrometry (HPLC-MS/MS). Specifically, system consisted of a Thermo Q-Exactive in line with an electrospray source and an Ultimate3000 (Thermo) series HPLC consisting of a binary pump, degasser, and auto-sampler outfitted with a Xbridge Amide column (Waters; dimensions of 4.6 mm × 100 mm and a 3.5 μm particle size). The mobile phase A contained 95% (vol/vol) water, 5% (vol/vol) acetonitrile, 20 mM ammonium hydroxide, 20 mM ammonium acetate, pH = 9.0; B was 100% Acetonitrile. The gradient was: 0-1 min, 15% A; 18.5 min, 76% A; 18.5-20.4 min, 24% A; 20.4-20.5 min, 15% A; 20.5-28 min, 15% A with a flow rate of 400 μL/min. The capillary of the ESI source was set to 275 °C, with sheath gas at 45 arbitrary units, auxiliary gas at 5 arbitrary units and the spray voltage at 4.0 kV. In positive/negative polarity switching mode, an m/z scan range from 70 to 850 was chosen and MS1 data was collected at a resolution of 70,000. The automatic gain control (AGC) target was set at 1 × 106 and the maximum injection time was 200 ms. The top 5 precursor ions were subsequently fragmented, in a data-dependent manner, using the higher energy collisional dissociation (HCD) cell set to 30% normalized collision energy in MS2 at a resolution power of 17,500. Data acquisition and peak extraction/integration were carried out by Xcalibur 4.0 software and Tracefinder 2.1 software, respectively (ThermoFisher). Low quality peaks were omitted from analysis. Ion counts for each sample were normalized by total ion counts and analyzed using multiple t-tests with a Benjamini-Kreiger false discovery rate of 10%.

Statistical Analyses

Data were analyzed statistically using Prism 7 (Graphpad), except RNA-seq and metabolomic data which was analyzed as described above. Statistical tests, error bar representations, p-values,

biological replicates, sample sizes, and independent experiments are specified in figure legends. Appropriate statistical tests were selected for each comparison based on type of data and assuming normality. Adjustments for multiple comparisons were performed when appropriate and are described in figure legends. Representative images of gels and histology are from at least 3 biological replicates. No outliers were removed from data analysis.

Chapter 3 – Hexokinase 2 is dispensable for T-cell dependent immunity

Background

T lymphocytes in the immune system and neoplastic cells in cancer are both highly proliferative cell types, relying on highly active metabolic pathways (Pearce, Poffenberger et al. 2013, DeBerardinis and Chandel 2016). T cells typically divide and expand in response to a specific antigen, while cancer cells exhibit uncontrolled proliferation. Nonetheless, similar molecular mechanisms underlie the ability of these different cell types to proliferate. Indeed, one of the major side effects of chemotherapies which target proliferating cancer cells is immunosuppression. One common mechanism utilized by both cancer and activated T cells to support their proliferation is an upregulation of glycolysis to provide intermediates for macromolecule synthesis (Lunt and Vander Heiden 2011, Andrejeva and Rathmell 2017).

Glucose metabolism is essential for both normal T cell mediated immunity and pathological T cell mediated inflammation (Wang, Marquardt et al. 1976, Michalek, Gerriets et al. 2011, Gerriets and Rathmell 2012, Chang, Curtis et al. 2013, Yang, Fujii et al. 2013, Blagih, Coulombe et al. 2015, Yin, Choi et al. 2015). Studies have similarly shown that glucose metabolism is required for tumor growth in a variety of cancer models (Shaw 2006). Furthermore, in the tumor microenvironment, evidence indicates that T cells and cancer cells may compete for glucose, and that cancer cells may upregulate glycolysis in part to deprive T cells of glucose as a means to evade and suppress the immune system (Chang, Qiu et al. 2015, Ho, Bihuniak et al. 2015). These studies have led to interest in using anti-glycolytic agents for cancer therapy. Clearly, glucose metabolism is essential for both cancer and T cells. However, it is not clear if glucose is utilized

differently in cancer and T cells and thus if glucose metabolism is a viable target for cancer therapy. Given that T cells also rely heavily on glucose, it is possible that anti-glycolytic therapy could lead to immunosuppression, leaving patients susceptible to infections. Furthermore, such immunosuppression would work at cross purposes with emerging cancer therapies such as check point blockade which rely on T cells. Therefore, any potential glycolytic target for cancer therapy should ideally spare T cell function.

One possible target for anti-glycolytic cancer therapy is Hexokinase (HK), first committed step of glycolysis. HK can be expressed as 4 different isoforms, with HK1 being a somewhat ubiquitous isoform and HK2 existing as a more selectively regulated isoform (Wilson 2003). Cancer cells highly upregulate HK2 compared to their normal tissue of origin and it is required for tumorigenesis in a variety of mouse cancer models, including breast and lung cancer and T-cell leukemia (Patra, Wang et al. 2013, Wang, Xiong et al. 2014, Botzer, Maman et al. 2016, Kishton, Barnes et al. 2016). However, HK2 is also highly upregulated in activated T cells (Shi, Wang et al. 2011, Tan, Yang et al. 2017). Furthermore, pan-hexokinase inhibition with 2-deoxyglucose (2DG) causes impaired differentiation of the inflammatory Th17 CD4+ T cell lineage and a shift from effector to memory cells in CD8+ T cells (Dang, Barbi et al. 2011, Shi, Wang et al. 2011, Sukumar, Liu et al. 2013). Presently, it is unknown whether loss of HK2 would impair T cell mediated inflammation and immunity.

In this study, we report that HK2 is largely dispensable in T cells for viral immunity and inflammation in several mouse models. Collectively, our data indicate that targeting HK2 may be

a promising avenue for further research in cancer therapy, as it may spare T cell function while inhibiting cancer growth.

HK2 is dispensable for T cells in vitro

To assess the necessity of HK2 for basic T cell function in vitro, we generated mice that have a conditional deletion of the Hk2 gene in T cells by crossing CD4-cre mice with mice harboring a floxed Hk2 allele ($Hk2^{fl/fl}$). Resulting CD4-cre;$Hk2^{fl/fl}$ mice are herein referred to as T-$Hk2^{-/-}$ mice. Spleens from the mice were removed and CD4+ and CD8+ cells were isolated and activated in vitro. As has been observed previously, CD4+ and CD8+ WT T cells highly upregulated Hk2 transcript upon activation (Shi, Wang et al. 2011), but T cells from T-$Hk2^{-/-}$ mice had no increase in HK2 mRNA or protein upon activation (Figure 3.1-3.3). Importantly, there was no compensatory increase in HK1 or HK3 mRNA or protein in CD4+ or CD8+ cells from T-$Hk2^{-/-}$ mice (Figure 3.1, 3.3, 3.4). Surprisingly, total HK activity measured in activated CD4+ and CD8+ cells was not statistically different between WT and T-$Hk2^{-/-}$ mice. (Figure 3.5A). Glucose uptake capacity was measured by the amount of 2-DG taken up by cells. 2-DG uptake was unaffected by HK2 deficiency in CD4+ and CD8+ T cells (Figure 3.5B). Basal and maximal extracellular acidification rate (ECAR) is a surrogate measure of lactate production and glycolytic activity. ECAR was similar between activated T cells from WT and T-$Hk2^{-/-}$ mice (Figure 3.5C). Oxygen consumption rate was also unchanged in activated CD4+ and CD8+ T cells (Figure 3.5D). Overall, our data show that HK2 deficiency causes only small changes in T cell glucose usage.

In order to determine if HK2 deficient T cells had any functional deficits in vitro, we measured their ability to activate and proliferate after stimulation. Surprisingly, HK2 deficient CD4+ and CD8+ T cells had no decrease in expression of the activation markers CD25 or CD69 after 24 hours (Figure 3.6). CD4+ T cells had no decrease in proliferation after 72 hours as measured by

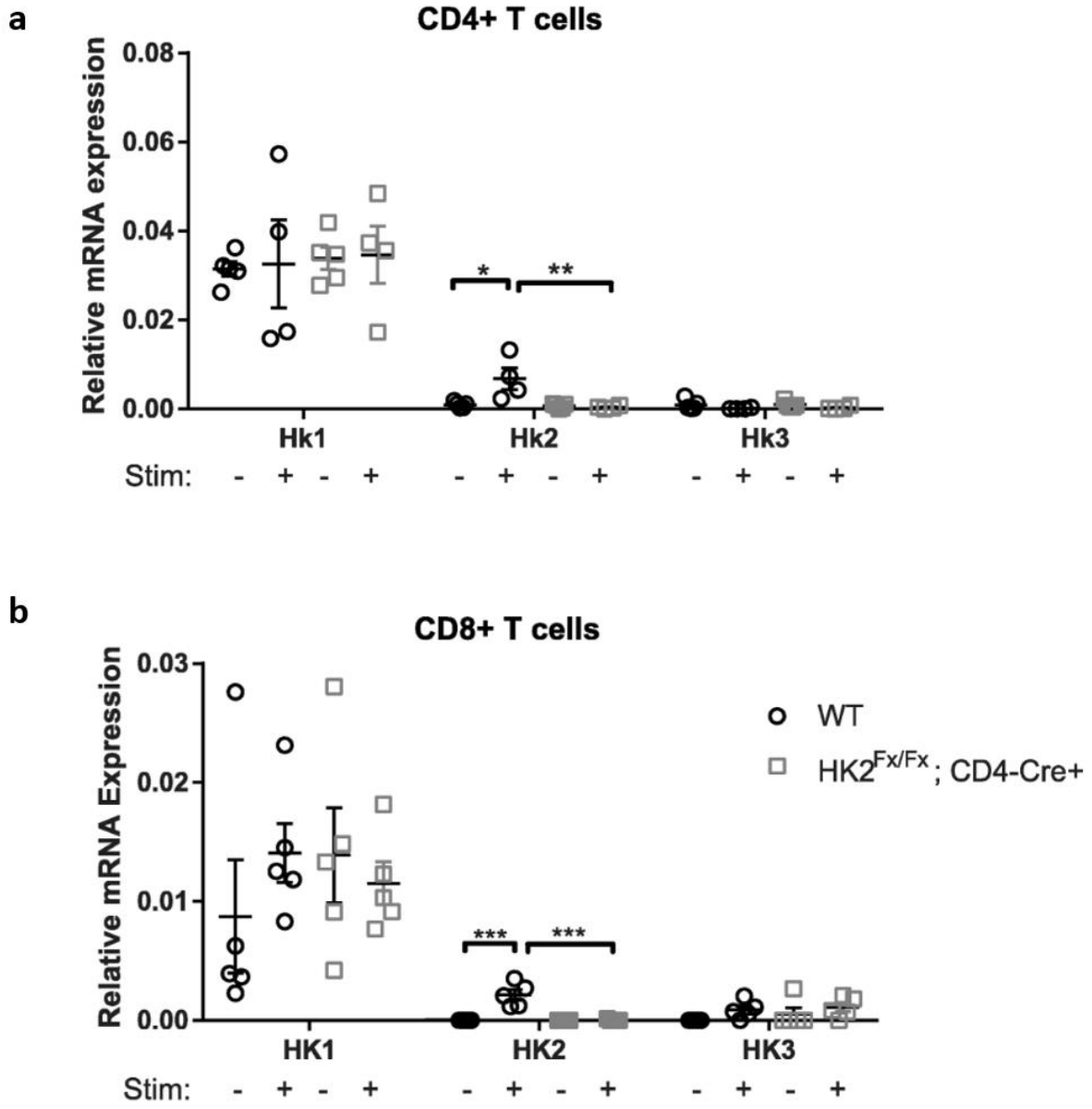

Figure 3.1. HK2 mRNA is decreased in T cells of T-Hk2-/- mice. Naïve CD4+ and CD8+ T cells were purified from splenocytes isolated from adult WT and T-Hk2−/− mice and compared to T cells activated in vitro with anti-CD3/28-coated beads for 24 hours. Expression of HK isoforms relative to β-actin and Rpl-19. Biological replicates from 2 independent experiments. Error bars represent mean ± SEM, ANOVA with Sidak multiple comparisons, *$p < 0.05$; **$p < 0.01$. NS = not significant

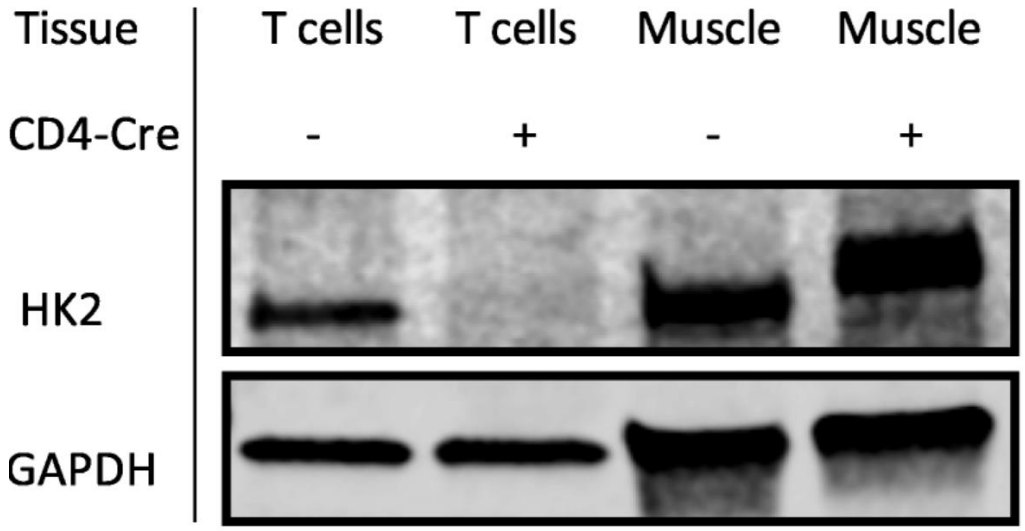

Figure 3.2. HK2 protein is decreased in CD4+ T cells of T-Hk2-/- mice. Purified naïve CD4+ T cells from WT and T-Hk2-/- mice were activated with anti-CD3/CD28 coated beads for 24 hr. Western blot for HK2 expression in T cells. Muscle protein from WT and T-Hk2-/- mice shown as positive control. GAPDH shown as loading control. Representative of 4 biological replicates.

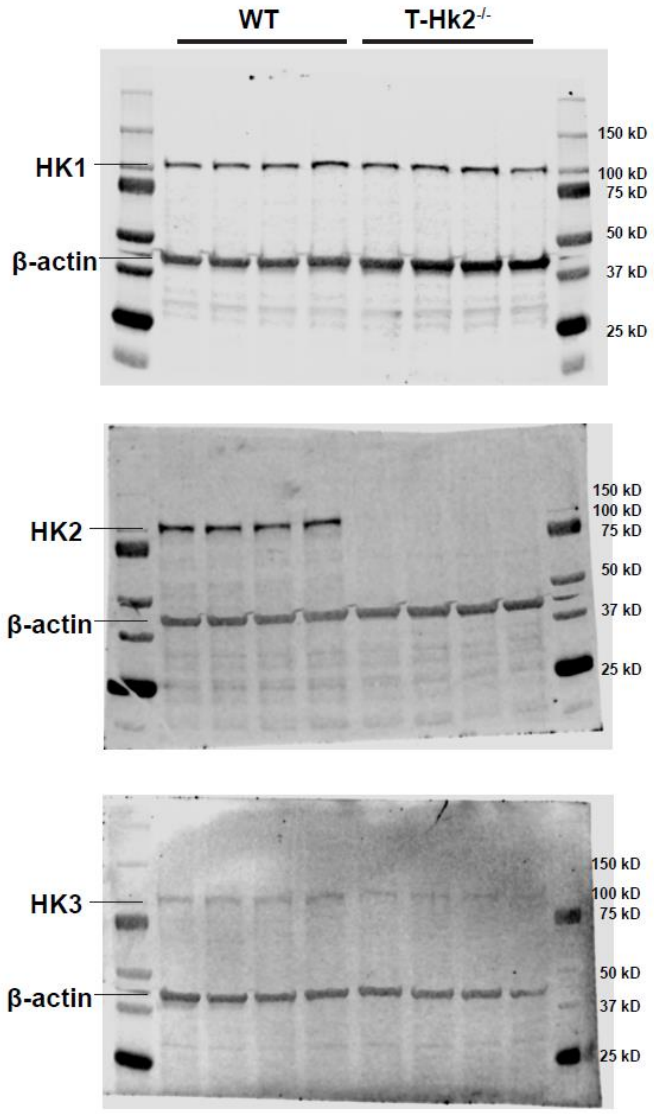

Figure 3.3. HK protein expression in CD8+ T cells of T-Hk2-/- mice. Purified CD4+ T cells from WT and T-Hk2-/- mice were activated with anti-CD3/CD28 coated beads for 72 hours. Western blot for HK1-3 expression in T cells. β-actin shown as loading control.

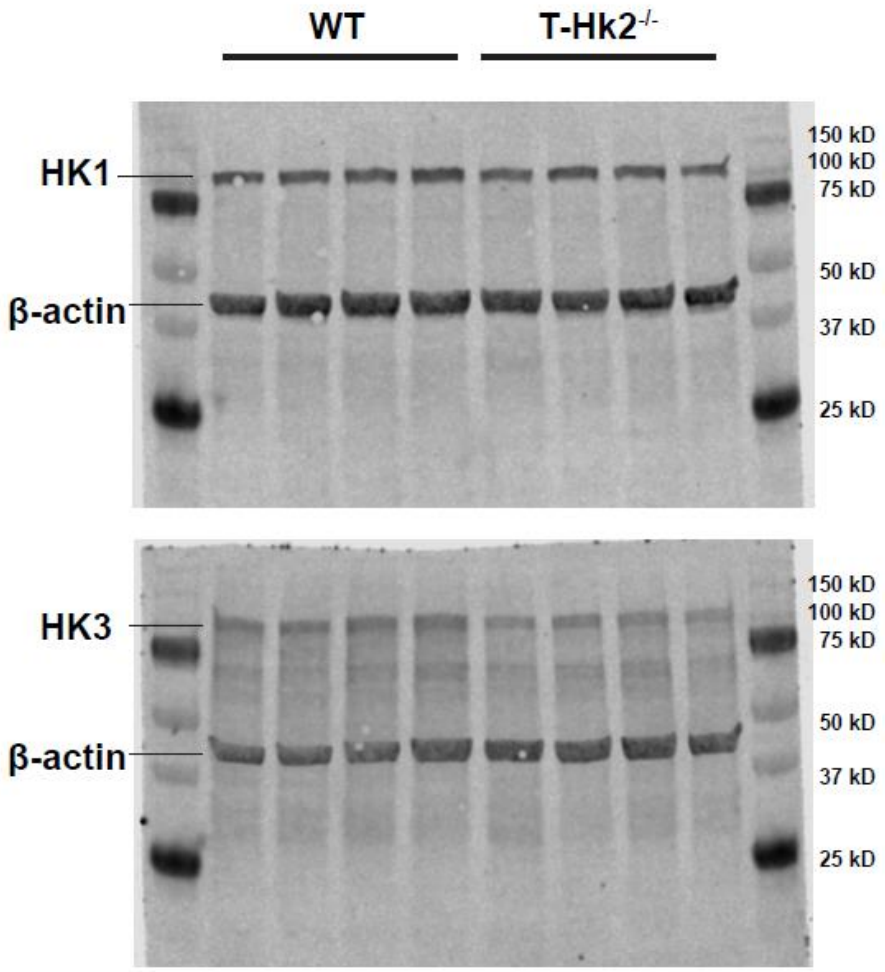

Figure 3.4. HK protein expression in CD4+ T cells of T-Hk2-/- mice. Purified CD4+ T cells from WT and T-Hk2-/- mice were activated with anti-CD3/CD28 coated beads for 72 hours. Western blot for HK1, HK3 expression in T cells. β-actin shown as loading control.

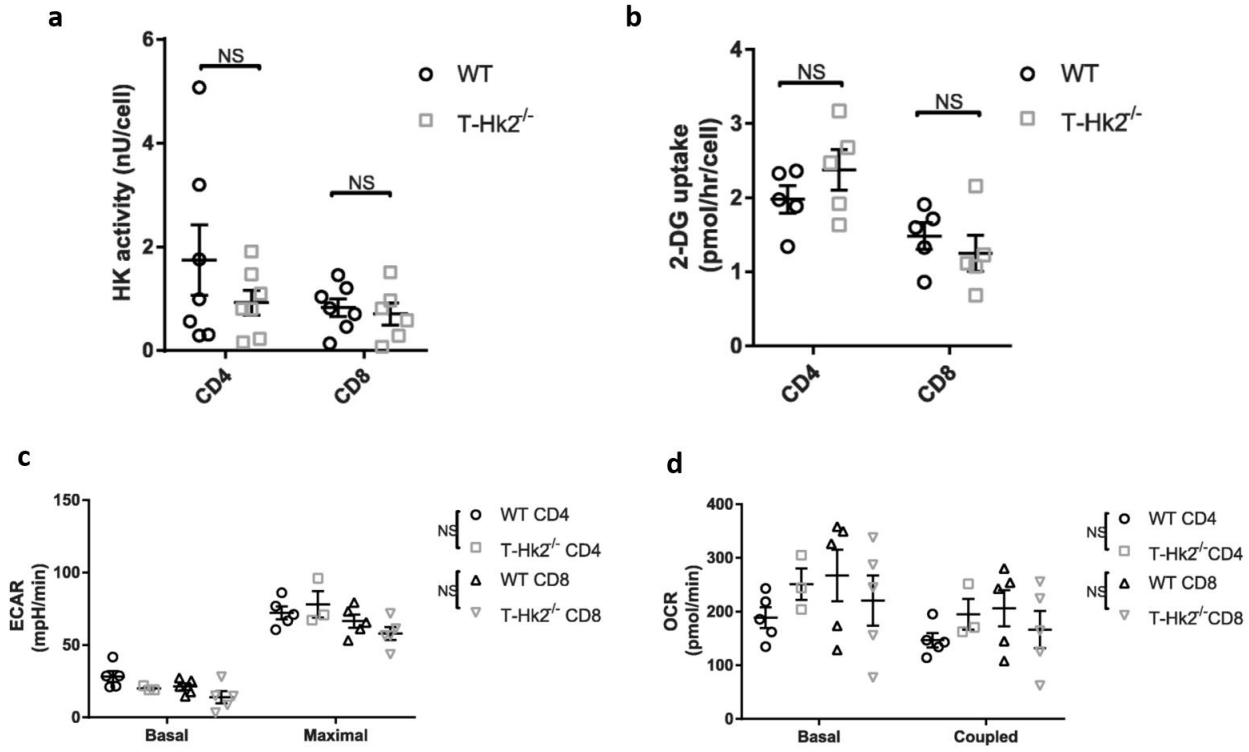

Figure 3.5 Hk2 is not necessary for T cell glucose metabolism. Purified naïve CD4+ or CD8+ T cells stimulated for 72 hr and assayed for **(A)** total HK activity, **(B)** 2-DG uptake, **(C)** extracellular acidification rate (ECAR), and **(D)** oxygen consumption rate (OCR). Biological replicates from at least 2 independent experiments. Error bars represent mean ± SEM, ANOVA with Sidak multiple comparisons, *$p < 0.05$; **$p < 0.01$. NS = not significant

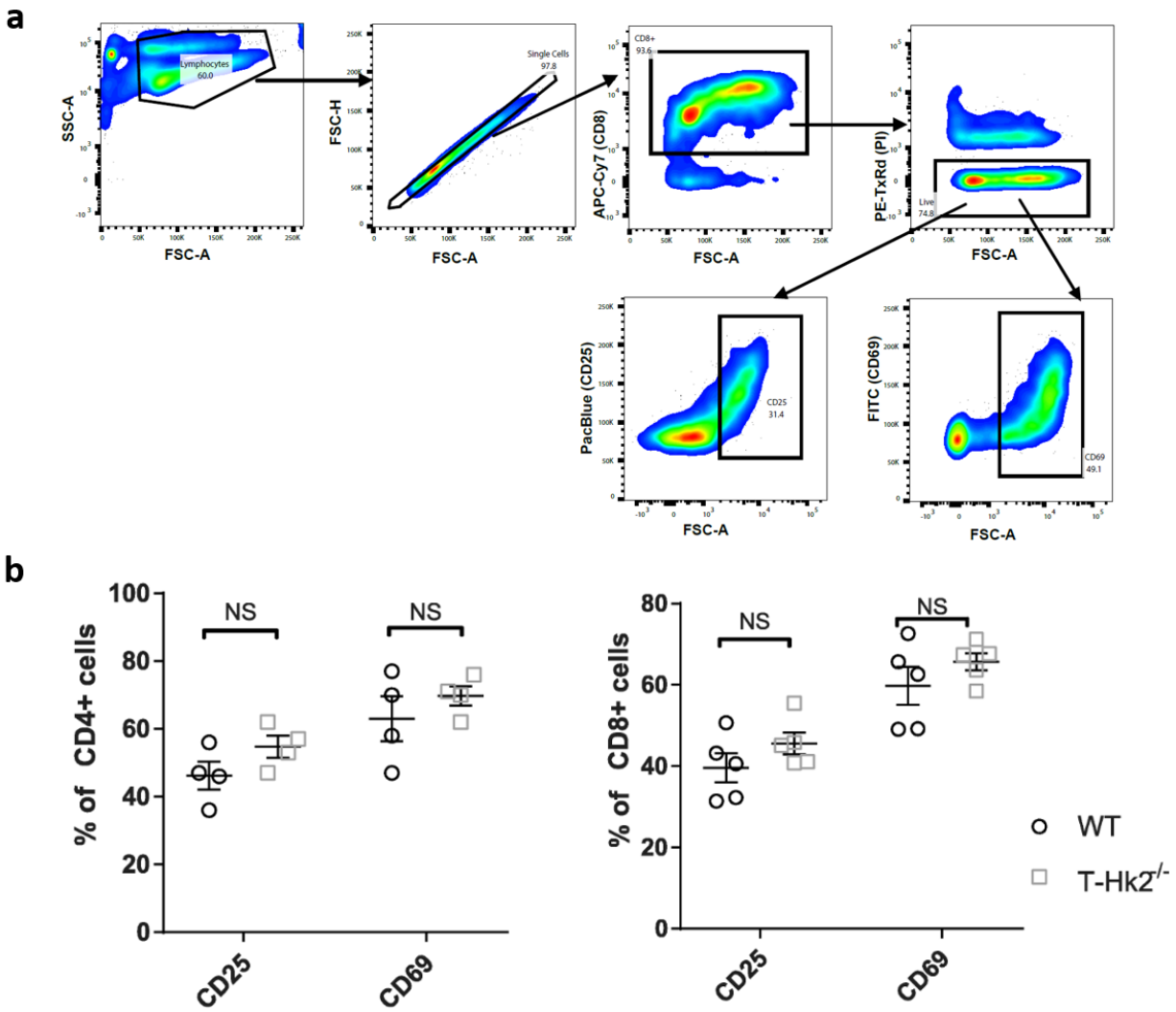

Figure 3.6. HK2 is not required for T cell activation. Naïve CD4+ and CD8+ T cells were enriched from splenocytes isolated from adult WT and T-Hk2−/− mice. T cells were activated in vitro with anti-CD3/28-coated beads for 24 hr. **(A)** Cells gated on live cells expressing CD4 or CD8. **(B)** Percent of cells positive for indicated activation markers by flow cytometry gated on CD4+ (left) or CD8+ (right) cells. Biological replicates from at least two independent experiments. Error bars represent mean ± SEM, ANOVA with Sidak multiple comparisons, *$p < 0.05$; **$p < 0.01$. NS = not significant

CFSE staining, while CD8+ T cells consistently showed a small but insignificant deficit (Figure 3.7). Together these data indicate that HK2 is not required for T cell viability, activation or proliferation in vitro.

Another important function of T cells is their ability to differentiate into specialized subsets. We tested the ability of CD4+ cells to differentiate in vitro by skewing them towards Th1, Th2, Th17, and Treg lineages. No major impairment was observed between WT and HK2 deficient T cells in any of these lineages as determined by viability and expression of lineage defining transcription factors (Figure 3.8-3.12). We also compared the steady state levels of different cell types in the spleens of WT and T-Hk2$^{-/-}$ mice. We observed no differences in percent of CD4+, CD8+, naïve (CD62L^{hi}CD44^{lo}), memory (CD44^{hi}), Th1, Th2, Th17, or Treg cells in T-Hk2$^{-/-}$ mice (Figure 3.13-3.15). Furthermore, there were no observed differences in other immune cell numbers (Figure 3.16). Together, these data demonstrate that T-Hk2$^{-/-}$ mice do not have an impairment in T cell differentiation in vitro or at steady state in vivo.

The unexpected dispensability for HK2 in vitro lead us to hypothesize that perhaps HK2 is upregulated in T cells to maintain glycolysis during conditions of low glucose availability. To this end, we activated CD4+ T cells in vitro under various glucose concentrations, from 5.5 mM (physiological blood glucose) to 0 mM. Previous work has shown that activation and viability at 24 hours should not be affected by low concentrations of glucose, but the complete absence of glucose will cause T cell death that can be rescued by pyruvate (Jacobs, Herman et al. 2008, Sena, Li et al. 2013). Consistent with previous findings, we observed a sharp decline in viability and activation in WT T cells between 0.1 mM glucose and 0 mM glucose that was restored with

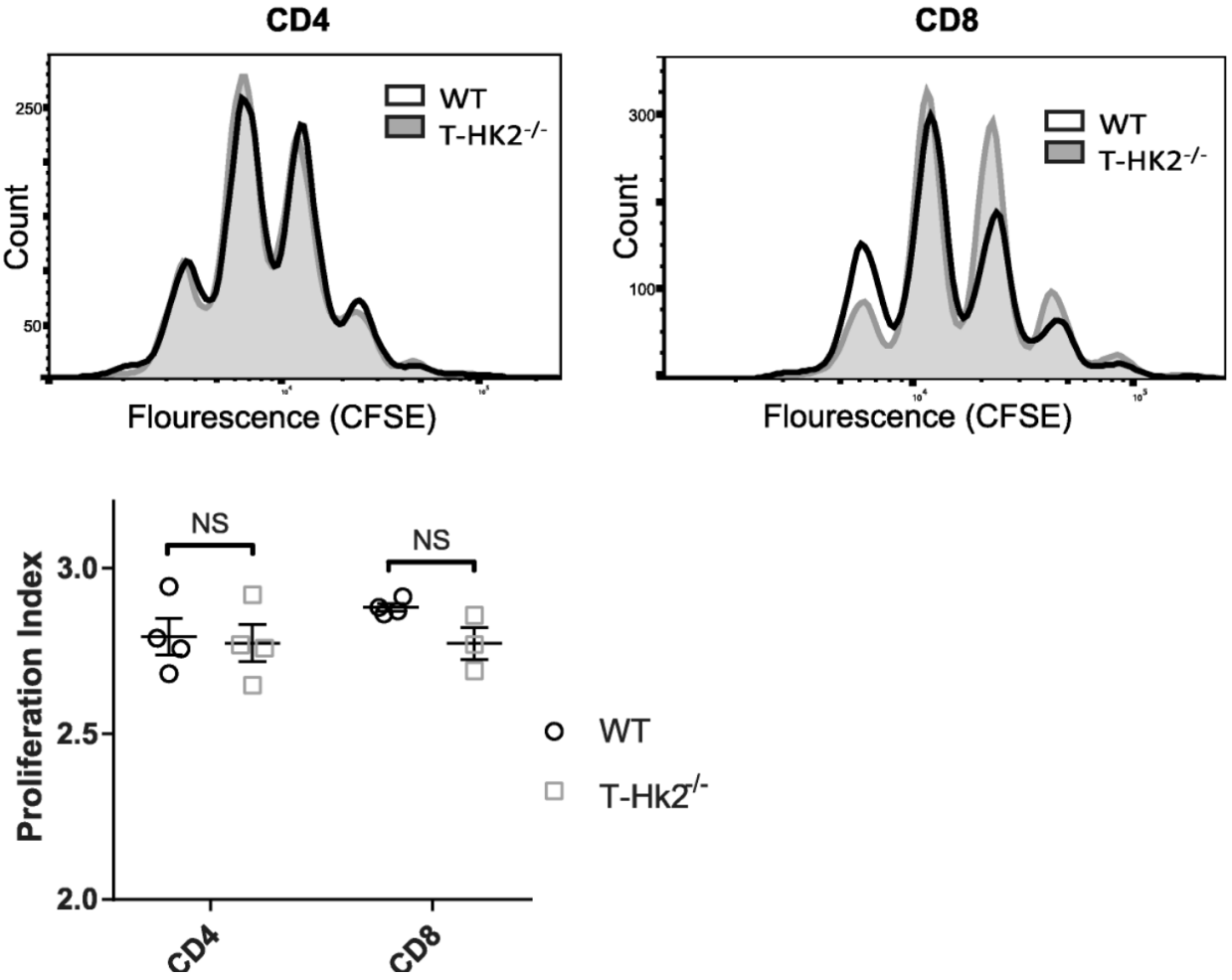

Figure 3.7. HK2 is not required for T cell proliferation. Naïve CD4+ and CD8+ T cells were enriched from splenocytes isolated from adult WT and T-Hk2−/− mice. T cells were activated in vitro with anti-CD3/28-coated beads for 72 hours after staining with CFSE. Representative images of CFSE dilution shown (top) as well as quantification (bottom). Biological replicates from at least two independent experiments. Error bars represent mean ± SEM, ANOVA with Sidak multiple comparisons, *$p < 0.05$; **$p < 0.01$. NS = not significant

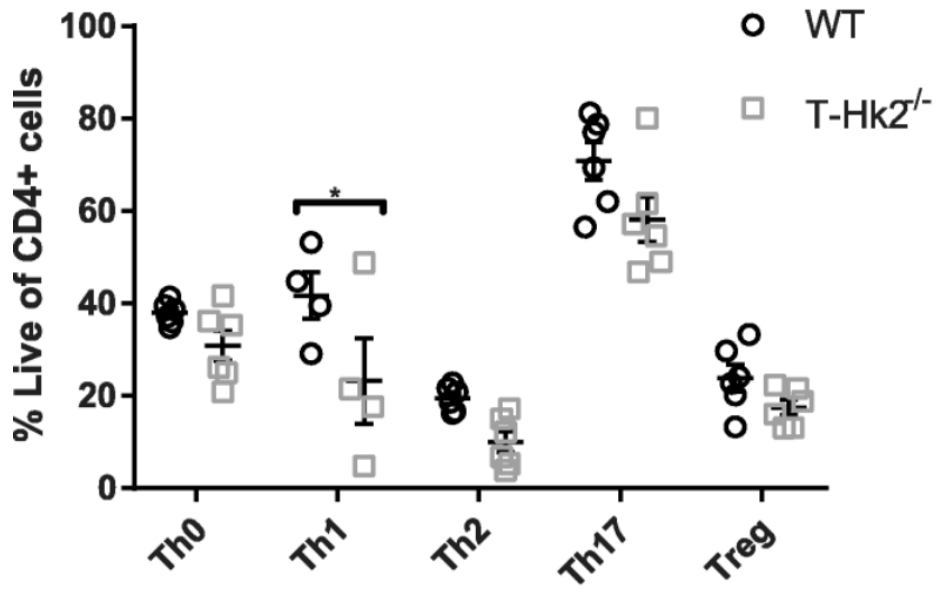

Figure 3.8. HK2 is not required for T cell viability. Naïve CD4+ T cells were enriched from splenocytes isolated from adult WT and T-Hk2−/− mice. Enriched naïve CD4+ T cells were stimulated with irradiated splenocytes under Th0, Th1, Th2, Th17, and Treg promoting conditions for 5 days. Percent of CD4+ cells excluding viability dye shown. Biological replicates from at least 2 independent experiments. Error bars represent mean ± SEM, ANOVA with Sidak multiple comparisons, *$p < 0.05$; **$p < 0.01$. NS = not significant

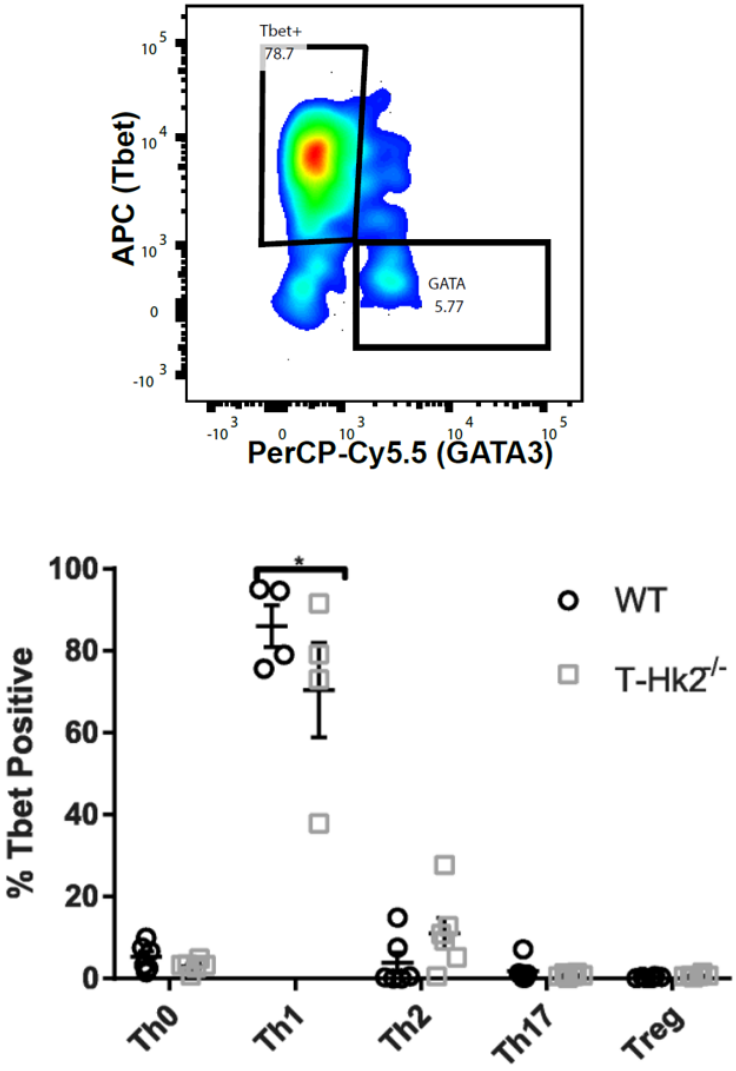

Figure 3.9. HK2 is not required for Tbet expression. Naïve CD4+ T cells were enriched from splenocytes isolated from adult WT and T-Hk2−/− mice. Enriched naïve CD4+ T cells were stimulated with irradiated splenocytes under Th0, Th1, Th2, Th17, and Treg promoting conditions for 5 days. Percent of viable CD4+ cells positive for Tbet staining shown. Biological replicates from at least 2 independent experiments. Error bars represent mean ± SEM, ANOVA with Sidak multiple comparisons, *$p < 0.05$; **$p < 0.01$. NS = not significant

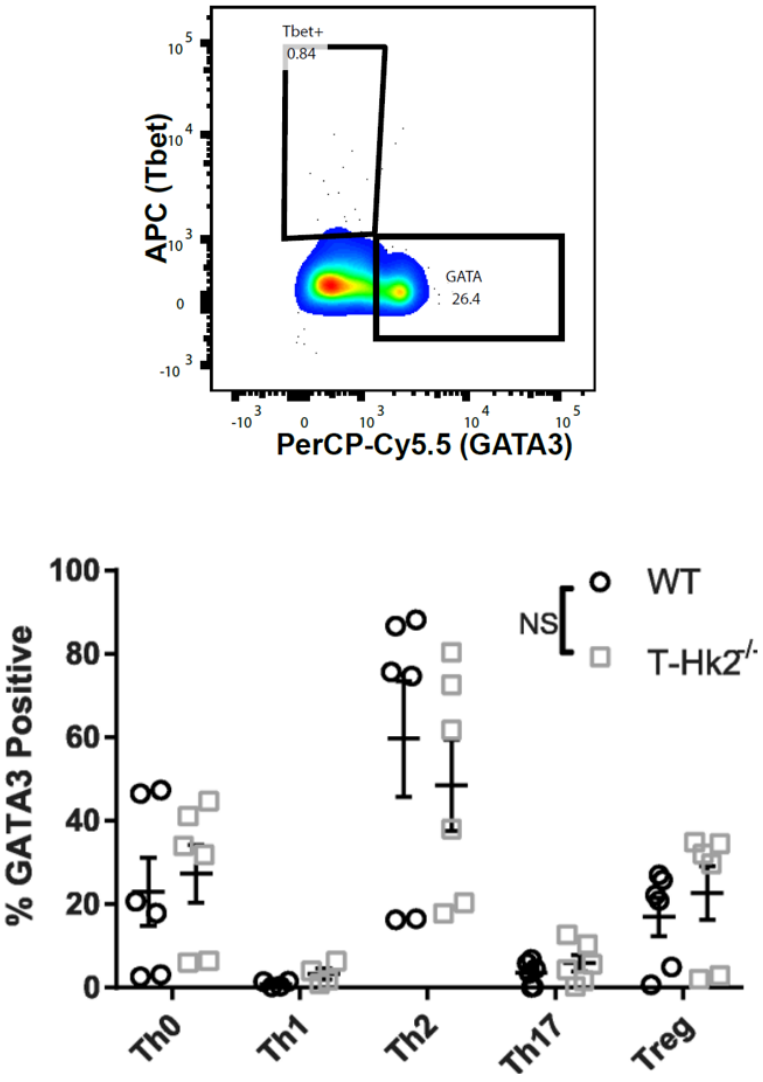

Figure 3.10. HK2 is not required for GATA3 expression. Naïve CD4+ T cells were enriched from splenocytes isolated from adult WT and T-Hk2−/− mice. Enriched naïve CD4+ T cells were stimulated with irradiated splenocytes under Th0, Th1, Th2, Th17, and Treg promoting conditions for 5 days. Percent of viable CD4+ cells positive for GATA3 staining shown. Biological replicates from at least 2 independent experiments. Error bars represent mean ± SEM, ANOVA with Sidak multiple comparisons, *$p < 0.05$; **$p < 0.01$. NS = not significant

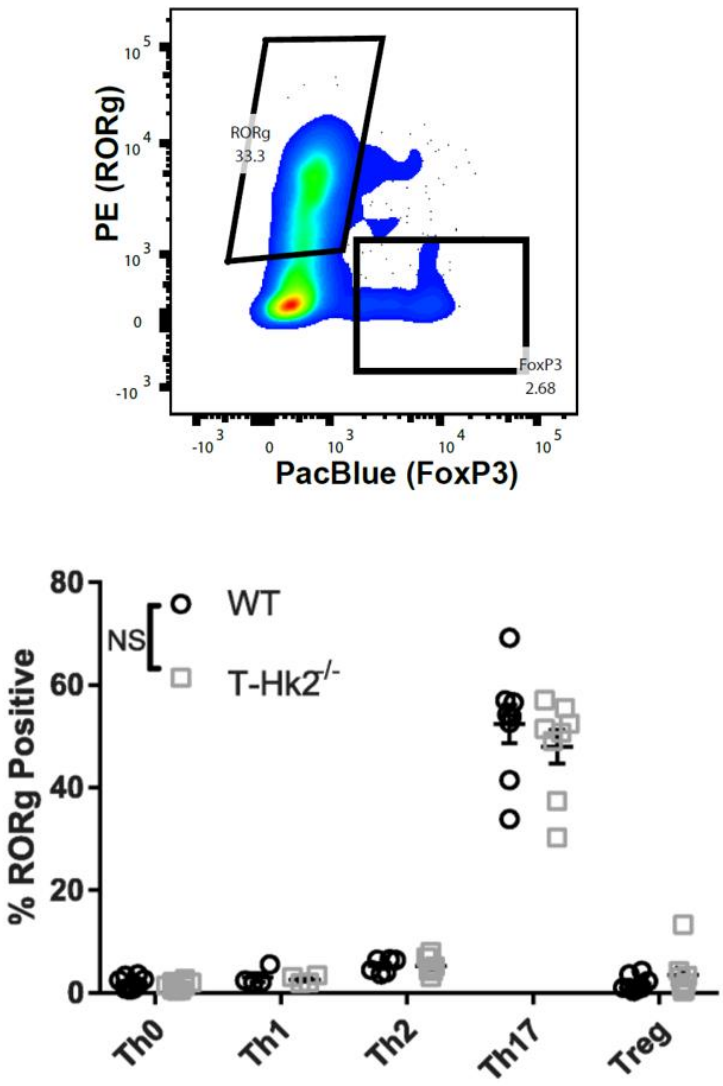

Figure 3.11. HK2 is not required for RORg expression. Naïve CD4+ T cells were enriched from splenocytes isolated from adult WT and T-Hk2−/− mice. Enriched naïve CD4+ T cells were stimulated with irradiated splenocytes under Th0, Th1, Th2, Th17, and Treg promoting conditions for 5 days. Percent of viable CD4+ cells positive for RORg staining shown. Biological replicates from at least 2 independent experiments. Error bars represent mean ± SEM, ANOVA with Sidak multiple comparisons, *$p < 0.05$; **$p < 0.01$. NS = not significant

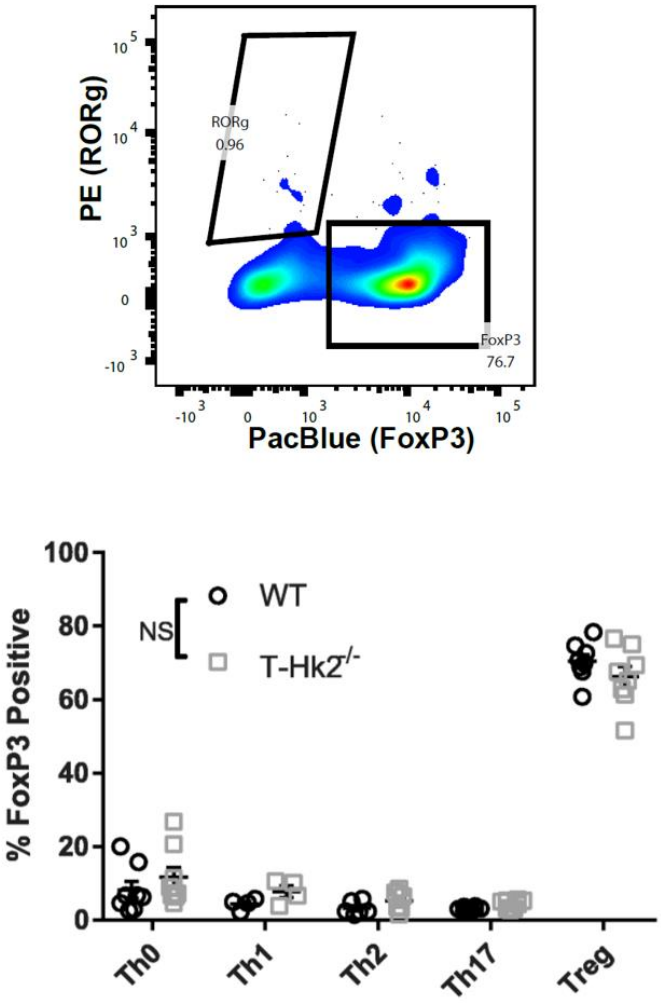

Figure 3.12. HK2 is not required for FoxP3 expression. Naïve CD4+ T cells were enriched from splenocytes isolated from adult WT and T-Hk2−/− mice. Enriched naïve CD4+ T cells were stimulated with irradiated splenocytes under Th0, Th1, Th2, Th17, and Treg promoting conditions for 5 days. Percent of viable CD4+ cells positive for FoxP3 staining shown. Biological replicates from at least 2 independent experiments. Error bars represent mean ± SEM, ANOVA with Sidak multiple comparisons, *$p < 0.05$; **$p < 0.01$. NS = not significant

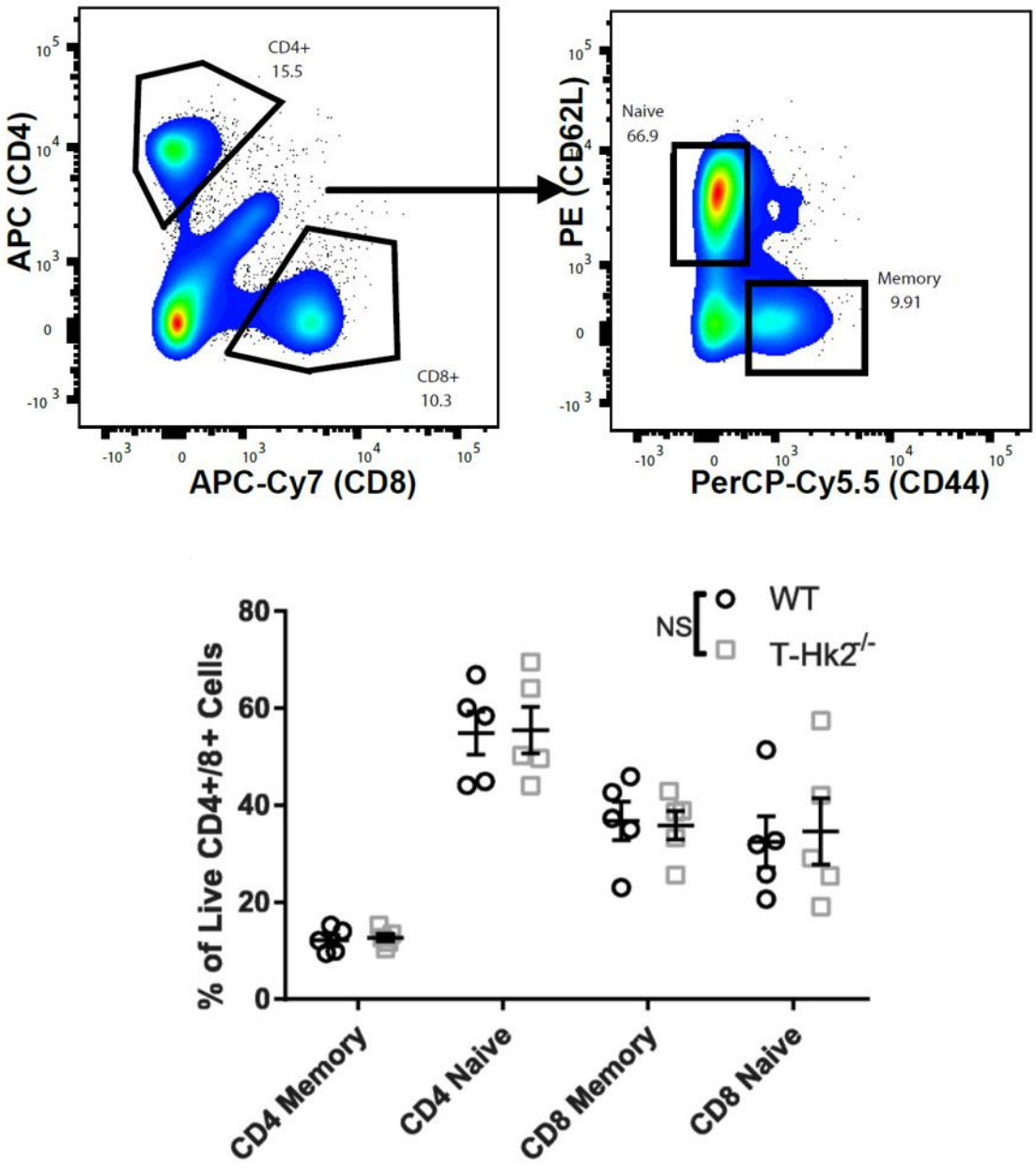

Figure 3.13. HK2 is not required for steady state memory populations. Splenocytes were isolated from 8 to 12 week old WT and T-Hk2−/− mice and stained and gated as indicated to analyze naïve and memory populations. Error bars represent mean ± SEM, ANOVA with Sidak multiple comparisons, *$p < 0.05$; **$p < 0.01$. NS = not significant

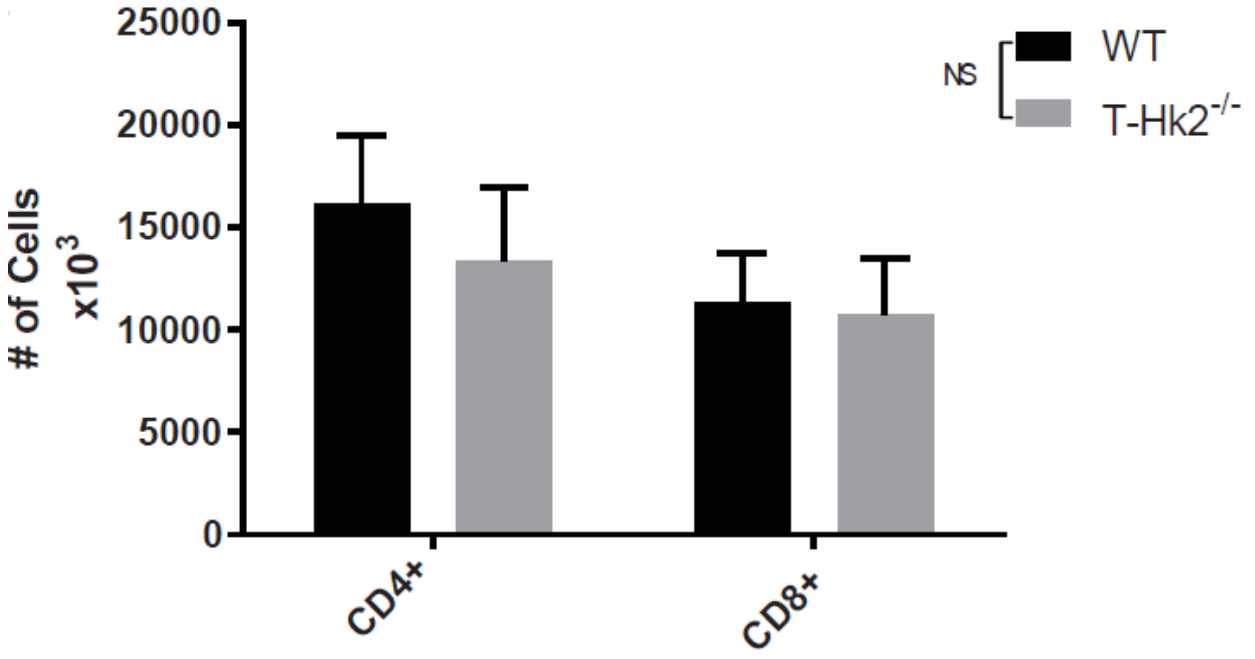

Figure 3.14. HK2 deficiency does not alter number of T cells at steady state. Splenocytes were isolated from 8 to 12 week old WT and T-Hk2−/− mice, stained for CD4+ and CD8+ cells, and counted. n=5 biological replicates. Error bars represent mean ± SEM, ANOVA with Sidak multiple comparisons, *$p < 0.05$; **$p < 0.01$. NS = not significant

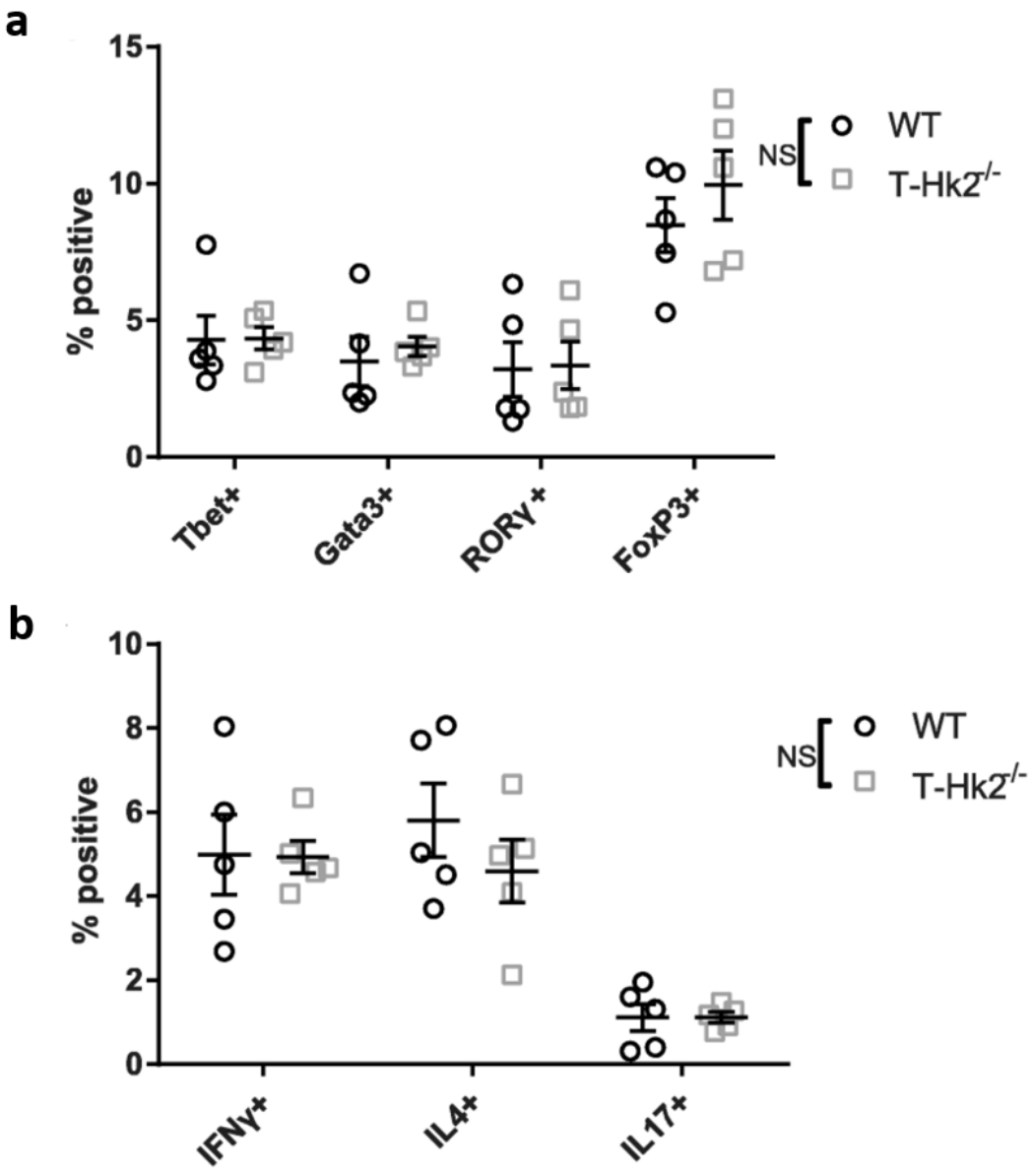

Figure 3.15. HK2 is not required for steady state CD4+ T cell subset populations.

Splenocytes were isolated from 8 to 12 week old WT and T-Hk2−/− mice to analyze percentage of viable CD4+ T cells positive for the indicated **(A)** transcription factor or **(B)** cytokine. Error bars represent mean ± SEM, ANOVA with Sidak multiple comparisons correction, *p 0.05; **p < 0.01. NS = not significant

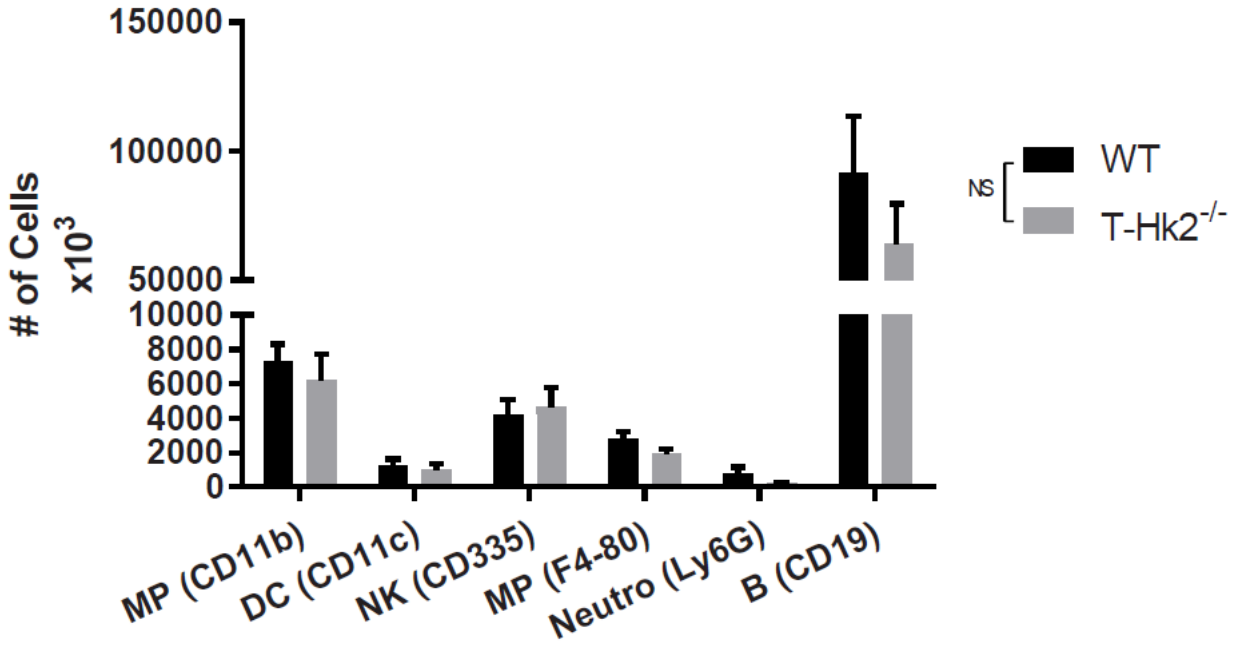

Figure 3.16. HK2 is not required for steady state immune cell populations. Splenocytes were isolated from 8 to 12 week old WT and T-Hk2−/− mice to analyze steady state levels of various populations by indicated marker, n = 5 mice. MP = macrophage, DC = dendritic cell, NK = natural killer cell, Neutro = neutrophil. Error bars represent mean ± SEM, ANOVA with Sidak multiple comparisons correction, *$p < 0.05$; **$p < 0.01$. NS = not significant

1 mM pyruvate (Figure 3.17). Remarkably, HK2 deficient T cells exhibited an identical response to glucose concentrations as WT T cells (Figure 3.17). Similarly, WT and HK2 deficient T cells stimulated for 3 days under varying concentrations of glucose showed comparable viability, proliferation as measured by CFSE proliferation index, and proliferation as measured by cell number (Figure 3.18). These data demonstrate that Hk2 is dispensable in vitro for T cell viability, activation, and proliferation even under limiting glucose levels.

HK2 deficiency mildly reduces T cell mediated inflammation in vivo

It is possible that though we did not see any differences in vitro from loss of HK2, there could be differences in vivo in T-Hk2$^{-/-}$ mice under inflammatory conditions. We tested whether HK2 deficiency in T cells would impair T cell mediated inflammation by using a mouse model of colitis driven by IL-10 deficiency. IL10$^{-/-}$ mice spontaneously develop colitis in a T cell dependent manner thought to be driven by Th1 and Th17 cytokine producing cells (Kuhn, Lohler et al. 1993, Berg, Davidson et al. 1996, Chichlowski, Sharp et al. 2008, Hoshi, Schenten et al. 2012). We generated Hk2$^{fl/fl}$;CD4-cre^{+};IL-10$^{-/-}$ mice that were globally deficient in IL-10 and had a T cell specific HK2 deficiency (herein referred to as IL-10$^{-/-}$; T-Hk2$^{-/-}$). IL-10$^{-/-}$ mice and IL-10$^{-/-}$;T-Hk2$^{-/-}$ mice both developed mild colitis marked by lymphocytic infiltrate in the colon, a failure to gain weight, splenomegaly, and rectal prolapse (Figure 3.19-3.21). IL-10 sufficient littermate control mice showed no signs of disease. Interestingly, IL-10$^{-/-}$;T-Hk2$^{-/-}$ mice developed spontaneous rectal prolapse at a significantly lower rate than IL-10$^{-/-}$ mice, though weight change and splenomegaly were similar between the two (Figure 3.19-3.20). To further investigate differences in the inflammation between IL-10$^{-/-}$ mice and IL-10$^{-/-}$;T-Hk2$^{-/-}$ mice, we analyzed tissues by flow cytometry which showed increase cellularity in the mesenteric lymph

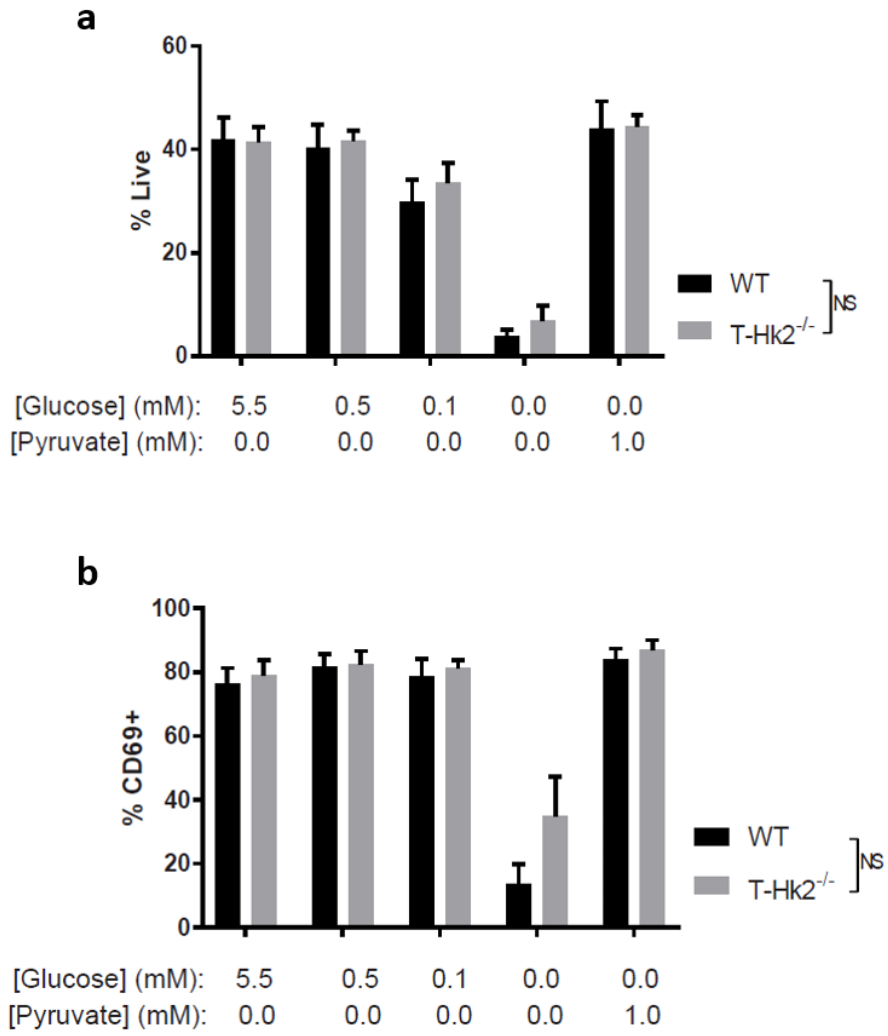

Figure 3.17. HK2 is dispensable for T cell activation under low glucose conditions. Naïve CD4+ and T cells were enriched from splenocytes isolated from adult WT and T-Hk2−/− mice. T cells were activated in vitro with anti-CD3/CD28 coated beads for 24 hours under indicated glucose and pyruvate concentrations. (A) Percent of CD4+ cells positive for viability and (B) percent of viable CD4+ cells expressing CD69 by flow cytometry. Biological replicates, n = 6, from 3 independent experiments. Error bars represent mean ± SEM, ANOVA with Sidak multiple comparisons correction, *$p < 0.05$; **$p < 0.01$. NS = not significant

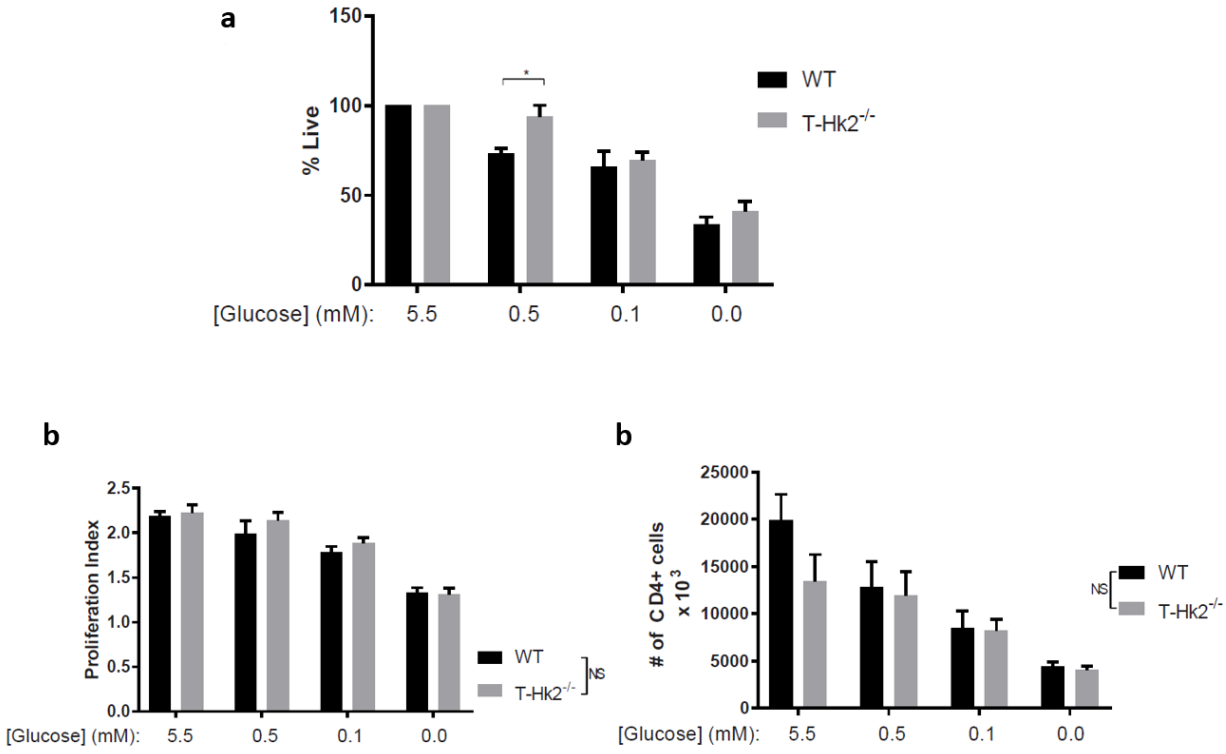

Figure 3.18. HK2 is dispensable for T cell proliferation under low glucose conditions. Naïve CD4+ and T cells were enriched from splenocytes isolated from adult WT and T-Hk2−/− mice. T cells were activated in vitro with anti-CD3/CD28 coated beads for 72 hours under indicated glucose conditions and 1 mM pyruvate. CD4+ T cells analyzed by flow cytometry for **(A)** percent of cells positive for viability, **(B)** proliferation as measured by CFSE dilution, and **(C)** proliferation as measured by cell number. Biological replicates, n = 4 WT, 5 T-Hk2−/− from 2 independent experiments. Error bars represent mean ± SEM, ANOVA with Sidak multiple comparisons correction, *$p < 0.05$; **$p < 0.01$. NS = not significant

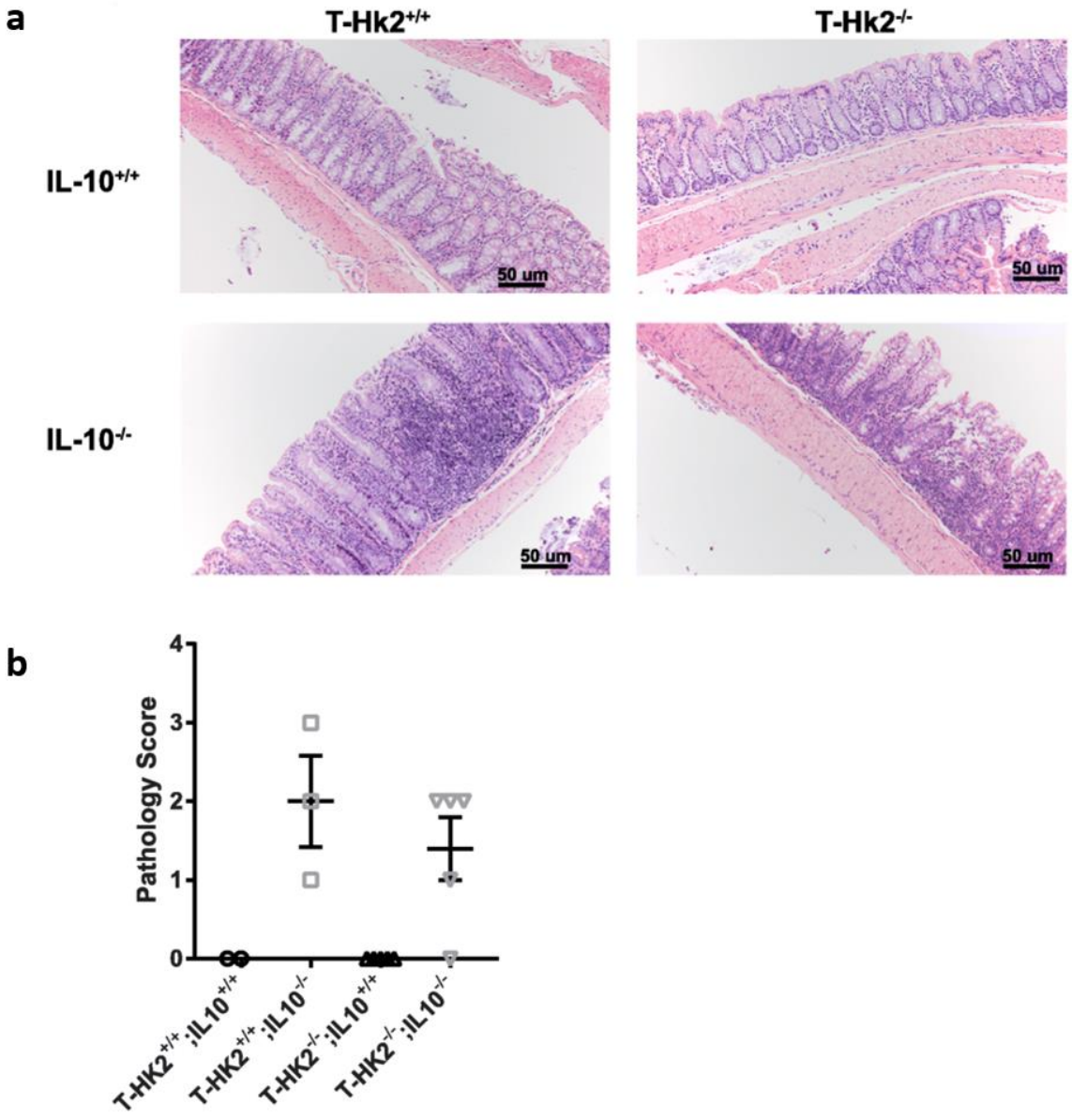

Figure 3.19. IL10 deficiency induces colitis. T-Hk2−/− mice were crossed to IL10−/− mice to induce colitis. Mice were euthanized at approximately 13–15 weeks of age or earlier if required due to weight loss or rectal prolapse. (A) Histology of mouse colon. (B) Scoring of pathological inflammation.

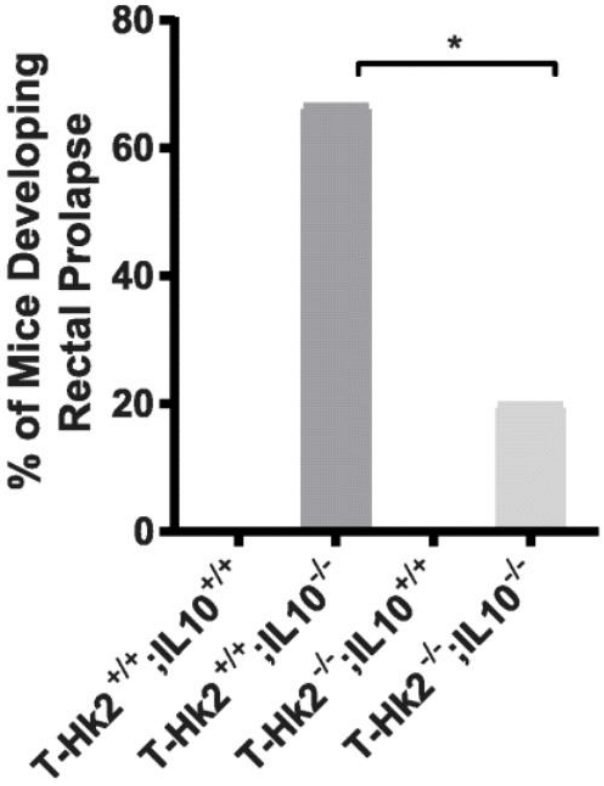

Figure 3.20. HK2 deficiency reduces rectal prolapse in IL-10 mediated colitis. T-Hk2−/− mice were crossed to IL10−/− mice to induce colitis. Mice were euthanized at approximately 13–15 weeks of age or earlier if required due to weight loss or rectal prolapse. Percentage of mice developing rectal prolapse shown. Chi-squared test. n = 4, 12, 10, 10 mice (left to right).

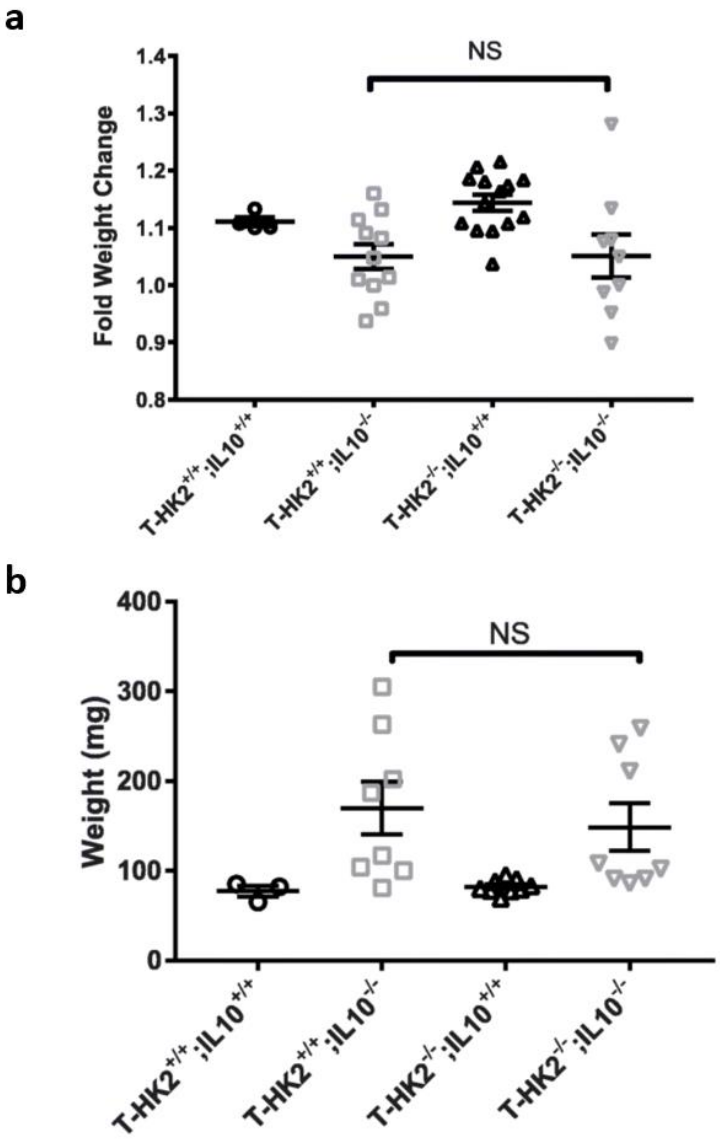

Figure 3.21. HK2 deficiency does not affect weight loss or splenomegaly in IL-10 colitis. T-Hk2−/− mice were crossed to IL10−/− mice to induce colitis. Mice were euthanized at approximately 13–15 weeks of age or earlier if required due to weight loss or rectal prolapse. **(A)** Fold change in weight between week 9 and euthanasia. **(B)** Spleen weight. Biological replicates, error bars represent mean ± SEM, ANOVA with Sidak multiple comparisons correction, *$p < 0.05$; **$p < 0.01$. NS = not significant

nodes and lamina propria of both IL10$^{-/-}$ mice and IL-10$^{-/-}$;T-Hk2$^{-/-}$ when compared to IL10$^{+/+}$ mice (Figure 3.22-3.23). There were no observed differences in CD4+, CD8+, CD69+, IFNγ +, IL17+, or FoxP3+ cell numbers in the mesenteric lymph nodes of IL10$^{-/-}$ mice and IL-10$^{-/-}$;T-Hk2$^{-/-}$ mice (Figure 3.22). However, there was a mild decrease in CD4+ T cells in the lamina propria of IL-10$^{-/-}$;T-Hk2$^{-/-}$ mice (Figure 3.23). Overall these data indicate that IL-10$^{-/-}$;T-Hk2$^{-/-}$ develop colitis, but with a lower severity than IL10$^{-/-}$ mice.

We also tested the necessity of HK2 in a mouse model of Th2 lung inflammation by sensitizing WT and T-Hk2$^{-/-}$ mice with ovalbumin/aluminum hydroxide (OVA/alum) and provoking airway inflammation subsequently with aerosolized OVA. Inflammation in the airway in response to OVA is known to be a Th2 driven process with a Th17 component (Afshar, Medoff et al. 2008). Non-sensitized WT and T-Hk2$^{-/-}$ mice lacked any pulmonary inflammation after challenge with OVA while both WT and T-Hk2$^{-/-}$ sensitized mice developed significant inflammation (Figure 3.24). Bronchoalveolar lavage after OVA challenge showed both WT and T-Hk2$^{-/-}$ mice had an increase in BAL cellularity when compared to mice that were not previously sensitized (Figure 3.25). Absolute levels of T cells and Eosinophils were increased in the BAL of both WT and Hk2$^{-/-}$ mice, but T-Hk2$^{-/-}$ mice had a small decrease in eosinophils when compared to WT mice (Figure 3.25). Th2 cytokines in the BAL were increased in both WT and T-Hk2$^{-/-}$ mice (Figure 3.26). While T-Hk2$^{-/-}$ mice had cytokine levels that trended downward compared to WT mice, the decrease was not statistically significant. Whole lung RNA cytokine levels showed similar results with a significant increase in Th2 and Th17 cytokines in both WT and T-Hk2$^{-/-}$ mice when compared to unsensitized mice; IFNγ, a Th1 cytokine, was not increased (Figure 3.27). Furthermore, similar to BAL levels, RNA levels showed a descending trend in cytokine levels

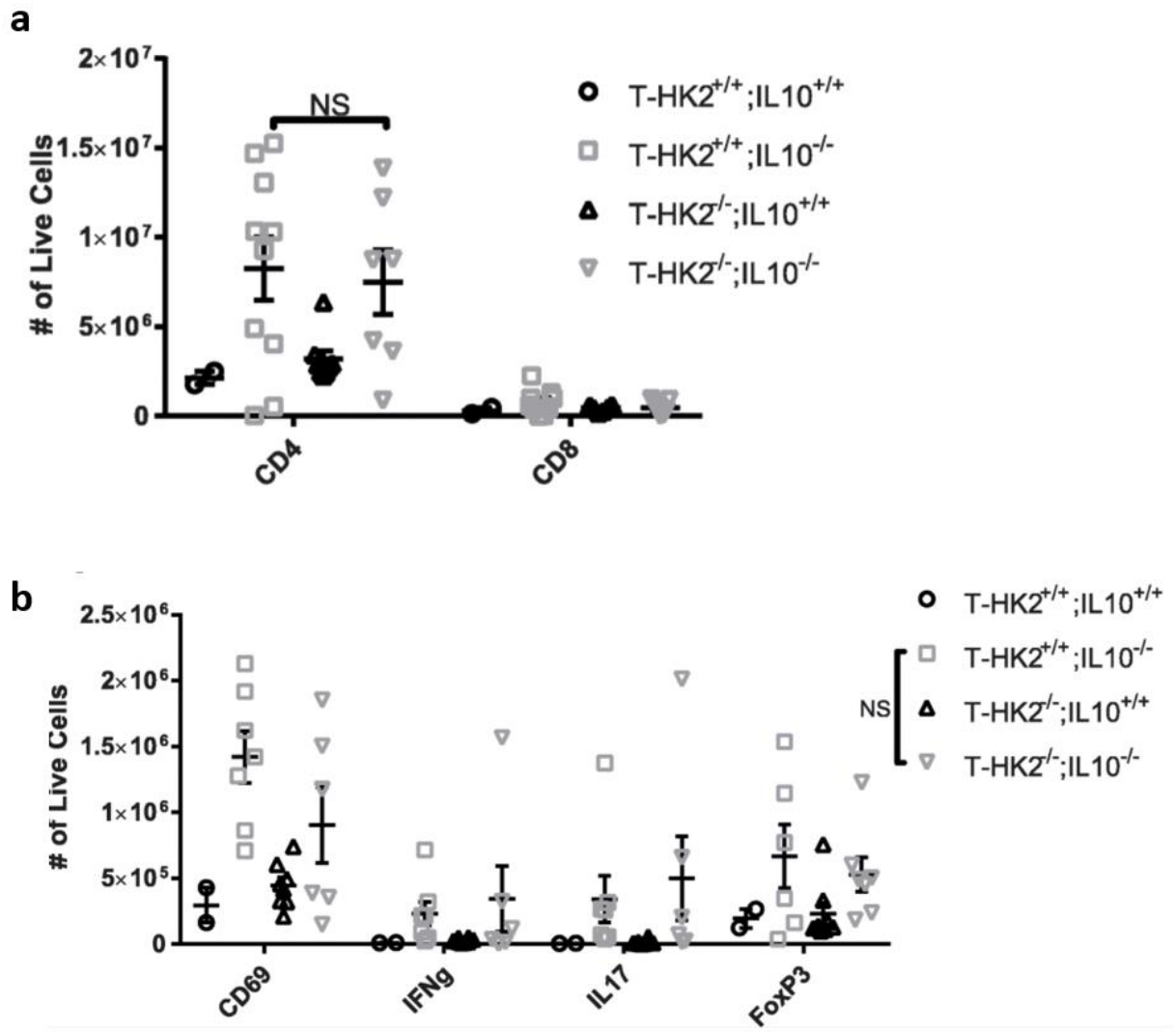

Figure 3.22. HK2 deficiency does not impair lymph node inflammation in IL-10 colitis. T-Hk2−/− mice were crossed to IL10−/− mice to induce colitis. Mice were euthanized at approximately 13–15 weeks of age or earlier if required due to weight loss or rectal prolapse. Total number of indicated cell type isolated from mesenteric lymph nodes. Biological replicates, error bars represent mean ± SEM, ANOVA with Sidak multiple comparisons correction, *$p < 0.05$; **$p < 0.01$. NS = not significant. Data generated with help of Elizabeth Steinert.

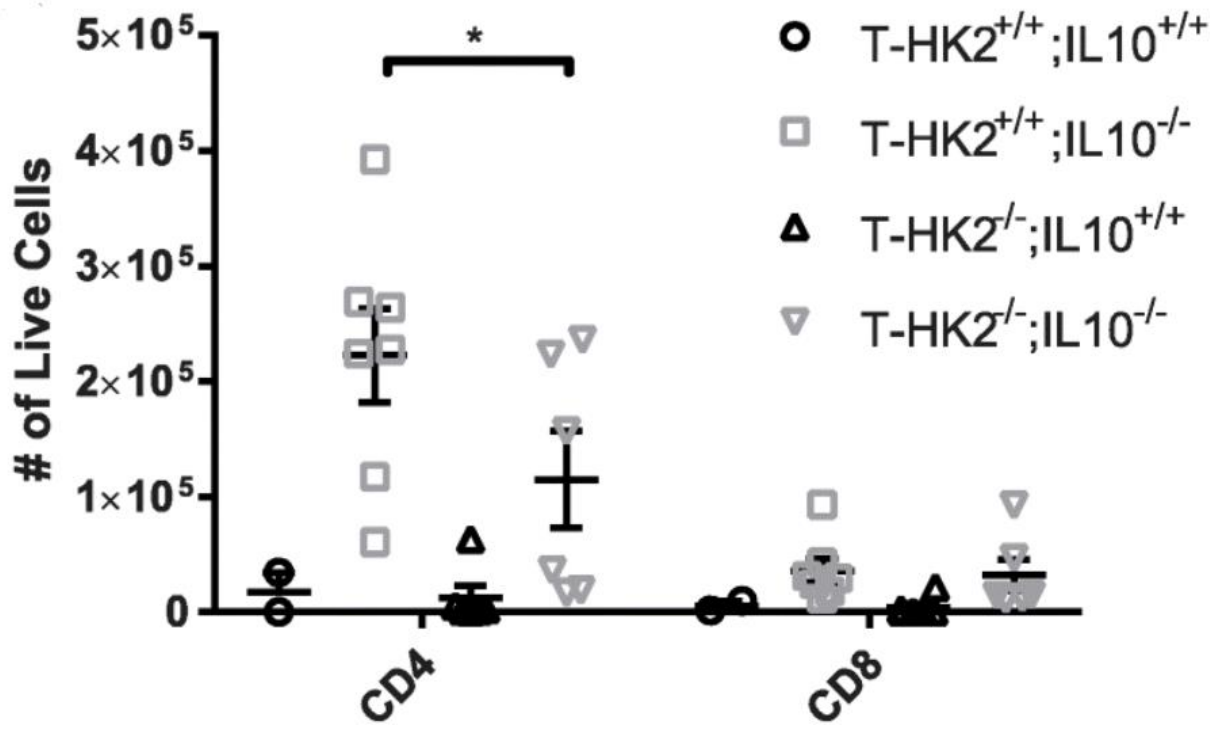

Figure 3.23. HK2 deficiency reduces lamina propria inflammation in IL-10 colitis. T-Hk2−/− mice were crossed to IL10−/− mice to induce colitis. Mice were euthanized at approximately 13–15 weeks of age or earlier if required due to weight loss or rectal prolapse. Total number of indicated cell type isolated from colon lamina propria. Biological replicates, error bars represent mean ± SEM, ANOVA with Sidak multiple comparisons correction, *$p < 0.05$; **$p < 0.01$. NS = not significant. Data generated with help of Elizabeth Steinert.

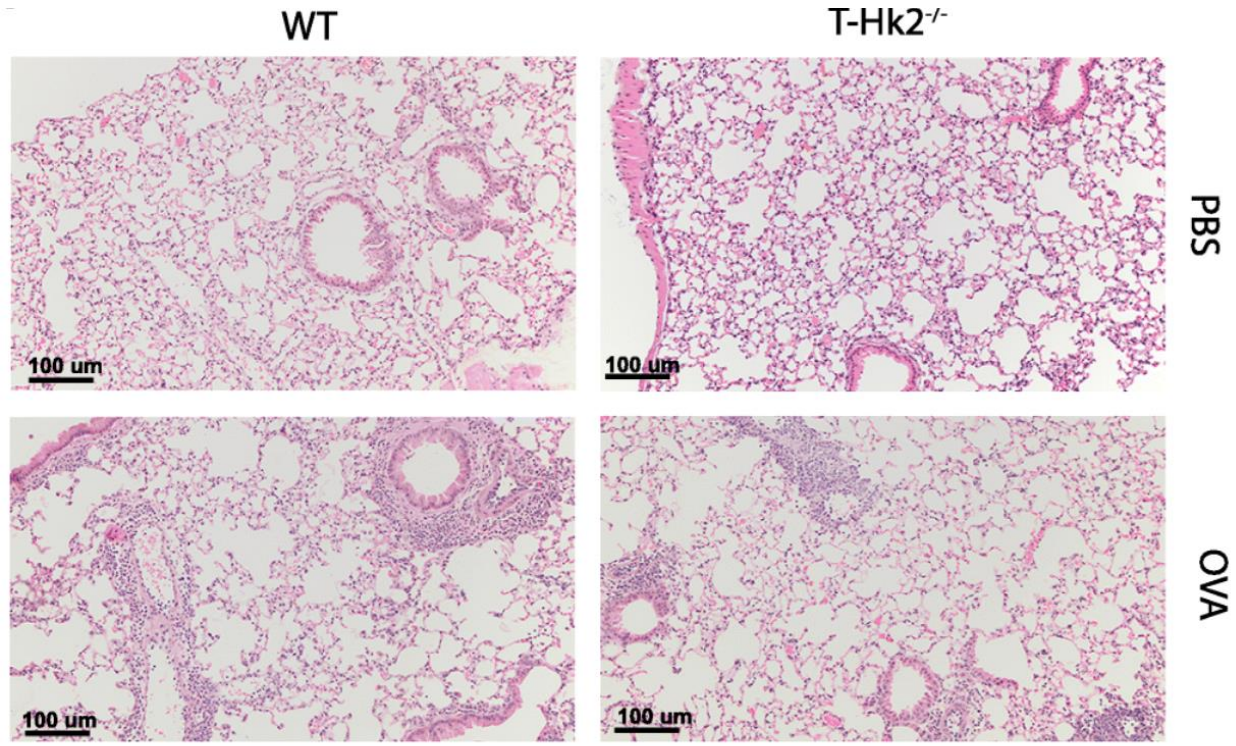

Figure 3.24. OVA induces inflammation in lungs of OVA-sensitized mice. Six to eight-week old WT and T-Hk2−/− mice were pre-sensitized to OVA twice, 14 days apart with intraperitoneal injection of OVA/alum or PBS/alum. Twenty-one days after initial pre-sensitization, mice were challenged with aerosolized OVA daily for 3 days. Mice were euthanized for analysis on the fourth day. H&E staining of lung tissue shown, representative of 4 biological replicates. Data generated with help of Krishan Chhiba.

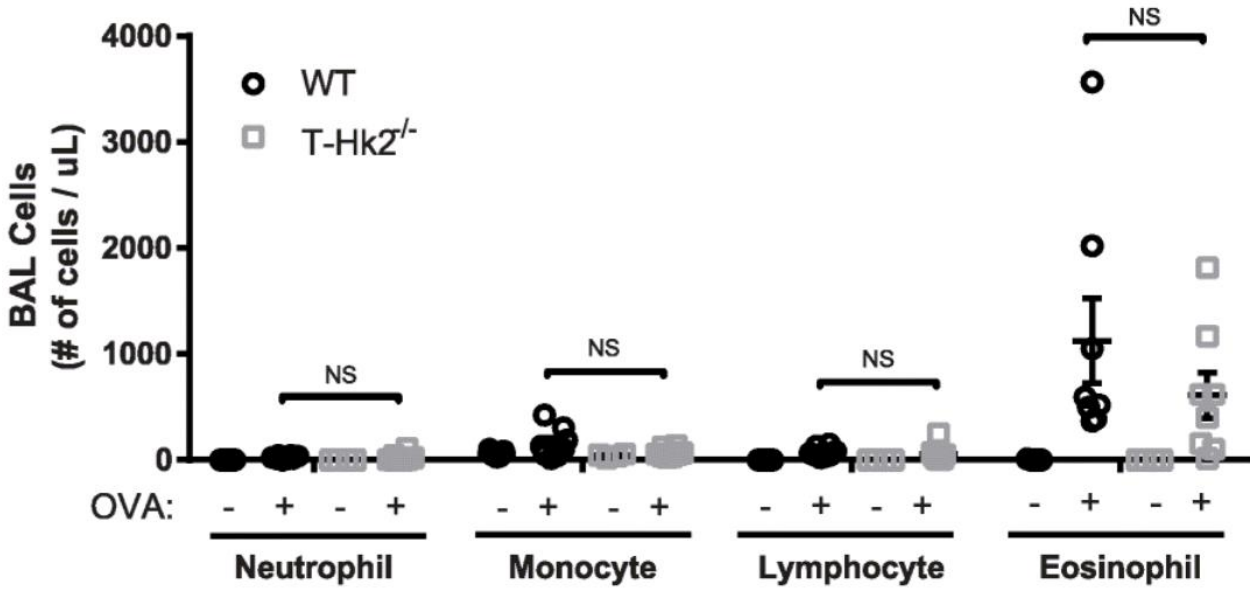

Figure 3.25. HK2 is not essential for inflammation in OVA-induced inflammation. WT and T-Hk2−/− mice were pre-sensitized to OVA/alum or PBS/alum. After aerosolized OVA challenge, brochoalveolar lavage fluid was analyzed for cellular infiltrate. Multiple t tests with Holm-Sidak correction for multiple comparisons. Biological replicates, error bars represent mean ± SEM, *$p < 0.05$; **$p < 0.01$. NS = not significant. Data generated with help of Krishan Chhiba.

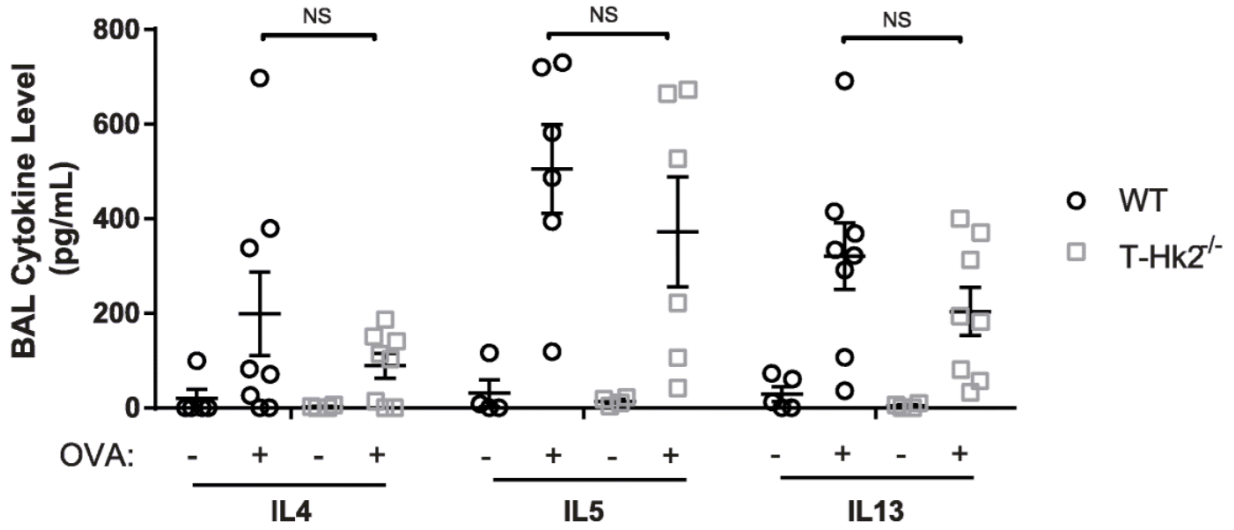

Figure 3.26. HK2 is not essential for cytokine production in OVA-induced inflammation. WT and T-Hk2−/− mice were pre-sensitized to OVA/alum or PBS/alum. After aerosolized OVA challenge, brochoalveolar lavage fluid was analyzed for cytokines by ELISA. Multiple t tests with Holm-Sidak correction for multiple comparisons. Biological replicates, error bars represent mean ± SEM, *$p < 0.05$; **$p < 0.01$. NS = not significant. Data generated with help of Krishan Chhiba.

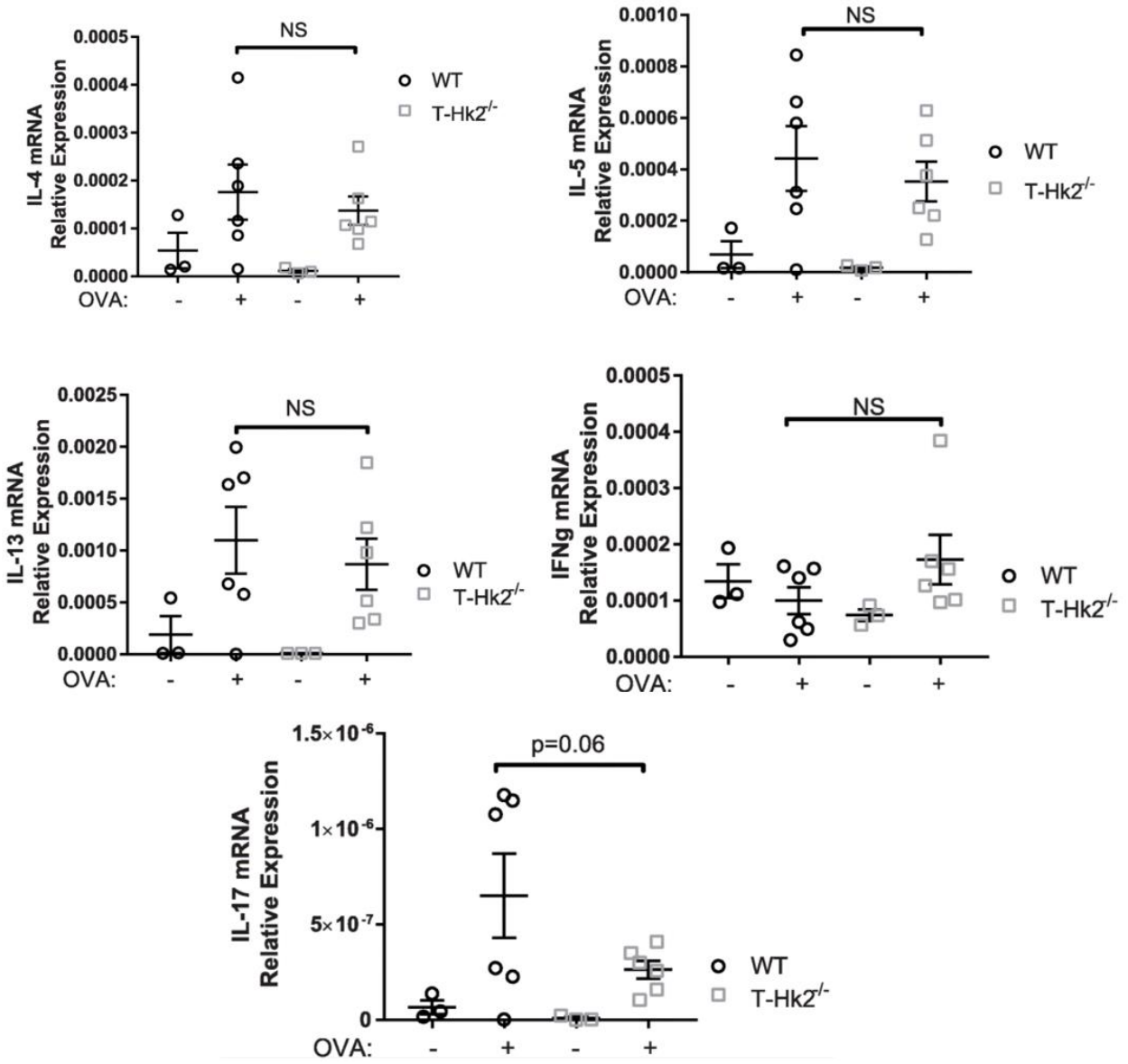

Figure 3.27. HK2 is not essential for cytokine RNA in OVA-induced inflammation. WT and T-Hk2−/− mice were pre-sensitized to OVA/alum or PBS/alum. After aerosolized OVA challenge, whole lung RNA was isolated and evaluated for expression of indicated cytokines relative to β-actin. Biological replicates, error bars represent mean ± SEM, ANOVA with Sidak multiple comparisons correction, *$p < 0.05$; **$p < 0.01$. NS = not significant. Data generated with help of Krishan Chhiba.

when comparing T-Hk2$^{-/-}$ mice to WT mice. However, again the decrease in cytokine levels of T-Hk2$^{-/-}$ mice was not statistically significant, though the decrease in IL-17 approached significance (p=0.06). Taken together, these results indicate that Hk2 is not strictly required for development of Th2 inflammation, but its presence may modulate the extent of inflammation.

HK2 is not required for T cell mediated viral immunity

To test the role of HK2 in viral immunity, we infected T-Hk2$^{-/-}$ mice intraperitoneally with lymphocytic choriomeningitis virus (LCMV). Rapid clearance of the virus after acute infection requires function of CD8+ T cells and maintenance of a LCMV-specific memory population requires CD4+ and CD8+ T cell function (Fung-Leung, Kundig et al. 1991, Shedlock and Shen 2003). As we observed a small difference in proliferation of CD8+ T cells in vitro, we hypothesized there could be a defect in the anti-viral proliferative response, but T-Hk2$^{-/-}$ mice show an antigen specific CD8+ T cell expansion following infection with LCMV identical to that of WT mice; CD8+ T cells expand rapidly and then slowly contract (Figure 3.28A). However, the percentage of CD8+ cells specific for the gp33 epitope of LCMV in the blood lags in T-Hk2$^{-/-}$ mice compared to WT mice at 5 days post-infection (DPI), though it catches up by 8 DPI and remains at comparable levels for at least 60 days (Figure 3.28B). Notably, the T-Hk2$^{-/-}$ mice memory population expands and contracts just as the respective population in WT mice (Figure 3.28C). Numbers of antigen specific memory cells in the spleen are also similar between WT and T-Hk2$^{-/-}$ mice at 60 DPI (Figure 3.29) and T-Hk2$^{-/-}$ mice were able to clear infection by 8 DPI just as WT mice and had a similar viral load at 3 DPI (Figure 3.30). Furthermore, antigen specific memory cells at 60 DPI are also functional, as they retain their ability to secrete IFNγ and TNFα following restimulation with exogenous gp33 peptide (Figure 3.31).

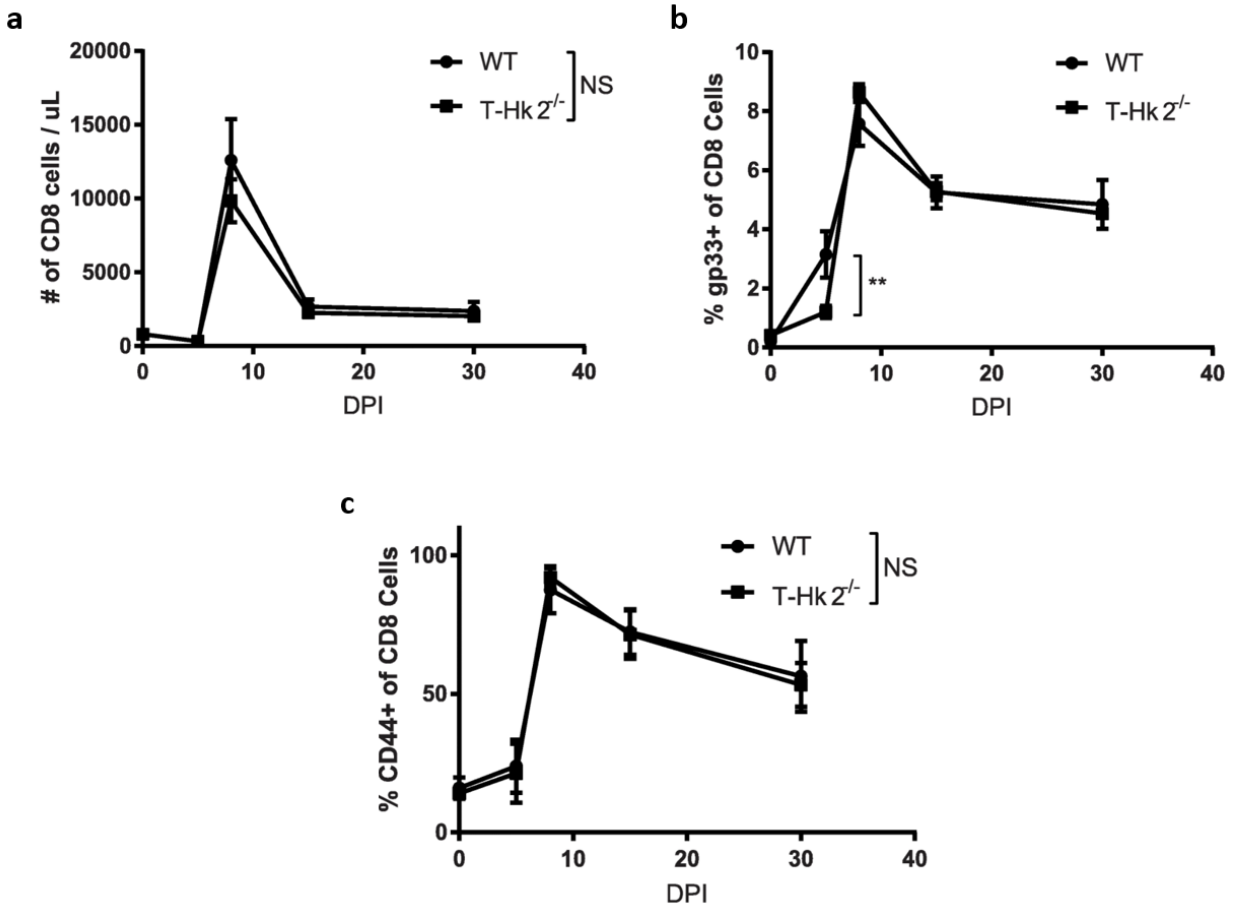

Figure 3.28. HK2 is not required for T cell expansion in LCMV infection. Eight to twelve-week old WT and T-Hk2−/− mice were injected intraperitoneally with 2×10^5 pfu LCMV. Peripheral blood was monitored at indicated time points by flow cytometry. **(A)** Number of CD8+ cells. **(B)** Percentage of CD8+ cells positive for gp-33 tetramer (D(b)/LCMV.GP33.KAVYNFATM) or **(C)** CD44. Biological replicates, error bars represent mean ± SEM, ANOVA (repeated measures) with Sidak multiple comparisons correction, *$p < 0.05$; **$p < 0.01$. NS = not significant, DPI = days post infection

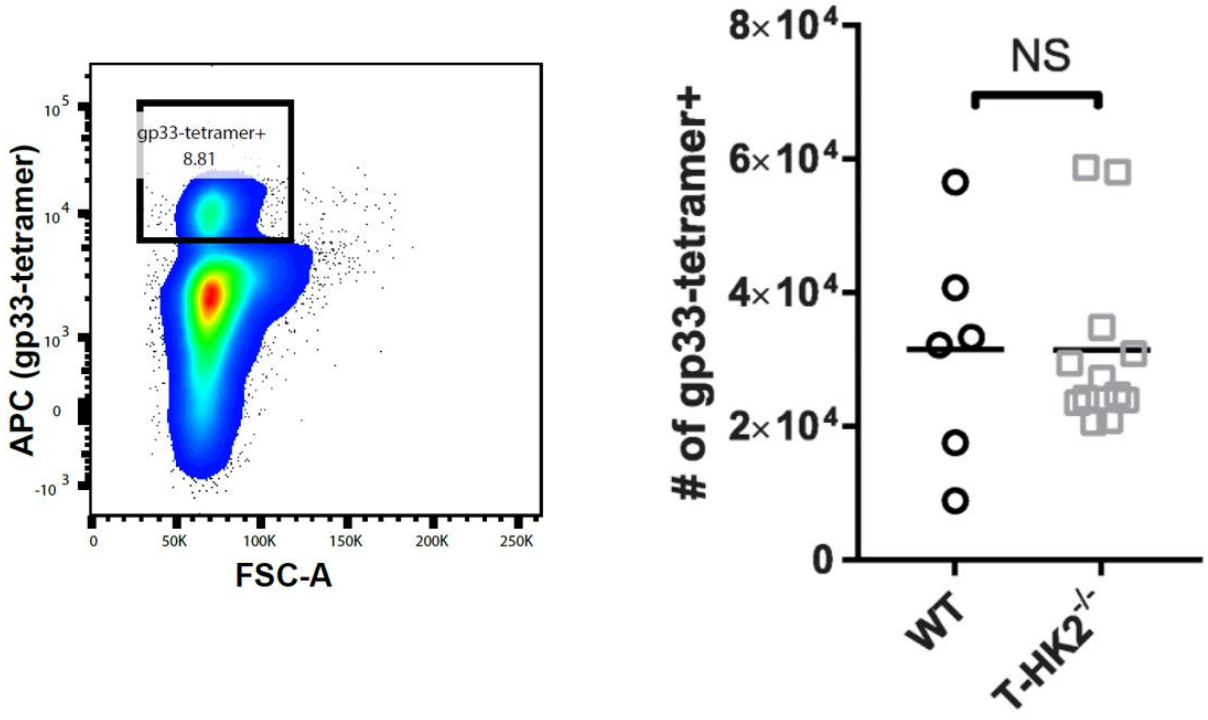

Figure 3.29. HK2 is not required for maintenance of antigen specific cells. Eight to twelve-week old WT and T-Hk2−/− mice were injected intraperitoneally with 2×10^5 pfu LCMV. Number of gp33-tetramer+ CD8+ T cells in spleen of WT and T-Hk2−/− mice at 60 DPI. Biological replicates, error bars represent mean ± SEM, ANOVA with Sidak multiple comparisons correction, *$p < 0.05$; **$p < 0.01$. NS = not significant, DPI = days post infection

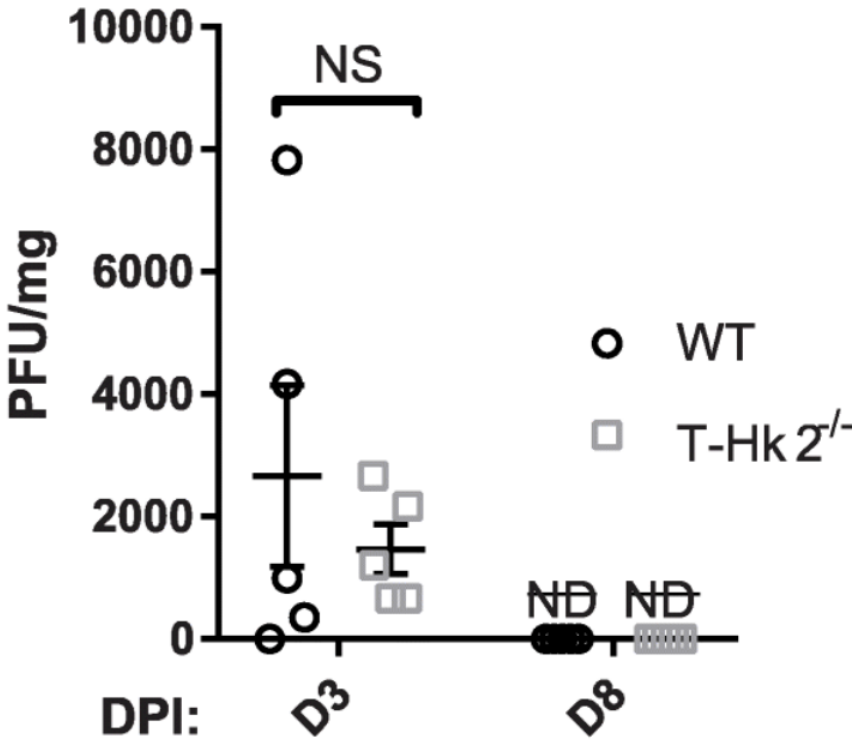

Figure 3.30. HK2 is not required for clearance of LCMV infection. Eight to twelve-week old WT and T-Hk2−/− mice were injected intraperitoneally with 2×10^5 pfu LCMV. Viral load as measured by plaque assay from right lobe of liver from 3 and 8 DPI. Biological replicates, error bars represent mean ± SEM, ANOVA with Sidak multiple comparisons correction, *$p < 0.05$; **$p < 0.01$. NS = not significant, DPI = days post infection

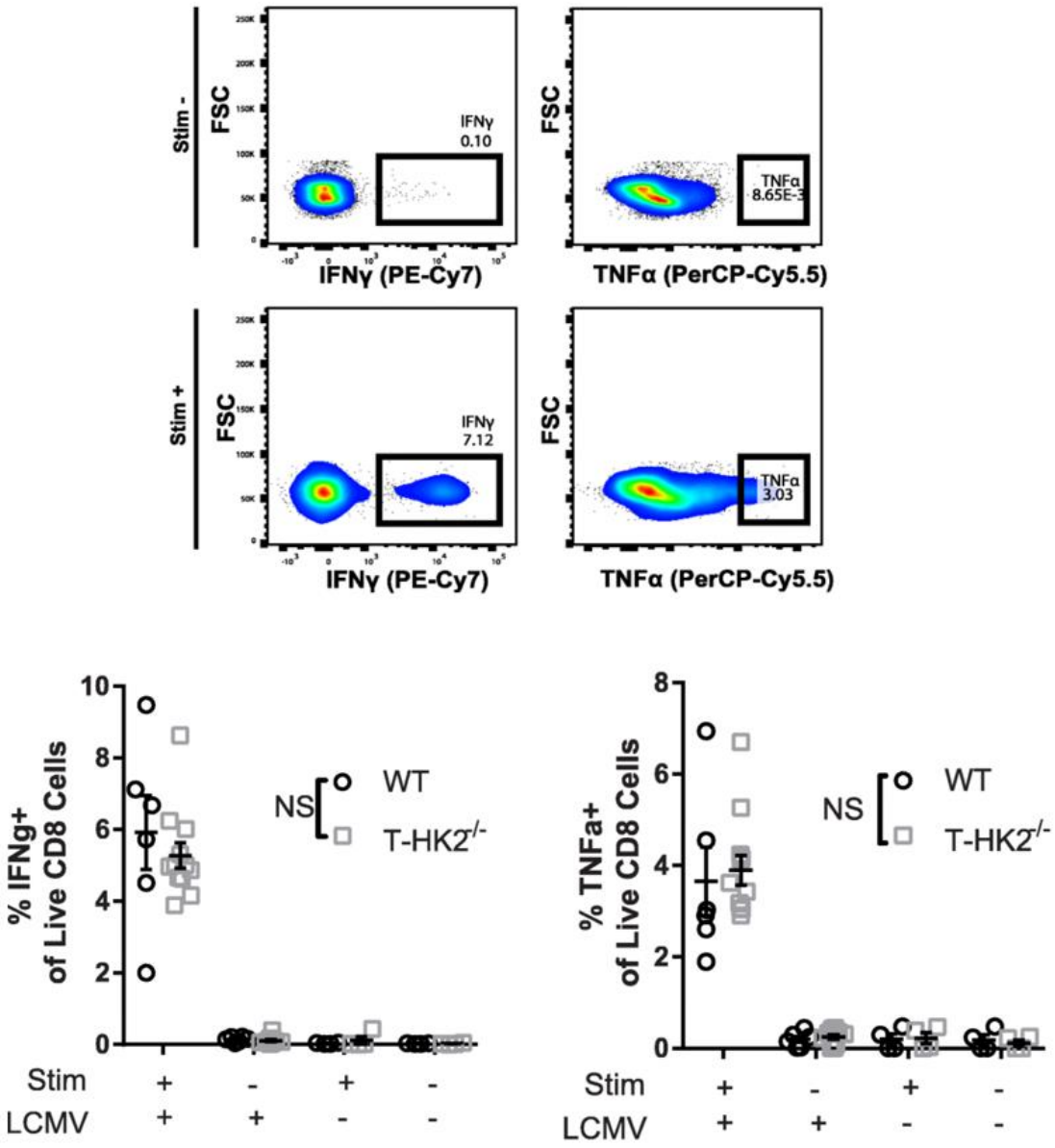

Figure 3.31. HK2 is not required for memory T cell function in LCMV infection. Eight to twelve-week old WT and T-Hk2−/− mice were injected intraperitoneally with 2×10^5 pfu LCMV. Splenocytes from uninfected mice and mice 60 DPI were stimulated in vitro for 5 h with 30 ng/mL $gp_{33–41}$ peptide or vehicle control and stained for IFNγ and TNFα secretion. Biological replicates, error bars represent mean ± SEM, ANOVA with Sidak multiple comparisons correction, *$p < 0.05$; **$p < 0.01$. NS = not significant, DPI = days post infection

In order to determine if there were any in vivo differences in metabolism between WT and T-Hk2$^{-/-}$ mice we analyzed metabolite and transcript profiles of CD8+ T cells from the spleens of mice at 8 DPI. We found no significant difference in metabolite levels and only four differentially expressed genes between WT and T-Hk2$^{-/-}$ mice (Figure 3.32-3.33). Predictably, of the few genes that were differentially expressed, Hk2 stood out as the most downregulated gene in CD8+ T cells from T-Hk2$^{-/-}$ mice. Importantly, HK1 was unchanged in both WT and HK2 deficient T cells. These data indicate that HK2 is dispensable for CD8+ T cell mediated viral immunity.

HK2 is not required for Treg function in vivo

Although HK2 is not necessary for inflammatory CD4+ and CD8+ lineages, we next determined if HK2 was required for the function of the regulatory T cell lineage (Treg cells). We generated mice with Treg specific deletion of the Hk2 gene by crossing Hk2$^{fl/fl}$ mice with FoxP3-YFP-cre mice. Tregs isolated from these mice (FP3-Hk2$^{-/-}$) did not show appreciable levels of Hk2 mRNA transcript (Figure 3.34). FP3-Hk2$^{-/-}$ mice did not develop any indications of autoimmune disease as would be expected of mice with deficiencies in Treg function (Zheng and Rudensky 2007, Shrestha, Yang et al. 2015), as determined by histology, serum ANA titers, weight, and presence of splenomegaly (Figures 3.35-3.36). Furthermore, they had normal numbers of Tregs in the spleen, as well as normal numbers of naïve and memory CD4 and CD8 T cells (Figure 3.37). These data indicate that HK2 is dispensable for Treg function in vivo.

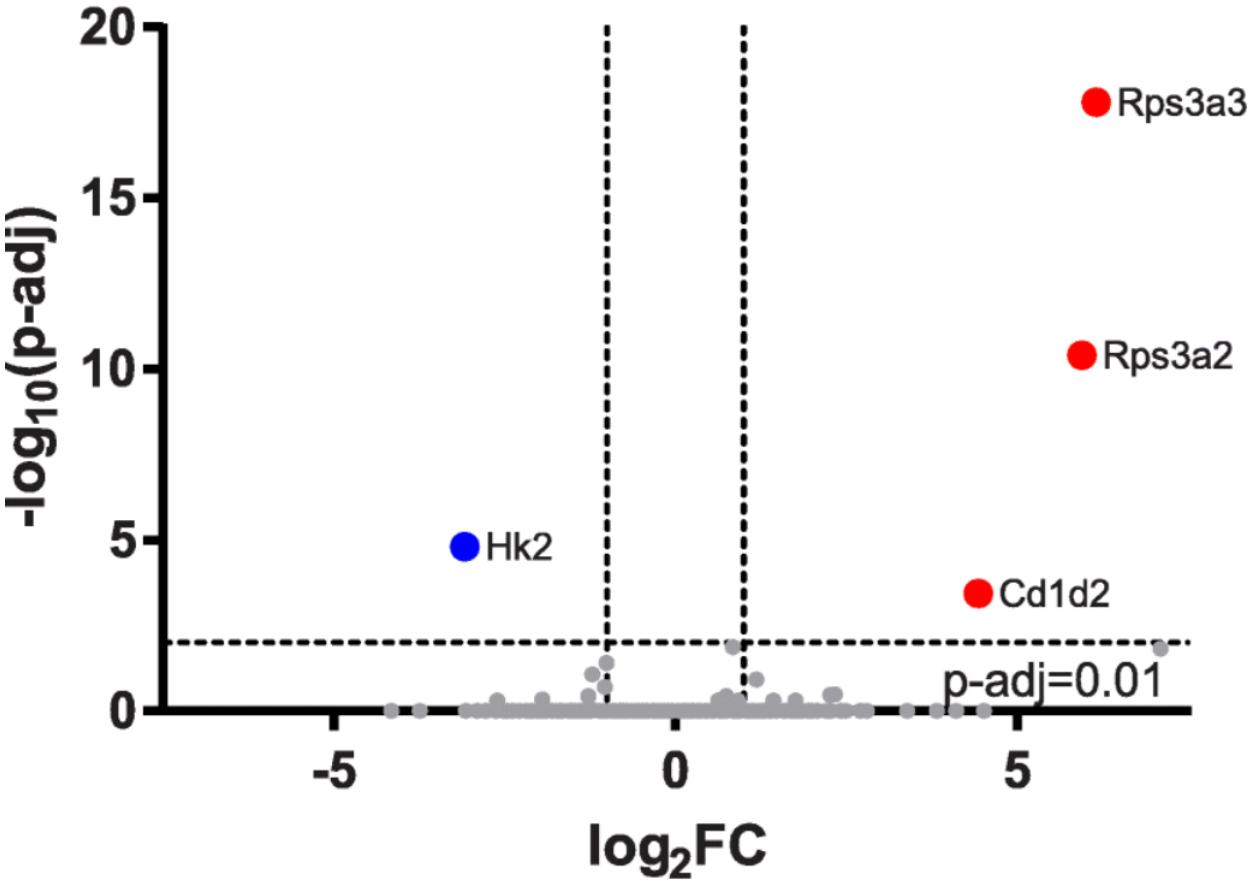

Figure 3.32. HK2 deficiency causes minimal changes in transcription in vivo in T cells.

Eight to twelve-week old WT and T-Hk2−/− mice were injected intraperitoneally with 2×10^5 pfu LCMV. CD8+ T cells were sorted 8 DPI, RNA was isolated, and RNA-seq performed. Volcano plot of gene expression differences. Differentially regulated genes include those with greater than 2 fold change in expression and multiplicity adjusted p value < 0.01, DPI = days post infection. Data generated with help of Carlos Martinez.

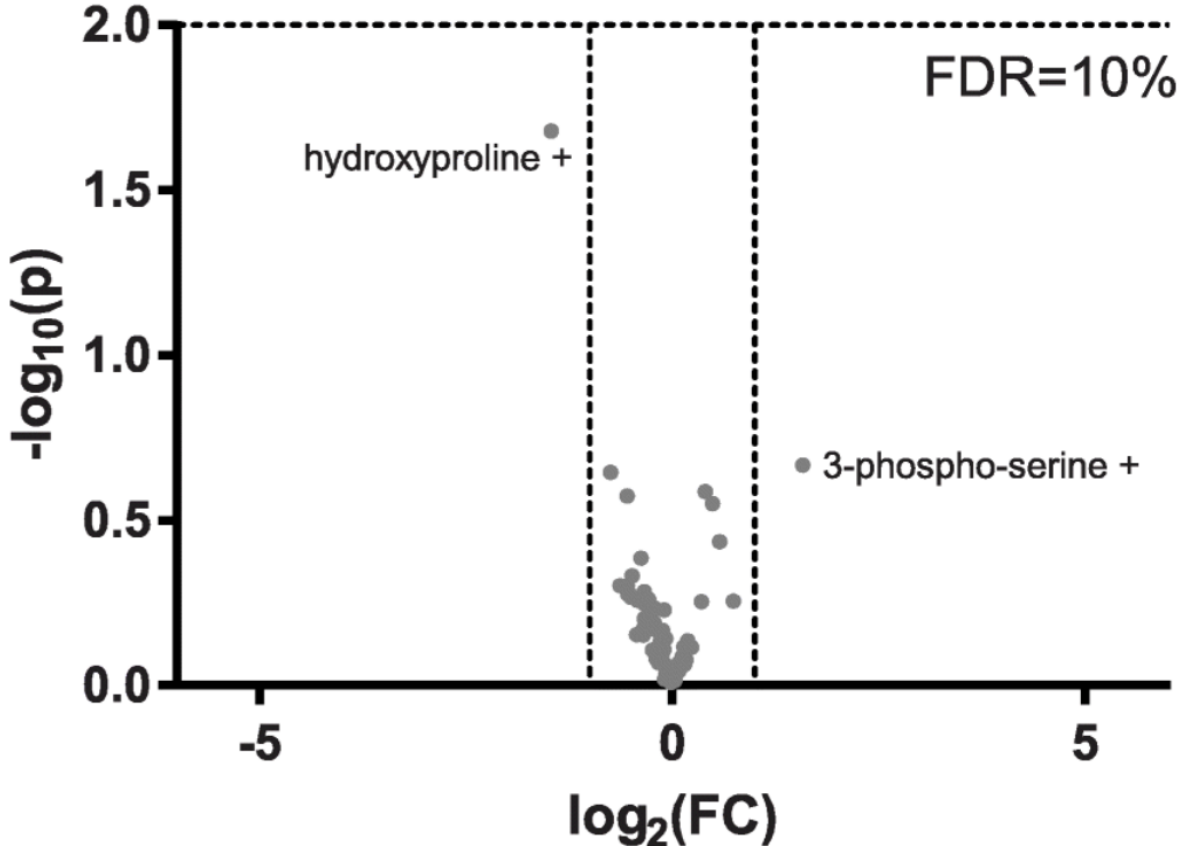

Figure 3.33. HK2 deficiency causes minimal changes in metabolites in vivo in T cells. Eight to twelve-week old WT and T-Hk2−/− mice were injected intraperitoneally with 2×10^5 pfu LCMV. CD8+ T cells were sorted 8 DPI, metabolites were isolated, and targeted metabolomics performed. Volcano plot of metabolite concentration differences. Vertical dashed lines indicate 2 fold change in metabolite concentration. Horizontal dashed line indicates no discoveries made (False Discovery Rate of 0.1, two-stage Benjamini-Krieger method, n = 5 mice), DPI = days post infection. Data generated with help of Peng Gao.

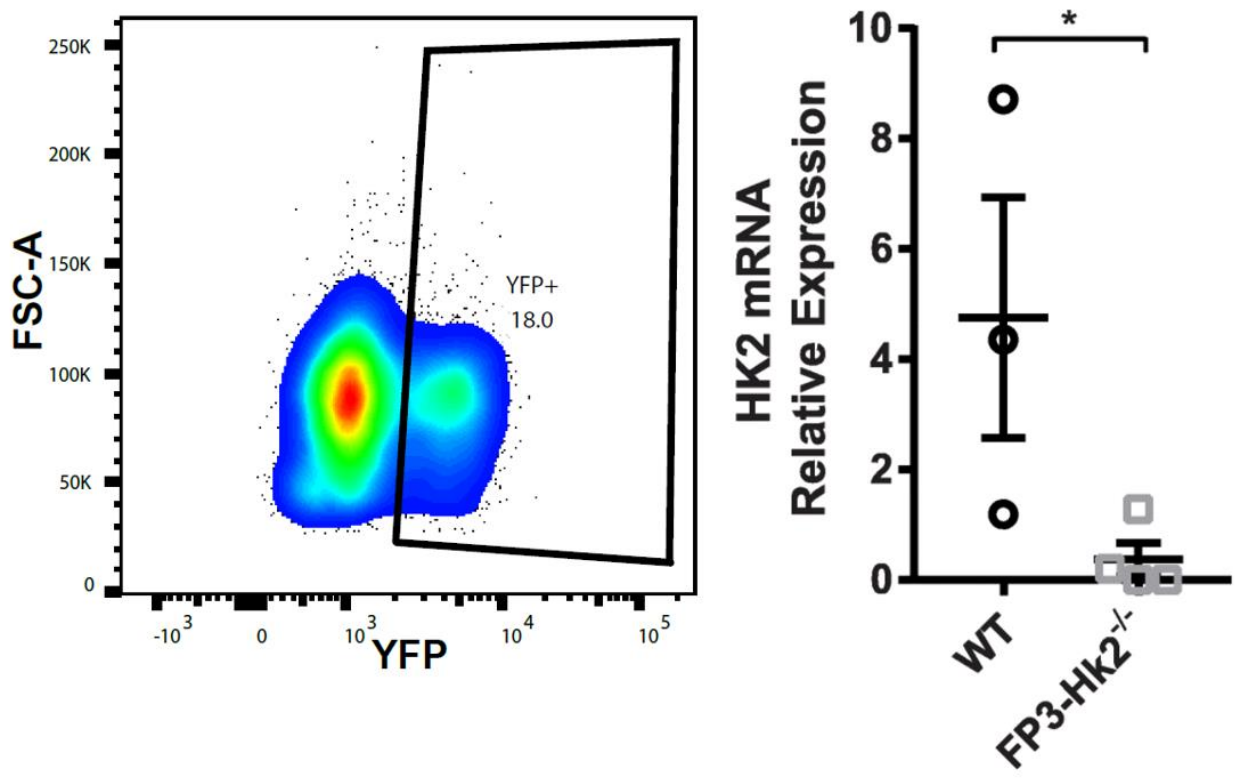

Figure 3.34 HK2 expression is decreased in Tregs from FP3-Hk2-/- mice. Mice with YFP+ HK2-deficient Treg cells were generated (FP3-Hk2$^{-/-}$ mice). CD4+ cells from spleens of adult WT and FP3-Hk2$^{-/-}$ mice were stimulated under Treg promoting conditions and RNA was isolated from sorted YFP+ cells. Hk2 expression relative to β-actin shown. Biological replicates, error bars represent mean ± SEM, single-tailed Student's t test, *$p < 0.05$; **$p < 0.01$. NS = not significant

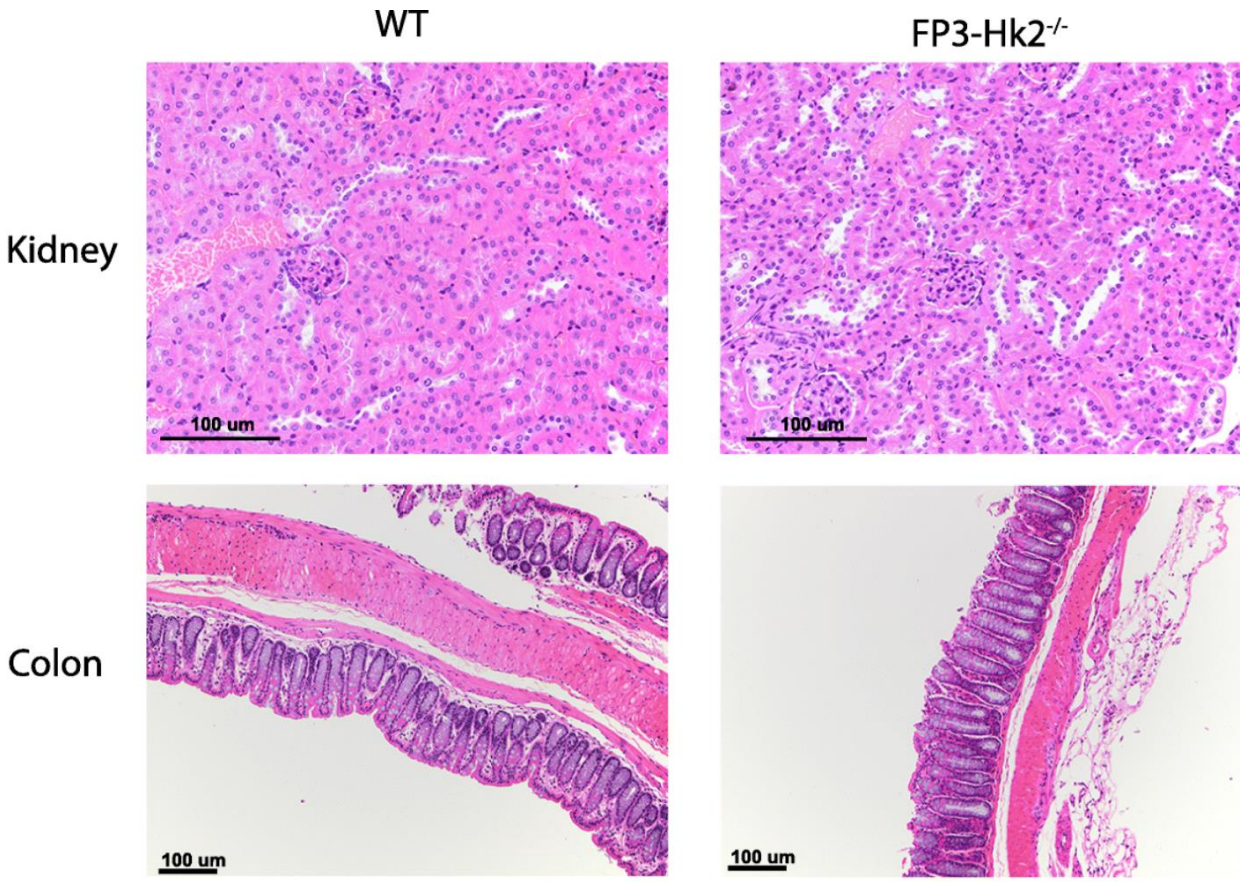

Figure 3.35. Treg specific HK2 deficiency does not cause spontaneous inflammation. WT and FP3-Hk2−/− mice were aged to 6 months. Representative H&E stained sections of indicated tissues shown.

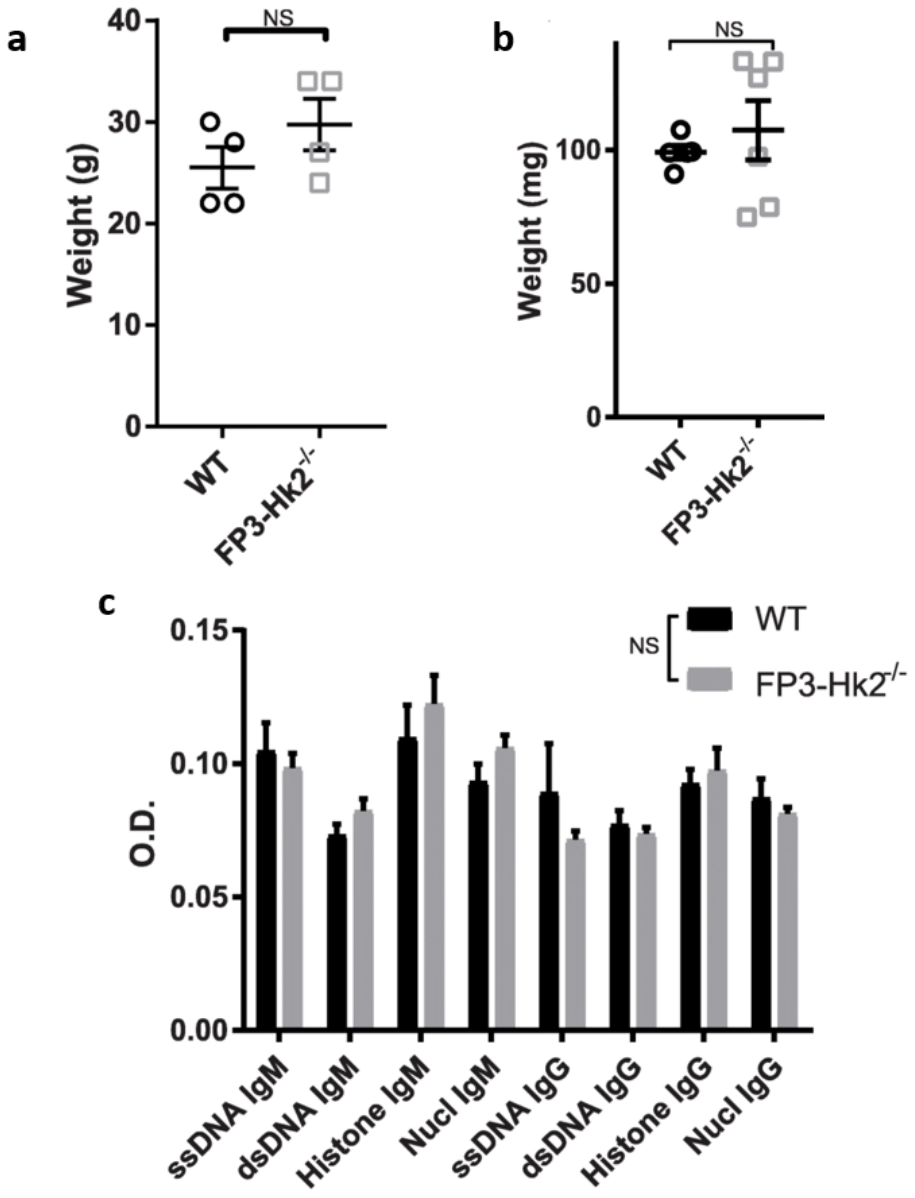

Figure 3.36. Treg specific HK2 deficiency does not cause spontaneous inflammation. WT and FP3-Hk2−/− mice were aged to 6 months. **(A)** Body weight, single-tailed Student's t test **(B)** Spleen weight, single-tailed Student's t test **(C)** Autoantibody titers in serum, ANOVA with Sidak multiple comparisons. In all panels, biological replicates shown, error bars represent mean ± SEM, *$p < 0.05$; **$p < 0.01$. NS = not significant. Data generated with help of Perlman lab.

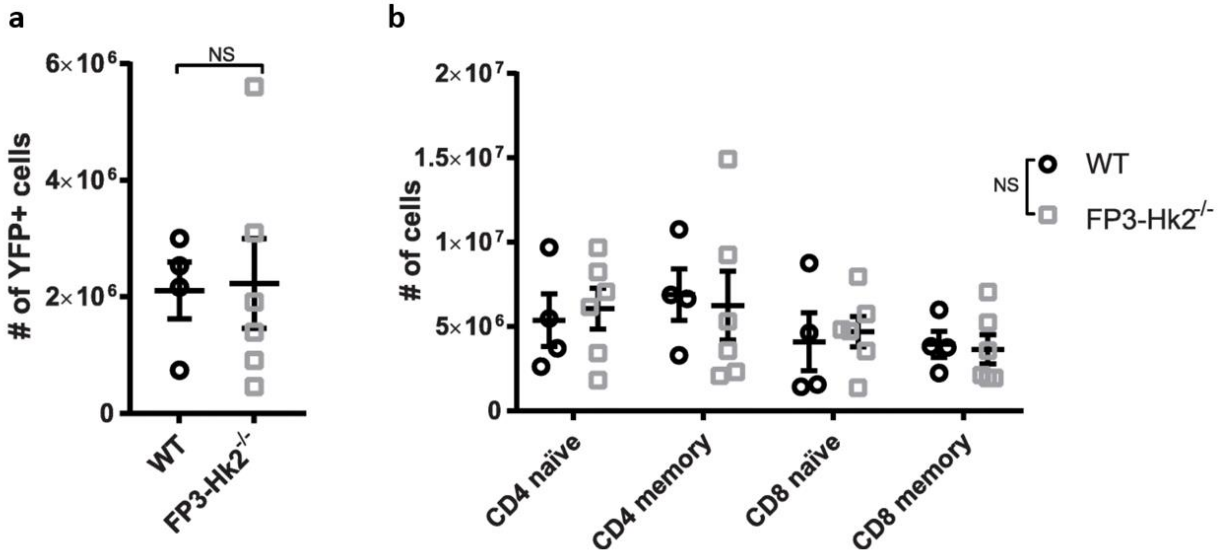

Figure 3.37. Treg specific HK2 deficiency does not cause changes in T cell numbers. WT and FP3-Hk2−/− mice were aged to 6 months. Number of splenic Treg cells and viable CD4+ or CD8+ T cells that are $CD62L^{hi}CD44^{lo}$ (naive) or $CD44^{hi}$(memory). Biological replicates, error bars represent mean ± SEM, ANOVA with Sidak multiple comparisons correction, *$p < 0.05$; **$p < 0.01$. NS = not significant, DPI = days post infection

HK2 is not required for normal hematopoiesis

To determine if there is any defect in the ability of other hematopoetic lineages to differentiate without HK2, we abolished HK2 function in hematopoetic stem cells by crossing Hk2 floxed mice with Vav1-iCre, which expresses Cre in hematopoietic stem cells during development (de Boer, Williams et al. 2003). Resulting BM-Hk2$^{-/-}$ mice did not have any significant HK2 expression as determined by western blot (Figure 3.38). Furthermore, HK2 deficiency did not impair hematopoiesis as assessed by platelet, white and red blood cell counts (Figure 3.39). Collectively, these data indicate HK2 is not required for normal hematopoesis.

Transcriptome differences between T cells and T cell leukemia in vivo

While cancer cells and T cells both upregulated HK2 expression, our data indicate it is only required in the former. For example, HK2 deficiency has been shown to decrease tumor burden in a mouse model of T cell acute lymphoblastic leukemia (T-ALL) (Kishton, Barnes et al. 2016). Finding therapeutics that target neoplastic T cells while sparing normal T cells represents an interesting challenge in cancer therapy, as the two share a common origin and common proliferative goals. In order to identify other potential metabolic targets for T-ALL beyond HK2 that would preferentially inhibit leukemia while sparing lymphocytes, we compared in vivo proliferating T cells and primary mouse T-ALL cells by RNA-seq. WT bone marrow was transduced with retrovirus expressing a constitutively active Notch protein (Notch1-deltaE) and injected into congenic CD45.1 mice. Mice developed CD4+CD8+ lymphoblasts in their blood and lymphoid organs. WT primary leukemia cells were isolated from the spleens of recipient mice after 6 weeks (Figure 3.40) and compared to WT CD8+ T cells isolated from mouse spleens 8 days after infection with LCMV. A wide range of differentially expressed genes were

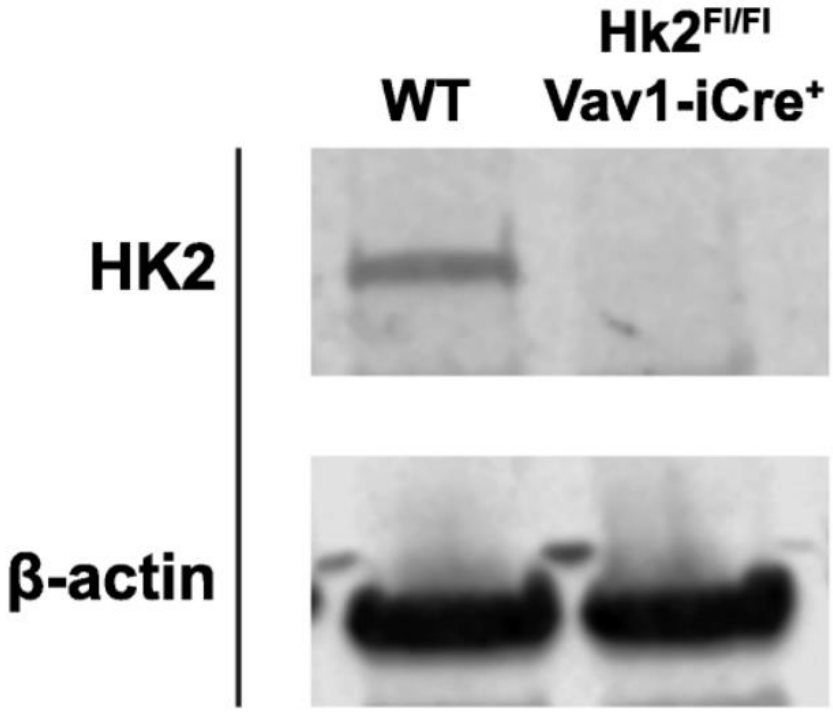

Figure 3.38. Hk2$^{Fl/Fl}$;Vav1-iCre mice have no observable HK2 in bone marrow. Western blot for protein expression of HK2 and β-actin in bone marrow. Representative of four independent experiments.

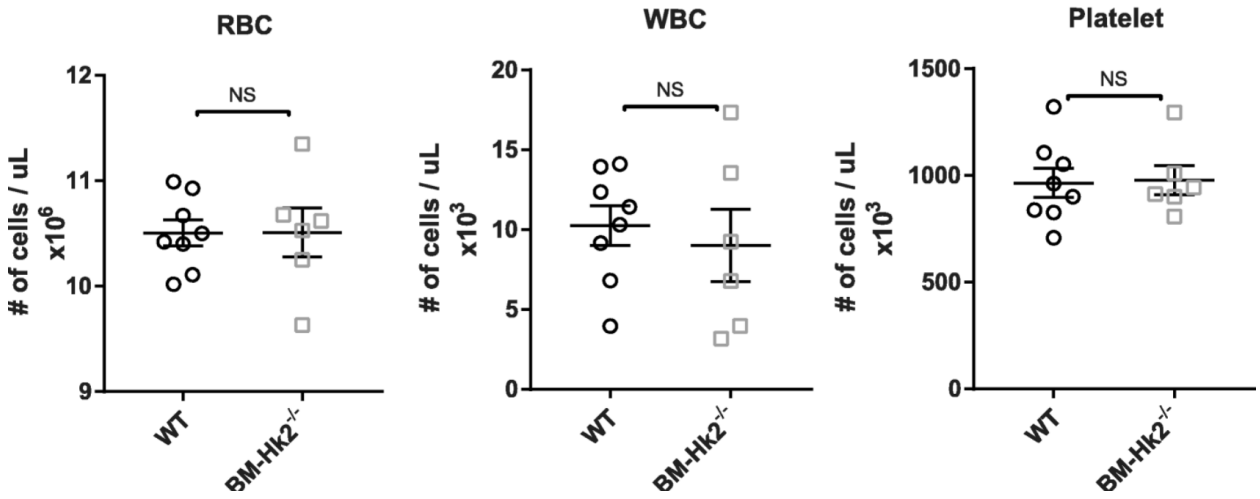

Figure 3.39. HK2 is not required for normal hematopoiesis. Mice with HK2-deficient bone marrow were generated ($Hk2^{Fl/Fl}$;Vav1-iCre, referred to as BM-$Hk2^{-/-}$). Biological replicates, unpaired t test, error bars represent mean ± SEM. NS = not significant.

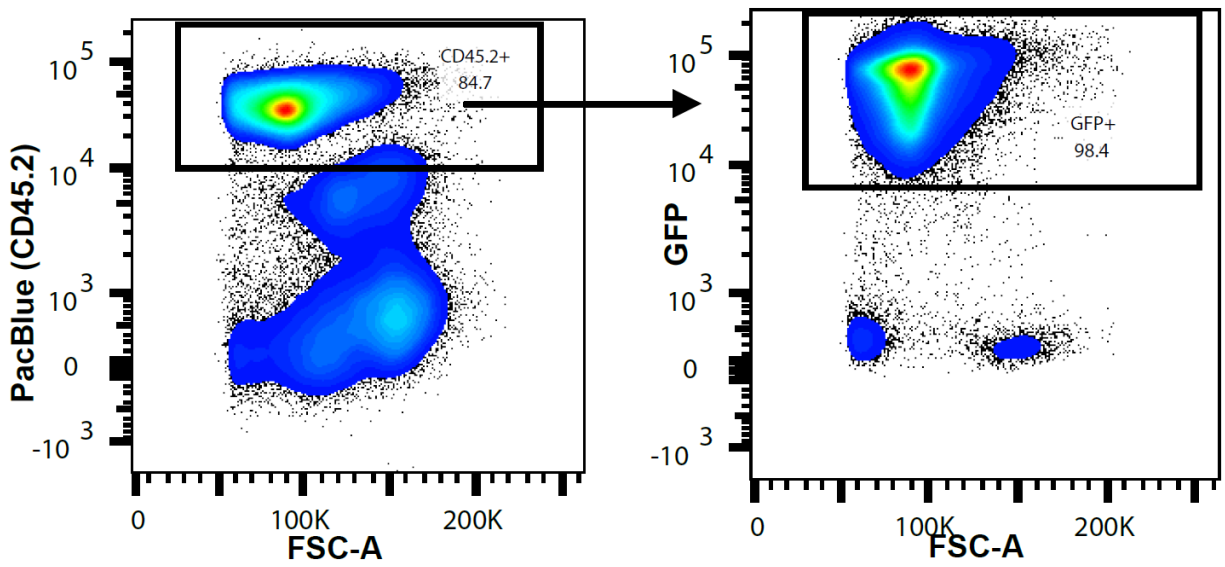

Figure 3.40. T-ALL leukemia cells sorted by congenic marker and GFP expression.

Example gating strategy shown for sorting leukemic cells after adoptive transfer of bone marrow expressing constitutively active Notch1. Initial population also gated based on FSC/SSC and viability.

identified between T cells and leukemic cells (Figure 3.41). 3331 genes were identified as being significantly differentially expressed between T cells and leukemia (Figure 3.41), with leukemic samples enriched in expected gene sets such as myc targets, beta-catenin pathway, and notch1 signaling (Figure 3.42). T cells were unsurprisingly enriched for gene sets involved in T cell processes such as allograft rejection and IFNγ response (Figure 3.42). Of the differentially expressed genes, 167 were metabolic genes in the KEGG database, including 61 upregulated metabolic genes in leukemia (Figure 3.43). 5 of the top metabolic genes upregulated in leukemia when compared to CD8+ T cells were Hmgcs2, Chdh, Fbp1, Prodh, and Ldhb. These genes consistently showed higher expression in leukemia cells when re-evaluated by RT-PCR (Figure 3.44). While some differences were statistically significant after T-tests, no individual gene reached statistical significance on multiple comparisons correction. Taken together, these data reveal essential differences in T cell and T-ALL cell metabolism that may be harnessed to selectively inhibit leukemic proliferation.

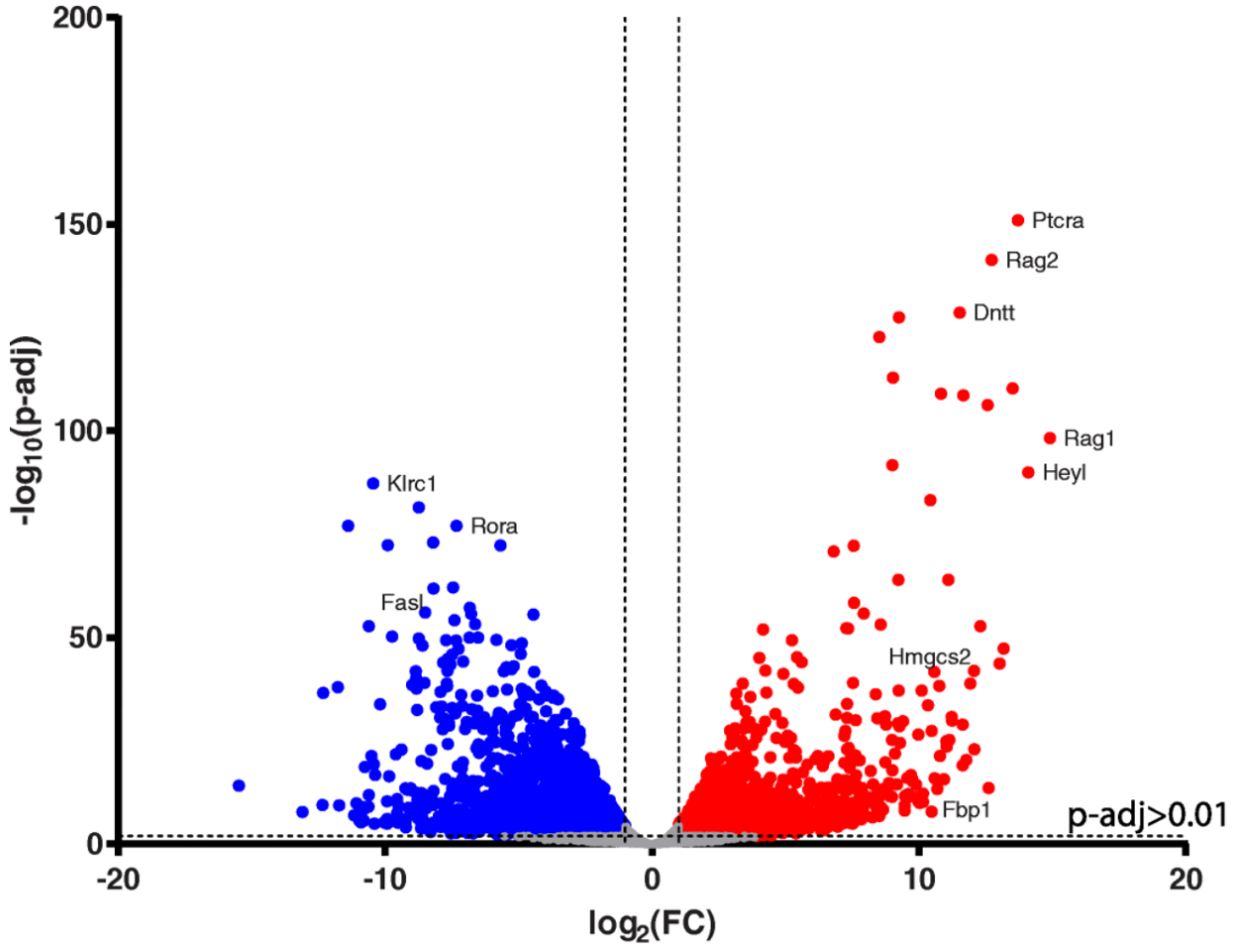

Figure 3.41. Transcriptomic differences between T cells and leukemia. Sorted splenic CD8+ T cells from WT mice 8 days after LCMV infection, compared to sorted T-ALL cells from WT mice 6 weeks after adoptive transfer. RNA isolated from sorted cells and analyzed by RNA-seq. Volcano plot of gene expression differences shown. Differentially regulated genes include those with greater than 2 fold change in expression and multiplicity adjusted *p* value < 0.01. Blue dots are overexpressed in CD8+ T cells, red in T-ALL. Data generated with help of Carlos Martinez.

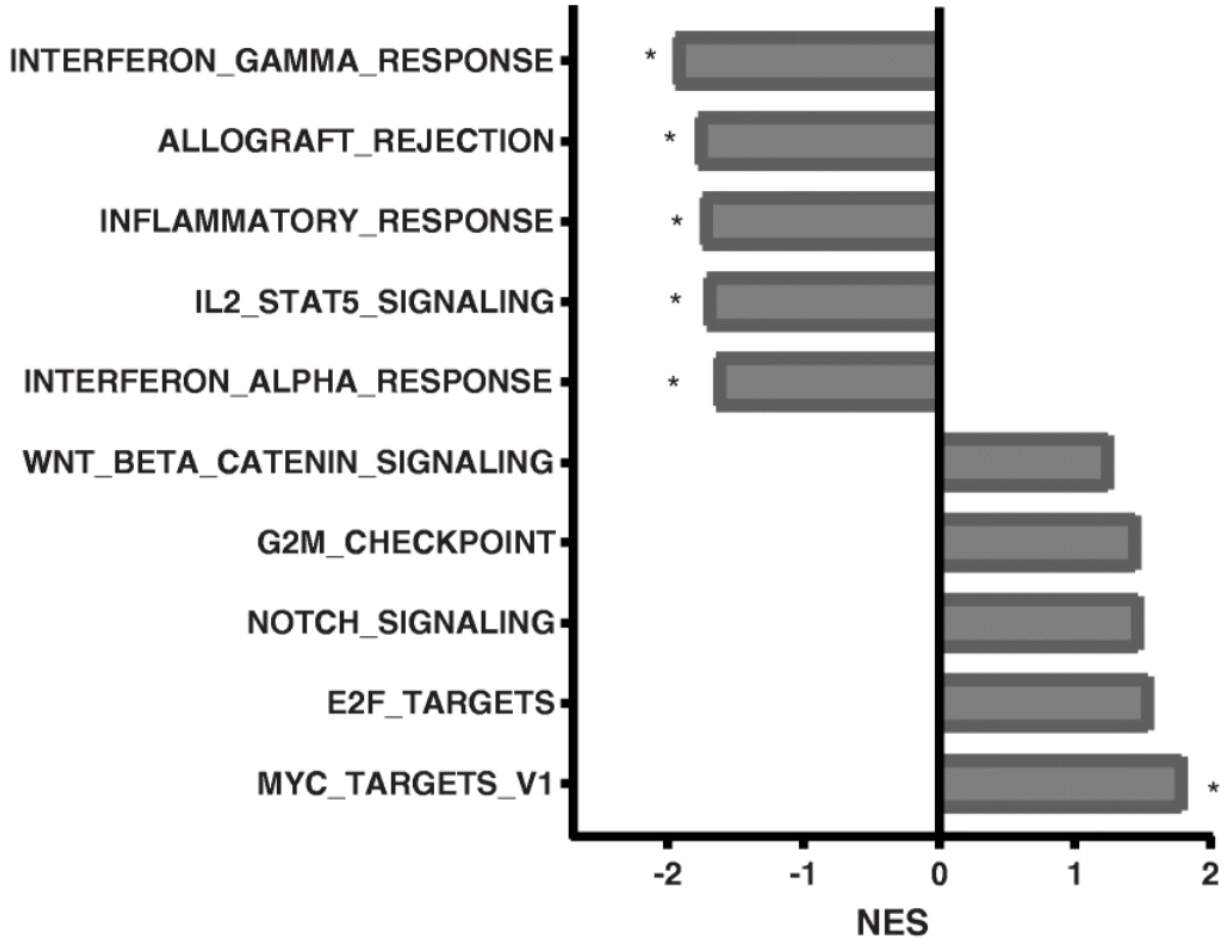

Figure 3.42. Hallmark pathways enriched in T cells and leukemia. Sorted splenic CD8+ T cells from WT mice 8 days after LCMV infection, compared to sorted T-ALL cells from WT mice 6 weeks after adoptive transfer. RNA isolated from sorted cells and analyzed by RNA-seq. Hallmark pathways shown that are enriched in leukemia (positive values) or T cells (negative values) and their normalized enrichment score. Statistical significance shown by * (FWER $p < 0.05$). Data generated with help of Carlos Martinez.

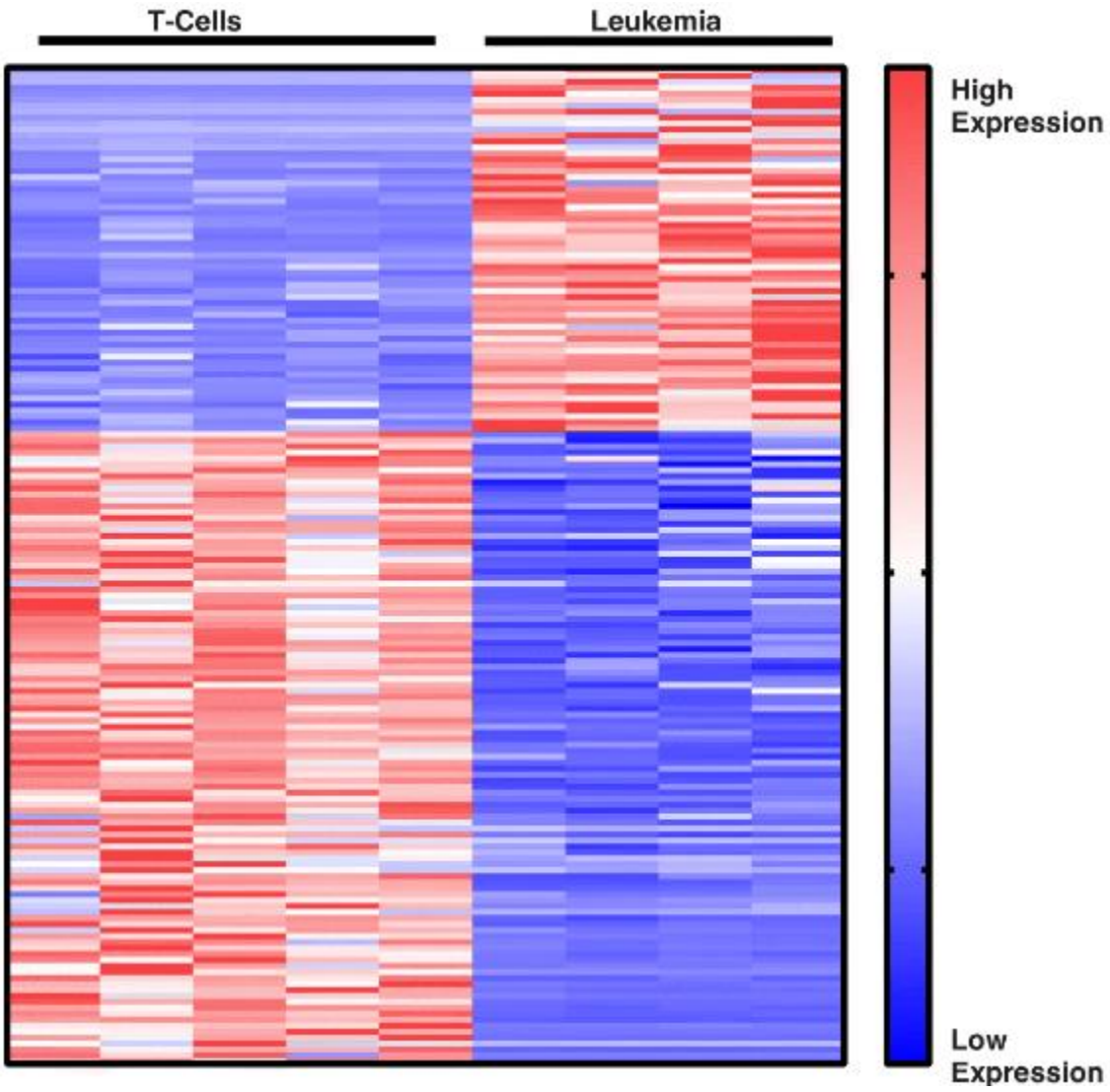

Figure 3.43. Metabolic differences exist between T cells and leukemia. Sorted splenic CD8+ T cells from WT mice 8 days after LCMV infection, compared to sorted T-ALL cells from WT mice 6 weeks after adoptive transfer. RNA isolated from sorted cells and analyzed by RNA-seq. Expression of differentially regulated metabolic genes from KEGG database shown. Data generated with help of Carlos Martinez.

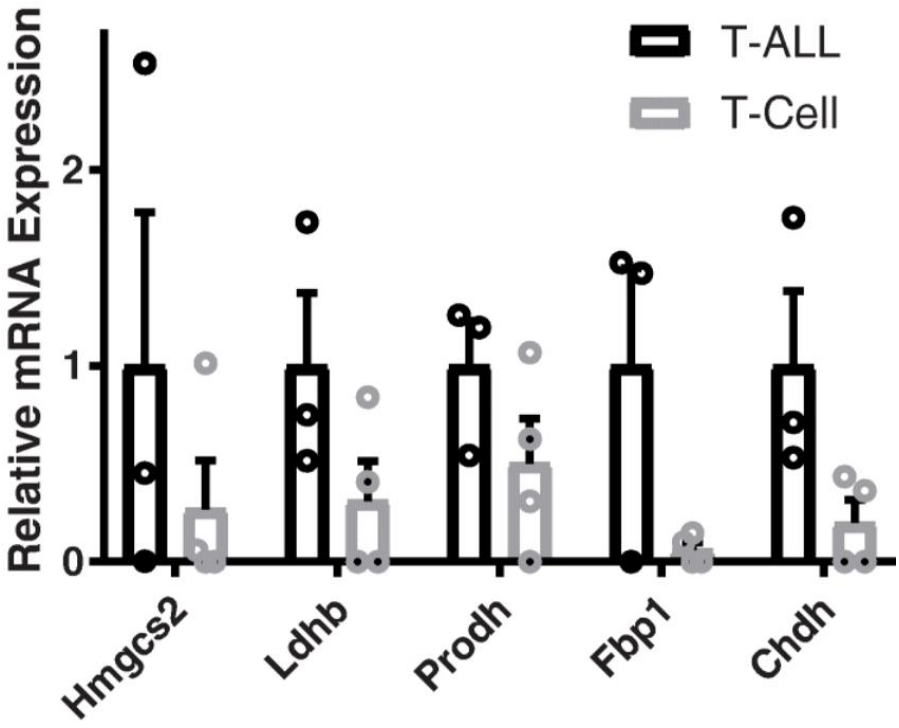

Figure 3.44. Differential expression of metabolic genes by RT-PCR. Sorted splenic CD8+ T cells from WT mice 8 days after LCMV infection, compared to sorted T-ALL cells from WT mice 6 weeks after adoptive transfer. RNA isolated from sorted cells. Expression of select metabolic genes shown by RT-PCR relative to β-actin and Rpl-19.

Chapter 4. Conclusions

In the past decade, there has been a resurgence of targeting metabolism for cancer therapy. Cancer cells undergo metabolic reprogramming to acquire sufficient nutrients to fuel macromolecule synthesis for growth and proliferation (Shaw 2006, Lunt and Vander Heiden 2011, DeBerardinis and Chandel 2016). However, the therapeutic window is limited by metabolic rewiring that cancer cells quickly undergo upon inhibition of a particular metabolic pathway thus becoming resistant to therapies targeting metabolism. Normal proliferating T cells, stem and progenitor cells also display features of metabolic reprogramming similar to cancer cells, further limiting the therapeutic index in targeting metabolism of cancer cells (Gerriets and Rathmell 2012, Pearce, Poffenberger et al. 2013, Andrejeva and Rathmell 2017). Moreover, targeting metabolism within T cells to diminish their proliferation and function could leave patients susceptible to life threatening infections while also rendering useless cutting-edge immunotherapies such as check point blockade and CAR-T cells.

A similar metabolic feature of proliferating cancer cells and T cells, is that they both highly upregulate glycolytic enzymes (Lunt and Vander Heiden 2011, Michalek, Gerriets et al. 2011, Gerriets and Rathmell 2012, Patra, Wang et al. 2013, Wang, Xiong et al. 2014, Botzer, Maman et al. 2016). HK2 is the one the most highly upregulated glycolytic enzymes in activated T cells and oncogenic transformed cells (Shi, Wang et al. 2011, Patra, Wang et al. 2013, Wang, Xiong et al. 2014, Botzer, Maman et al. 2016, Tan, Yang et al. 2017). Thus, we were surprised with our observation that HK2 is dispensable for the essential function of T cells – viral immunity. Clearance of acute LCMV infection was completely intact in mice with $Hk2^{-/-}$ T cells, as was the

ability of those mice to develop T cell memory. Unexpectedly, we found minimal differences in metabolite levels and gene expression between wild-type and HK2 deficient proliferating CD8 T cells in response to LCMV. Moreover, HK2 deficiency did not impair Treg function. Loss of HK2 also did not impair normal hematopoiesis indicating normal stem and progenitor cell function. Recent work has also shown that HK2 is required for angiogenesis (Yu, Wilhelm et al. 2017), and this inhibition could theoretically further synergize with cancer cell HK2 inhibition to improve response to therapy. In contrast to the observed dispensability of HK2 in immunity, we found that HK2 may play a small role in pathological T cell mediated inflammation. In a mouse model of colitis, HK2 deficiency conferred a limited degree of protection against inflammation. We speculate that the simplest explanation for this is that pathogenic T cells have a higher demand for glucose which HK2 deficient cells are unable to meet. Indeed, this effect has been observed in other models of inflammation, and 2-DG has been proposed as a potential therapeutic in autoimmune diseases (Yang, Fujii et al. 2013, Yin, Choi et al. 2015). However, it is also possible the microenvironment specific to these models may play a potential role, and it is also possible that HK2 could have non-metabolic functions contributing to pathogenesis.

It is important to note that recent work from another group supports our finding of HK2 dispensability in T cells, but in a model of herpes virus infection (Varanasi, Jaggi et al. 2018). However, while they propose a compensatory upregulation of HK1 in HK2 deficient T cells, we are unable to confirm that conclusion in our system. There was no observed compensatory increase in HK1 or HK3 expression at the RNA or protein level. Rather, we believe HK2 is dispensable because HK2-mediated glucose phosphorylation only constitutes a small percentage of total glucose phosphorylation in CD4+ and CD8+ T cells.

To identify other targets which could be utilized to selectively inhibit cancer cells, we compared the transcriptome and metabolome of proliferating T cell leukemia with T cells proliferating physiologically in response to infection. This analysis revealed striking differences in how the metabolism of a leukemic cell differs from that of a T cell and identified specific potential targets for cancer therapy, including Hmgcs2, Prodh, Ldhb, Fbp1, and Chdh. This dataset may serve as a significant resource for future studies in cancer therapy to determine if any of the identified highly expressed metabolic genes are also required for leukemia.

In conclusion, multiple studies have shown HK2 is essential for cancer growth and development, including in models of breast cancer, lung cancer, and leukemia, leading to interest in HK2 as a potential drug target for cancer therapy. We sought to determine the role of HK2 in T cells, considering the high expression of HK2 in T cells and the potential for HK2 inhibition to adversely affect immunity. We have demonstrated through various animal models that HK2 serves as a mostly redundant enzyme in T cells. We propose that our findings make HK2 an attractive target for cancer therapy, as it would be expected to have limited immunosuppressive side effects.

Chapter 5. Future Directions

While this thesis begins to answer some of the questions regarding the effects of HK2 inhibition on the immune system, it also raises several questions. One particular question is why do T cells upregulate HK2 at all? Every function, enzyme, and attribute in every cell has a cost and a benefit associated with it. Evolution selects against attributes that have a high cost and little benefit for the organism. Even in a T cell, the small bioenergetic and biosynthetic cost of upregulating the expression of HK2 should theoretically be selected against over time if the increase in HK2 does not afford any additional benefit to the organism. Yet our findings suggest that T cells needlessly upregulate this enzyme. The most likely explanation for this is that there may be certain types of infections that require T cell HK2 expression for an adequate response. In this way, though HK2 is not required for the T cell functions tested in this thesis, HK2 may be necessary in other infections. Perhaps the occasional occurrence of these non-tested infections over time has given organisms expressing HK2 in T cells a survival advantage that justifies its considerable upregulation in T cell activation.

Some of our findings may hint at possible scenarios where HK2 is necessary for immunity. For example, we observed small differences in the ability of CD8+ cells to expand early in response to infection with LCMV. It is therefore possible that if mice were infected with a much higher initial viral load, the decreased initial expansion of T cells would be insufficient to control the infection. Such a hypothesis could be tested by infecting mice with a lethal dose of virus, such that half of WT mice succumb to the infection. If HK2 were required in this scenario, the infection would be lethal to a larger portion of HK2 deficient mice.

Alternatively, the necessity for HK2 may be pathogen or site specific. For example, our colitis data show that HK2 deficiency caused a small decrease in T cell expansion or infiltration in the lamina propria but not in the lymph nodes. One reasonable hypothesis from this finding is that the microenvironment of the lamina propria elicits the proliferative defect of HK2 deficient T cells. In this case, it is possible that mice with HK2 deficiency in the context of viral or bacterial colitis could have more severe disease and higher mortality. If this were true, it would also be interesting to determine the mechanism by which the microenvironment alters T cell metabolism. For example, the colon microenvironment may have different availability of substrates for T cell growth and proliferation, in which case an unbiased metabolomic approach could show how substrate usage may vary between WT and HK2 deficient T cells in the lamina propria.

Another potential area of further research could help determine if HK2 is required in T cells across a wide variety of infections. Different infections interact differently with the immune system, and it is certainly possible that immunity to certain pathogens could be more dependent on T cell HK2 expression than other pathogens. This is particularly important considering the potential for use of HK2 inhibition in cancer therapy. Several different opportunistic pathogens are known to commonly take advantage of immunosuppression in cancer patients, and such pathogens could specifically be tested to determine if HK2 is required for T cells to mediate clearance and immunity.

Future studies are also necessary to further investigate the role HK2 inhibition could play specifically in the setting of cancer therapy. Testing the dispensability of HK2 in T cell dependent tumor immunity would be an important step to making more generalizable

conclusions. For example, HK2 could be deleted in CAR T cells to determine its necessity for tumor immunity. Alternatively, HK2 could be deleted in conjunction with a checkpoint inhibitor therapy to similarly test necessity in the context of tumor immunity. These studies could help determine if HK2 inhibition may be used in conjunction with existing immunotherapies without hindering their effectiveness.

Finally, other immune cells could also be dependent on HK2, such as B cells and macrophages, which are important for adaptive and innate immunity, respectively. Both cell types are known to require glycolysis for their function. Macrophages rely on glycolysis after exposure to LPS (a signal for potential bacterial infection) for production of the inflammatory cytokine IL1-β (Tannahill, Curtis et al. 2013). Similarly, B cells rely on glycolysis to utilize glucose in antibody production (Caro-Maldonado, Wang et al. 2014). It is therefore conceivable that inhibition of glycolysis could adversely affect immune cells other than T cells.

If HK2 inhibition were to adversely affect other immune cells, that would also limit its potential efficacy in cancer therapy. Initial studies may be wise to first determine the relative contribution of HK2 to total HK expression in other immune cells with simple methods such as RT-PCR and ELISA. If HK2 constitutes a large fraction of total HK in these cells, future studies may further examine the role of HK2 in these cell types by deleting HK2 from each cell type (by crossing to multiple individual Cre mice), from all immune cells (by crossing HK2 to Vav1-iCre), or all adult cells (by crossing to an inducible ubiquitin CreERT2). These deficiencies could be studied in the context of infections such as influenza, pneumonia, and relevant diseases known to require

B cell or macrophage function. Together, these potential future studies could help to clarify the role HK2 inhibition may play in cancer therapy.

References

Afshar, R., B. D. Medoff and A. D. Luster (2008). "Allergic asthma: a tale of many T cells." Clin Exp Allergy **38**(12): 1847-1857.

Andrejeva, G. and J. C. Rathmell (2017). "Similarities and Distinctions of Cancer and Immune Metabolism in Inflammation and Tumors." Cell Metab **26**(1): 49-70.

Berg, D. J., N. Davidson, R. Kuhn, W. Muller, S. Menon, G. Holland, L. Thompson-Snipes, M. W. Leach and D. Rennick (1996). "Enterocolitis and colon cancer in interleukin-10-deficient mice are associated with aberrant cytokine production and CD4(+) TH1-like responses." J Clin Invest **98**(4): 1010-1020.

Blagih, J., F. Coulombe, E. E. Vincent, F. Dupuy, G. Galicia-Vazquez, E. Yurchenko, T. C. Raissi, G. J. van der Windt, B. Viollet, E. L. Pearce, J. Pelletier, C. A. Piccirillo, C. M. Krawczyk, M. Divangahi and R. G. Jones (2015). "The energy sensor AMPK regulates T cell metabolic adaptation and effector responses in vivo." Immunity **42**(1): 41-54.

Botzer, L. E., S. Maman, O. Sagi-Assif, T. Meshel, I. Nevo, I. Yron and I. P. Witz (2016). "Hexokinase 2 is a determinant of neuroblastoma metastasis." Br J Cancer **114**(7): 759-766.

Bryce, P. J., C. B. Mathias, K. L. Harrison, T. Watanabe, R. S. Geha and H. C. Oettgen (2006). "The H1 histamine receptor regulates allergic lung responses." J Clin Invest **116**(6): 1624-1632.

Buck, M. D., D. O'Sullivan, R. I. Klein Geltink, J. D. Curtis, C. H. Chang, D. E. Sanin, J. Qiu, O. Kretz, D. Braas, G. J. van der Windt, Q. Chen, S. C. Huang, C. M. O'Neill, B. T. Edelson, E. J. Pearce, H. Sesaki, T. B. Huber, A. S. Rambold and E. L. Pearce (2016).

"Mitochondrial Dynamics Controls T Cell Fate through Metabolic Programming." Cell **166**(1): 63-76.

Caro-Maldonado, A., R. Wang, A. G. Nichols, M. Kuraoka, S. Milasta, L. D. Sun, A. L. Gavin, E. D. Abel, G. Kelsoe, D. R. Green and J. C. Rathmell (2014). "Metabolic reprogramming is required for antibody production that is suppressed in anergic but exaggerated in chronically BAFF-exposed B cells." J Immunol **192**(8): 3626-3636.

Carr, E. L., A. Kelman, G. S. Wu, R. Gopaul, E. Senkevitch, A. Aghvanyan, A. M. Turay and K. A. Frauwirth (2010). "Glutamine uptake and metabolism are coordinately regulated by ERK/MAPK during T lymphocyte activation." J Immunol **185**(2): 1037-1044.

Champagne, D. P., K. M. Hatle, K. A. Fortner, A. D'Alessandro, T. M. Thornton, R. Yang, D. Torralba, J. Tomas-Cortazar, Y. W. Jun, K. H. Ahn, K. C. Hansen, L. Haynes, J. Anguita and M. Rincon (2016). "Fine-Tuning of CD8(+) T Cell Mitochondrial Metabolism by the Respiratory Chain Repressor MCJ Dictates Protection to Influenza Virus." Immunity **44**(6): 1299-1311.

Chandel, N. S., D. S. McClintock, C. E. Feliciano, T. M. Wood, J. A. Melendez, A. M. Rodriguez and P. T. Schumacker (2000). "Reactive oxygen species generated at mitochondrial complex III stabilize hypoxia-inducible factor-1alpha during hypoxia: a mechanism of O2 sensing." J Biol Chem **275**(33): 25130-25138.

Chang, C. H., J. D. Curtis, L. B. Maggi, Jr., B. Faubert, A. V. Villarino, D. O'Sullivan, S. C. Huang, G. J. van der Windt, J. Blagih, J. Qiu, J. D. Weber, E. J. Pearce, R. G. Jones and E. L. Pearce (2013). "Posttranscriptional control of T cell effector function by aerobic glycolysis." Cell **153**(6): 1239-1251.

Chang, C. H., J. Qiu, D. O'Sullivan, M. D. Buck, T. Noguchi, J. D. Curtis, Q. Chen, M. Gindin, M. M. Gubin, G. J. van der Windt, E. Tonc, R. D. Schreiber, E. J. Pearce and E. L. Pearce (2015). "Metabolic Competition in the Tumor Microenvironment Is a Driver of Cancer Progression." Cell **162**(6): 1229-1241.

Chichlowski, M., J. M. Sharp, D. A. Vanderford, M. H. Myles and L. P. Hale (2008). "Helicobacter typhlonius and Helicobacter rodentium differentially affect the severity of colon inflammation and inflammation-associated neoplasia in IL10-deficient mice." Comp Med **58**(6): 534-541.

Cui, G., M. M. Staron, S. M. Gray, P. C. Ho, R. A. Amezquita, J. Wu and S. M. Kaech (2015). "IL-7-Induced Glycerol Transport and TAG Synthesis Promotes Memory CD8+ T Cell Longevity." Cell **161**(4): 750-761.

Dang, E. V., J. Barbi, H. Y. Yang, D. Jinasena, H. Yu, Y. Zheng, Z. Bordman, J. Fu, Y. Kim, H. R. Yen, W. Luo, K. Zeller, L. Shimoda, S. L. Topalian, G. L. Semenza, C. V. Dang, D. M. Pardoll and F. Pan (2011). "Control of T(H)17/T(reg) balance by hypoxia-inducible factor 1." Cell **146**(5): 772-784.

de Boer, J., A. Williams, G. Skavdis, N. Harker, M. Coles, M. Tolaini, T. Norton, K. Williams, K. Roderick, A. J. Potocnik and D. Kioussis (2003). "Transgenic mice with hematopoietic and lymphoid specific expression of Cre." Eur J Immunol **33**(2): 314-325.

DeBerardinis, R. J. and N. S. Chandel (2016). "Fundamentals of cancer metabolism." Sci Adv **2**(5): e1600200.

Erben, U., C. Loddenkemper, K. Doerfel, S. Spieckermann, D. Haller, M. M. Heimesaat, M. Zeitz, B. Siegmund and A. A. Kuhl (2014). "A guide to histomorphological evaluation of intestinal inflammation in mouse models." Int J Clin Exp Pathol **7**(8): 4557-4576.

Fesnak, A. D., C. H. June and B. L. Levine (2016). "Engineered T cells: the promise and challenges of cancer immunotherapy." Nat Rev Cancer **16**(9): 566-581.

Frauwirth, K. A., J. L. Riley, M. H. Harris, R. V. Parry, J. C. Rathmell, D. R. Plas, R. L. Elstrom, C. H. June and C. B. Thompson (2002). "The CD28 signaling pathway regulates glucose metabolism." Immunity **16**(6): 769-777.

Fung-Leung, W. P., T. M. Kundig, R. M. Zinkernagel and T. W. Mak (1991). "Immune response against lymphocytic choriomeningitis virus infection in mice without CD8 expression." J Exp Med **174**(6): 1425-1429.

Gerriets, V. A., R. J. Kishton, M. O. Johnson, S. Cohen, P. J. Siska, A. G. Nichols, M. O. Warmoes, A. A. de Cubas, N. J. MacIver, J. W. Locasale, L. A. Turka, A. D. Wells and J. C. Rathmell (2016). "Foxp3 and Toll-like receptor signaling balance Treg cell anabolic metabolism for suppression." Nat Immunol **17**(12): 1459-1466.

Gerriets, V. A., R. J. Kishton, A. G. Nichols, A. N. Macintyre, M. Inoue, O. Ilkayeva, P. S. Winter, X. Liu, B. Priyadharshini, M. E. Slawinska, L. Haeberli, C. Huck, L. A. Turka, K. C. Wood, L. P. Hale, P. A. Smith, M. A. Schneider, N. J. MacIver, J. W. Locasale, C. B. Newgard, M. L. Shinohara and J. C. Rathmell (2015). "Metabolic programming and PDHK1 control CD4+ T cell subsets and inflammation." J Clin Invest **125**(1): 194-207.

Gerriets, V. A. and J. C. Rathmell (2012). "Metabolic pathways in T cell fate and function." Trends Immunol **33**(4): 168-173.

Hamanaka, R. B. and N. S. Chandel (2012). "Targeting glucose metabolism for cancer therapy." J Exp Med **209**(2): 211-215.

Hatfield, S. M., J. Kjaergaard, D. Lukashev, T. H. Schreiber, B. Belikoff, R. Abbott, S. Sethumadhavan, P. Philbrook, K. Ko, R. Cannici, M. Thayer, S. Rodig, J. L. Kutok, E. K.

Jackson, B. Karger, E. R. Podack, A. Ohta and M. V. Sitkovsky (2015). "Immunological mechanisms of the antitumor effects of supplemental oxygenation." Sci Transl Med **7**(277): 277ra230.

Ho, P. C., J. D. Bihuniak, A. N. Macintyre, M. Staron, X. Liu, R. Amezquita, Y. C. Tsui, G. Cui, G. Micevic, J. C. Perales, S. H. Kleinstein, E. D. Abel, K. L. Insogna, S. Feske, J. W. Locasale, M. W. Bosenberg, J. C. Rathmell and S. M. Kaech (2015). "Phosphoenolpyruvate Is a Metabolic Checkpoint of Anti-tumor T Cell Responses." Cell **162**(6): 1217-1228.

Hoshi, N., D. Schenten, S. A. Nish, Z. Walther, N. Gagliani, R. A. Flavell, B. Reizis, Z. Shen, J. G. Fox, A. Iwasaki and R. Medzhitov (2012). "MyD88 signalling in colonic mononuclear phagocytes drives colitis in IL-10-deficient mice." Nat Commun **3**: 1120.

Intlekofer, A. M., R. G. Dematteo, S. Venneti, L. W. Finley, C. Lu, A. R. Judkins, A. S. Rustenburg, P. B. Grinaway, J. D. Chodera, J. R. Cross and C. B. Thompson (2015). "Hypoxia Induces Production of L-2-Hydroxyglutarate." Cell Metab **22**(2): 304-311.

Jacobs, S. R., C. E. Herman, N. J. MacIver, J. A. Wofford, H. L. Wieman, J. J. Hammen and J. C. Rathmell (2008). "Glucose Uptake Is Limiting in T Cell Activation and Requires CD28-Mediated Akt-Dependent and Independent Pathways." The Journal of Immunology **180**(7): 4476-4486.

Kaminski, M. M., S. W. Sauer, M. Kaminski, S. Opp, T. Ruppert, P. Grigaravicius, P. Grudnik, H. J. Grone, P. H. Krammer and K. Gulow (2012). "T cell activation is driven by an ADP-dependent glucokinase linking enhanced glycolysis with mitochondrial reactive oxygen species generation." Cell Rep **2**(5): 1300-1315.

Kawalekar, O. U., R. S. O'Connor, J. A. Fraietta, L. Guo, S. E. McGettigan, A. D. Posey, Jr., P. R. Patel, S. Guedan, J. Scholler, B. Keith, N. W. Snyder, I. A. Blair, M. C. Milone and C. H. June (2016). "Distinct Signaling of Coreceptors Regulates Specific Metabolism Pathways and Impacts Memory Development in CAR T Cells." Immunity **44**(2): 380-390.

Kishton, R. J., C. E. Barnes, A. G. Nichols, S. Cohen, V. A. Gerriets, P. J. Siska, A. N. Macintyre, P. Goraksha-Hicks, A. A. de Cubas, T. Liu, M. O. Warmoes, E. D. Abel, A. E. Yeoh, T. R. Gershon, W. K. Rathmell, K. L. Richards, J. W. Locasale and J. C. Rathmell (2016). "AMPK Is Essential to Balance Glycolysis and Mitochondrial Metabolism to Control T-ALL Cell Stress and Survival." Cell Metab **23**(4): 649-662.

Kuhn, R., J. Lohler, D. Rennick, K. Rajewsky and W. Muller (1993). "Interleukin-10-deficient mice develop chronic enterocolitis." Cell **75**(2): 263-274.

Lee, J. H., C. Elly, Y. Park and Y. C. Liu (2015). "E3 Ubiquitin Ligase VHL Regulates Hypoxia-Inducible Factor-1alpha to Maintain Regulatory T Cell Stability and Suppressive Capacity." Immunity **42**(6): 1062-1074.

Lunt, S. Y. and M. G. Vander Heiden (2011). "Aerobic glycolysis: meeting the metabolic requirements of cell proliferation." Annu Rev Cell Dev Biol **27**: 441-464.

Ma, E. H., G. Bantug, T. Griss, S. Condotta, R. M. Johnson, B. Samborska, N. Mainolfi, V. Suri, H. Guak, M. L. Balmer, M. J. Verway, T. C. Raissi, H. Tsui, G. Boukhaled, S. Henriques da Costa, C. Frezza, C. M. Krawczyk, A. Friedman, M. Manfredi, M. J. Richer, C. Hess and R. G. Jones (2017). "Serine Is an Essential Metabolite for Effector T Cell Expansion." Cell Metab **25**(2): 345-357.

Macintyre, A. N., V. A. Gerriets, A. G. Nichols, R. D. Michalek, M. C. Rudolph, D. Deoliveira, S. M. Anderson, E. D. Abel, B. J. Chen, L. P. Hale and J. C. Rathmell (2014). "The glucose transporter Glut1 is selectively essential for CD4 T cell activation and effector function." Cell Metab **20**(1): 61-72.

Mamlouk, S., J. Kalucka, R. P. Singh, K. Franke, A. Muschter, A. Langer, C. Jakob, M. Gassmann, G. B. Baretton and B. Wielockx (2014). "Loss of prolyl hydroxylase-2 in myeloid cells and T-lymphocytes impairs tumor development." Int J Cancer **134**(4): 849-858.

Mehta, M. M., S. E. Weinberg and N. S. Chandel (2017). "Mitochondrial control of immunity: beyond ATP." Nat Rev Immunol **17**(10): 608-620.

Michalek, R. D., V. A. Gerriets, S. R. Jacobs, A. N. Macintyre, N. J. MacIver, E. F. Mason, S. A. Sullivan, A. G. Nichols and J. C. Rathmell (2011). "Cutting edge: distinct glycolytic and lipid oxidative metabolic programs are essential for effector and regulatory CD4+ T cell subsets." J Immunol **186**(6): 3299-3303.

Michalek, R. D., V. A. Gerriets, A. G. Nichols, M. Inoue, D. Kazmin, C. Y. Chang, M. A. Dwyer, E. R. Nelson, K. N. Pollizzi, O. Ilkayeva, V. Giguere, W. J. Zuercher, J. D. Powell, M. L. Shinohara, D. P. McDonnell and J. C. Rathmell (2011). "Estrogen-related receptor-alpha is a metabolic regulator of effector T-cell activation and differentiation." Proc Natl Acad Sci U S A **108**(45): 18348-18353.

Mullen, A. R., Z. Hu, X. Shi, L. Jiang, L. K. Boroughs, Z. Kovacs, R. Boriack, D. Rakheja, L. B. Sullivan, W. M. Linehan, N. S. Chandel and R. J. DeBerardinis (2014). "Oxidation of alpha-ketoglutarate is required for reductive carboxylation in cancer cells with mitochondrial defects." Cell Rep **7**(5): 1679-1690.

Newton, R., B. Priyadharshini and L. A. Turka (2016). "Immunometabolism of regulatory T cells." Nat Immunol **17**(6): 618-625.

O'Sullivan, D., G. J. van der Windt, S. C. Huang, J. D. Curtis, C. H. Chang, M. D. Buck, J. Qiu, A. M. Smith, W. Y. Lam, L. M. DiPlato, F. F. Hsu, M. J. Birnbaum, E. J. Pearce and E. L. Pearce (2014). "Memory CD8(+) T cells use cell-intrinsic lipolysis to support the metabolic programming necessary for development." Immunity **41**(1): 75-88.

Pan, Y., T. Tian, C. O. Park, S. Y. Lofftus, S. Mei, X. Liu, C. Luo, J. T. O'Malley, A. Gehad, J. E. Teague, S. J. Divito, R. Fuhlbrigge, P. Puigserver, J. G. Krueger, G. S. Hotamisligil, R. A. Clark and T. S. Kupper (2017). "Survival of tissue-resident memory T cells requires exogenous lipid uptake and metabolism." Nature **543**(7644): 252-256.

Patra, K. C., Q. Wang, P. T. Bhaskar, L. Miller, Z. Wang, W. Wheaton, N. Chandel, M. Laakso, W. J. Muller, E. L. Allen, A. K. Jha, G. A. Smolen, M. F. Clasquin, R. B. Robey and N. Hay (2013). "Hexokinase 2 is required for tumor initiation and maintenance and its systemic deletion is therapeutic in mouse models of cancer." Cancer Cell **24**(2): 213-228.

Pearce, E. L., M. C. Poffenberger, C. H. Chang and R. G. Jones (2013). "Fueling immunity: insights into metabolism and lymphocyte function." Science **342**(6155): 1242454.

Pearce, E. L., M. C. Walsh, P. J. Cejas, G. M. Harms, H. Shen, L. S. Wang, R. G. Jones and Y. Choi (2009). "Enhancing CD8 T-cell memory by modulating fatty acid metabolism." Nature **460**(7251): 103-107.

Peng, M., N. Yin, S. Chhangawala, K. Xu, C. S. Leslie and M. O. Li (2016). "Aerobic glycolysis promotes T helper 1 cell differentiation through an epigenetic mechanism." Science **354**(6311): 481-484.

Phan, A. T., A. L. Doedens, A. Palazon, P. A. Tyrakis, K. P. Cheung, R. S. Johnson and A. W. Goldrath (2016). "Constitutive Glycolytic Metabolism Supports CD8+ T Cell Effector Memory Differentiation during Viral Infection." Immunity **45**(5): 1024-1037.

Postic, C., M. Shiota and M. A. Magnuson (2001). "Cell-specific roles of glucokinase in glucose homeostasis." Recent Prog Horm Res **56**: 195-217.

Rabinovich, G. A., D. Gabrilovich and E. M. Sotomayor (2007). "Immunosuppressive strategies that are mediated by tumor cells." Annu Rev Immunol **25**: 267-296.

Ron-Harel, N., D. Santos, J. M. Ghergurovich, P. T. Sage, A. Reddy, S. B. Lovitch, N. Dephoure, F. K. Satterstrom, M. Sheffer, J. B. Spinelli, S. Gygi, J. D. Rabinowitz, A. H. Sharpe and M. C. Haigis (2016). "Mitochondrial Biogenesis and Proteome Remodeling Promote One-Carbon Metabolism for T Cell Activation." Cell Metab **24**(1): 104-117.

Scharping, N. E., A. V. Menk, R. S. Moreci, R. D. Whetstone, R. E. Dadey, S. C. Watkins, R. L. Ferris and G. M. Delgoffe (2016). "The Tumor Microenvironment Represses T Cell Mitochondrial Biogenesis to Drive Intratumoral T Cell Metabolic Insufficiency and Dysfunction." Immunity **45**(2): 374-388.

Scharping, N. E., A. V. Menk, R. D. Whetstone, X. Zeng and G. M. Delgoffe (2017). "Efficacy of PD-1 Blockade Is Potentiated by Metformin-Induced Reduction of Tumor Hypoxia." Cancer Immunol Res **5**(1): 9-16.

Sena, L. A., S. Li, A. Jairaman, M. Prakriya, T. Ezponda, D. A. Hildeman, C. R. Wang, P. T. Schumacker, J. D. Licht, H. Perlman, P. J. Bryce and N. S. Chandel (2013). "Mitochondria are required for antigen-specific T cell activation through reactive oxygen species signaling." Immunity **38**(2): 225-236.

Sharma, P., K. Wagner, J. D. Wolchok and J. P. Allison (2011). "Novel cancer immunotherapy agents with survival benefit: recent successes and next steps." Nat Rev Cancer **11**(11): 805-812.

Shaw, R. J. (2006). "Glucose metabolism and cancer." Curr Opin Cell Biol **18**(6): 598-608.

Shedlock, D. J. and H. Shen (2003). "Requirement for CD4 T cell help in generating functional CD8 T cell memory." Science **300**(5617): 337-339.

Shi, L. Z., R. Wang, G. Huang, P. Vogel, G. Neale, D. R. Green and H. Chi (2011). "HIF1alpha-dependent glycolytic pathway orchestrates a metabolic checkpoint for the differentiation of TH17 and Treg cells." J Exp Med **208**(7): 1367-1376.

Shrestha, S., K. Yang, C. Guy, P. Vogel, G. Neale and H. Chi (2015). "Treg cells require the phosphatase PTEN to restrain TH1 and TFH cell responses." Nat Immunol **16**(2): 178-187.

Steinert, E. M., J. M. Schenkel, K. A. Fraser, L. K. Beura, L. S. Manlove, B. Z. Igyarto, P. J. Southern and D. Masopust (2015). "Quantifying Memory CD8 T Cells Reveals Regionalization of Immunosurveillance." Cell **161**(4): 737-749.

Sukumar, M., J. Liu, Y. Ji, M. Subramanian, J. G. Crompton, Z. Yu, R. Roychoudhuri, D. C. Palmer, P. Muranski, E. D. Karoly, R. P. Mohney, C. A. Klebanoff, A. Lal, T. Finkel, N. P. Restifo and L. Gattinoni (2013). "Inhibiting glycolytic metabolism enhances CD8+ T cell memory and antitumor function." J Clin Invest **123**(10): 4479-4488.

Sukumar, M., J. Liu, G. U. Mehta, S. J. Patel, R. Roychoudhuri, J. G. Crompton, C. A. Klebanoff, Y. Ji, P. Li, Z. Yu, G. D. Whitehill, D. Clever, R. L. Eil, D. C. Palmer, S. Mitra, M. Rao, K. Keyvanfar, D. S. Schrump, E. Wang, F. M. Marincola, L. Gattinoni, W. J. Leonard, P. Muranski, T. Finkel and N. P. Restifo (2016). "Mitochondrial

Membrane Potential Identifies Cells with Enhanced Stemness for Cellular Therapy." Cell Metab **23**(1): 63-76.

Tan, H., K. Yang, Y. Li, T. I. Shaw, Y. Wang, D. B. Blanco, X. Wang, J. H. Cho, H. Wang, S. Rankin, C. Guy, J. Peng and H. Chi (2017). "Integrative Proteomics and Phosphoproteomics Profiling Reveals Dynamic Signaling Networks and Bioenergetics Pathways Underlying T Cell Activation." Immunity **46**(3): 488-503.

Tannahill, G. M., A. M. Curtis, J. Adamik, E. M. Palsson-McDermott, A. F. McGettrick, G. Goel, C. Frezza, N. J. Bernard, B. Kelly, N. H. Foley, L. Zheng, A. Gardet, Z. Tong, S. S. Jany, S. C. Corr, M. Haneklaus, B. E. Caffrey, K. Pierce, S. Walmsley, F. C. Beasley, E. Cummins, V. Nizet, M. Whyte, C. T. Taylor, H. Lin, S. L. Masters, E. Gottlieb, V. P. Kelly, C. Clish, P. E. Auron, R. J. Xavier and L. A. O'Neill (2013). "Succinate is an inflammatory signal that induces IL-1beta through HIF-1alpha." Nature **496**(7444): 238-242.

Tyrakis, P. A., A. Palazon, D. Macias, K. L. Lee, A. T. Phan, P. Velica, J. You, G. S. Chia, J. Sim, A. Doedens, A. Abelanet, C. E. Evans, J. R. Griffiths, L. Poellinger, A. W. Goldrath and R. S. Johnson (2016). "S-2-hydroxyglutarate regulates CD8+ T-lymphocyte fate." Nature **540**(7632): 236-241.

van der Windt, G. J., B. Everts, C. H. Chang, J. D. Curtis, T. C. Freitas, E. Amiel, E. J. Pearce and E. L. Pearce (2012). "Mitochondrial respiratory capacity is a critical regulator of CD8+ T cell memory development." Immunity **36**(1): 68-78.

Varanasi, S. K., U. Jaggi, N. Hay and B. T. Rouse (2018). "Hexokinase II may be dispensable for CD4 T cell responses against a virus infection." PLoS One **13**(1): e0191533.

Wang, L., H. Xiong, F. Wu, Y. Zhang, J. Wang, L. Zhao, X. Guo, L. J. Chang, Y. Zhang, M. J. You, S. Koochekpour, M. Saleem, H. Huang, J. Lu and Y. Deng (2014). "Hexokinase 2-mediated Warburg effect is required for PTEN- and p53-deficiency-driven prostate cancer growth." Cell Rep **8**(5): 1461-1474.

Wang, R., C. P. Dillon, L. Z. Shi, S. Milasta, R. Carter, D. Finkelstein, L. L. McCormick, P. Fitzgerald, H. Chi, J. Munger and D. R. Green (2011). "The transcription factor Myc controls metabolic reprogramming upon T lymphocyte activation." Immunity **35**(6): 871-882.

Wang, T., C. Marquardt and J. Foker (1976). "Aerobic glycolysis during lymphocyte proliferation." Nature **261**(5562): 702-705.

Welsh, R. M. and M. O. Seedhom (2008). "Lymphocytic choriomeningitis virus (LCMV): propagation, quantitation, and storage." Curr Protoc Microbiol **Chapter 15**: Unit 15A 11.

Wheaton, W. W., S. E. Weinberg, R. B. Hamanaka, S. Soberanes, L. B. Sullivan, E. Anso, A. Glasauer, E. Dufour, G. M. Mutlu, G. S. Budigner and N. S. Chandel (2014). "Metformin inhibits mitochondrial complex I of cancer cells to reduce tumorigenesis." Elife **3**: e02242.

Wilson, J. E. (2003). "Isozymes of mammalian hexokinase: structure, subcellular localization and metabolic function." J Exp Biol **206**(Pt 12): 2049-2057.

Yang, Z., H. Fujii, S. V. Mohan, J. J. Goronzy and C. M. Weyand (2013). "Phosphofructokinase deficiency impairs ATP generation, autophagy, and redox balance in rheumatoid arthritis T cells." J Exp Med **210**(10): 2119-2134.

Yin, Y., S. C. Choi, Z. Xu, D. J. Perry, H. Seay, B. P. Croker, E. S. Sobel, T. M. Brusko and L. Morel (2015). "Normalization of CD4+ T cell metabolism reverses lupus." Sci Transl Med **7**(274): 274ra218.

Yu, P., K. Wilhelm, A. Dubrac, J. K. Tung, T. C. Alves, J. S. Fang, Y. Xie, J. Zhu, Z. Chen, F. De Smet, J. Zhang, S. W. Jin, L. Sun, H. Sun, R. G. Kibbey, K. K. Hirschi, N. Hay, P. Carmeliet, T. W. Chittenden, A. Eichmann, M. Potente and M. Simons (2017). "FGF-dependent metabolic control of vascular development." Nature **545**(7653): 224-228.

Zheng, Y. and A. Y. Rudensky (2007). "Foxp3 in control of the regulatory T cell lineage." Nat Immunol **8**(5): 457-462.